Develop a Tool for Sight Distance Analysis Using GIS and LiDAR Data

Final Report

Prepared By:

Huaguo Zhou, Ph.D. & P.E.
Fangjian Yang, Ph.D.

Highway Research Center
Department of Civil and Environmental Engineering
238 Harbert Engineering Center

Auburn University
Auburn, AL 36849

Sponsoring Agency:

Alabama Department of Transportation
1409 Coliseum Blvd
Montgomery, AL 36110

April 2025

1. Report No.	2. Government Accession No.	3. Recipient Catalog No.
4. Title and Subtitle Develop a Tool for Sight Distance Analysis Using GIS and LiDAR Data		5. Report Date April 2025
		6. Performing Organization Code
7. Author(s) Huaguo Zhou and Fangjian Yang		8. Performing Organization Report No. ALDOT 931-063
9. Performing Organization Name and Address Highway Research Center Department of Civil and Environmental Engineering 238 Harbert Engineering Center Auburn, AL 36849		10. Work Unit No. (TRAIS)
		11. Contract or Grant No. FHWA/ALDOT 931-063
12. Sponsoring Agency Name and Address Alabama Department of Transportation 1409 Coliseum Boulevard Montgomery, AL 36130		13. Type of Report and Period Covered: Technical Report
		14. Sponsoring Agency Code

15. Supplementary Notes

Project performed in collaboration with the Alabama Department of Transportation.

16. Abstract

Intersection Sight Distance (ISD) plays a critical role in ensuring roadway safety, particularly at unsignalized intersections where the lack of adequate visibility can result in severe accidents. Traditional ISD assessment methods often rely on manual measurements, which can be time-consuming, costly, and prone to inaccuracies. This study aims to address these limitations by developing an automated GIS-based tool that leverages LiDAR data to evaluate ISD at two-way stop-controlled (TWSC) intersections in Alabama. This tool facilitates efficient screening of large road networks, calculates the recommended ISD, and identifies sight distance obstructions. The method involves generating a digital surface model and conducting line-of-sight analyses while allowing users to customize such parameters as observer position, vehicle type, and vegetation exclusion. The developed method was applied to 13 intersections in Auburn, Alabama, and the results were validated against traditional field measurements. The comparison revealed that discrepancies mainly stemmed from human error in field assessments, dynamic changes in the environment, and the time lag between LiDAR data collection and field evaluation.

Furthermore, the study investigates the relationship between ISD and crash frequency, focusing on the unique traffic conditions in Alabama. Comprehensive LiDAR data covering 230 intersections were processed, and historical crash data from 2018 to 2022 were analyzed to identify target crashes influenced by sight distance deficiencies.

The LiDAR-based method proved to be a cost-effective, scalable, and reliable tool for assessing ISD, offering significant benefits for transportation agencies in planning and prioritizing intersection safety improvements. The study presents the development of ISD assessment tools, application of methodologies for evaluating ISD impact on intersection safety, and the formulation of region-specific Crash Modification Factors (CMFs). The findings provide actionable insights for optimizing intersection design to enhance roadway safety and guide future ISD-related research.

17. Key Words: Intersection Sight Distance, Sight Triangle, GIS, LiDAR Data, Unsignalized Intersection		18. Distribution Statement No restrictions	
19. Security Classification (of this report) Unclassified	20. Security Classification (of this page) Unclassified	21. No. of Pages 93	22. Price None.

Acknowledgment

The authors extend their gratitude to the project panel members for their valuable guidance throughout the project. The research team also thanks Stuart Manson, Wade Seymore, John Russell, Jared Horne, and Dalton L. Chamblee from ALDOT for their assistance with crash data and LiDAR data collection. A special appreciation goes to Md Roknuzzaman for his efforts in editing the final report.

TABLE OF CONTENTS

LIST OF FIGURES

LIST OF TABLES

1 INTRODUCTION

1.1 Background

Intersection Sight Distance (ISD) is a critical safety consideration in intersection design. ISD refers to the unobstructed distance along a driver's line of sight to a potential point of conflict, such as an oncoming vehicle or a pedestrian crossing. The adequacy of ISD is essential for drivers to detect hazards in time to react safely, make informed decisions, and avoid collisions. Insufficient ISD can lead to dangerous situations, such as drivers misjudging the speed or distance of approaching vehicles, resulting in failure to yield, improper turning maneuvers, or crashes. ISD is especially important at Two-Way Stop-Controlled (TWSC) intersections, where drivers on the minor road must stop and rely entirely on their ability to see oncoming traffic from the major road before proceeding. At these intersections, restricted sight distance has been linked to an increased risk of crashes, making it a crucial factor for ensuring the safety and efficiency of intersection operations. ISD is determined by several factors, including the height of the driver's eye, the height of any objects that might block the driver's view, and the clear space along the approach lanes and corners of the intersection that must remain free of obstructions. Additionally, ISD is influenced by factors such as vehicle speed, how quickly drivers can decelerate, their perception-reaction time (PRT), and their willingness to accept gaps in traffic. These variables can differ depending on the specific design of the intersection and the behavior of road users, making it essential to consider them when assessing ISD for safe intersection operations.

The American Association of State Highway and Transportation Officials (AASHTO) Policy on Geometric Design of Highways and Streets (Green Book) (AASHTO, 2018) defines the length of the sight triangle at the conflict leg as the ISD, which represents the area along the intersection approach legs and across their included corners that must be free of obstructions blocking a driver's view of potential conflicts with other vehicles. Additionally, the Green Book provides calculation methods for determining the recommended ISD for intersections with stop control on minor roads. **Figure 1** illustrates the clear sight triangles and ISD at an intersection with stop control on the minor road.

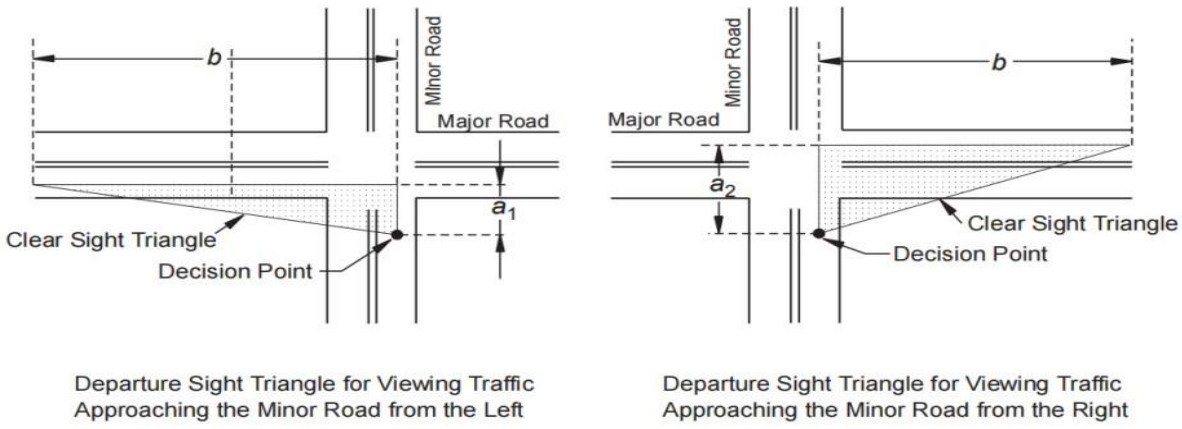

Figure 1 Clear Sight Triangle and Intersection Sight Distance (AASHTO, 2018)

The distance a_2 comprises distance a_1 plus the width of the departing lane(s) on the major road to the right and encompasses any median width on the major road. Distance b represents the ISD required for observing traffic approaching the minor road from the left or right. Adhering to these guidelines is essential for improving intersection safety and ensuring the overall safety of road users.

However, while the theory behind ISD is well understood, practical challenges remain. Traditional methods for assessing ISD often rely on manual, field-based measurements, which can be time-consuming, expensive, and prone to inaccuracies, especially across a large network of intersections. Additionally, these methods are limited in their ability to account for dynamic traffic conditions and the varying geometry of intersections. This gap between theory and practical assessment has created a need for more efficient, accurate, and scalable methods for ISD evaluation.

Recent technological advancements, including the use of Geographic Information Systems (GIS) and Light Detection and Ranging (LiDAR) data, have shown promise in automating and enhancing ISD assessments. GIS and LiDAR enable the capture of high-resolution spatial data, allowing for a more precise evaluation of visibility conditions at intersections. These technologies can provide detailed information about intersection geometry, obstructions, and other factors that influence sight distance. However, despite these advancements, existing methods still face several limitations that have created the research gap.

One major limitation of existing ISD assessment methods is the difficulty in efficiently screening large road networks to calculate both the recommended ISD and the occlusion rate for each intersection, which refers to the proportion of the sight triangle area that is obstructed by physical objects such as buildings, vegetation, or parked vehicles. This challenge prevents transportation agencies from systematically prioritizing intersections based on the severity of sight obstructions, limiting their ability to allocate resources effectively to critical locations. Furthermore, inconsistencies in ISD measurement across multiple intersections pose another challenge, as current methods often fail to align with standardized measurement used by various transportation agencies, leading to potential overestimation or underestimation of ISD values. This inconsistency undermines the reliability of ISD assessments and impedes informed decision-making for safety improvements. Additionally, ISD measurements are highly sensitive to the positions of the observer (typically the driver) and the target (e.g., oncoming vehicles or potential obstructions). Small variations in these positions can cause significant discrepancies in measurements, compromising the accuracy of evaluations. Existing methods struggle to determine these positions precisely, leading to errors that can impact the assessment of intersection safety.

Moreover, there is a need to better understand the relationship between ISD and traffic safety within the specific conditions of Alabama. While the general principles of ISD are well understood, there has been limited exploration into how ISD affects crash frequency and severity in varying regional contexts. Alabama's road network includes a diverse range of intersection types, spanning rural and urban settings, with differing road geometries and traffic volumes.

Investigating how ISD impacts traffic safety within this context can provide valuable insights for region-specific safety strategies and support data-driven decisions for intersection improvements.

Addressing these research gaps is crucial for improving the accuracy and effectiveness of intersection safety assessments, ultimately leading to better roadway safety outcomes. The current limitations in ISD evaluation methods, including inefficiencies in screening large road networks and inconsistencies in measurement across multiple intersections, impede the ability of transportation agencies to accurately prioritize high-risk intersections for targeted safety interventions. Without automated and standardized ISD assessments, agencies may misallocate resources or overlook intersections where inadequate sight distance significantly contributes to crash risks. Furthermore, the high sensitivity of ISD to the observer and target positions highlights the need for greater precision in these measurements, as inaccuracies can lead to erroneous safety evaluations. In addition, the limited exploration of how ISD impacts traffic safety in specific regional contexts, such as Alabama, suggests that current safety strategies may not fully consider the distinct characteristics of local road networks. By developing a scalable, automated tool that ensures consistent and precise ISD evaluations, this research addresses these critical gaps and enables transportation agencies to make more informed, data-driven decisions aimed at enhancing safety, reducing crash risks, and improving overall traffic operations.

1.2 Research Objectives

This study aims to develop and validate an automated GIS-based tool that leverages LiDAR data to assess ISD accurately and efficiently, addressing the limitations of traditional methods. Additionally, the study seeks to explore the relationship between ISD and crash frequency, particularly in Alabama, to provide valuable insights into how local traffic and environmental conditions influence intersection safety.

The first part of the research focuses on the development of a new measurement method for ISD. The primary objective is to create a GIS-based tool that uses high-resolution LiDAR data to automate the ISD measurement process. This tool addresses the limitations of traditional manual methods, which are often inefficient and labor-intensive, especially when applied to large networks of intersections. The goal is to develop a scalable, efficient, and accurate solution that can be applied across diverse intersection types. Additionally, the tool will be designed to incorporate the sensitivity of ISD to the positions of the observer (driver) and the target (e.g., oncoming vehicles or obstructions). Accurate determination of these positions is essential for minimizing measurement errors, ensuring that the ISD evaluations reflect real-world conditions. Furthermore, the tool will enable transportation agencies to efficiently screen large road networks by calculating the recommended ISD and occlusion rates for each intersection. This capability will allow agencies to prioritize high-risk intersections based on visibility issues, improving resource allocation for safety interventions. The tool will also provide detailed visual outputs, such as maps and 3D models, to facilitate decision-making by transportation planners and other stakeholders.

The second part of the research focuses on studying the impact of ISD on traffic safety. The objective is to analyze the relationship between ISD and crash frequency at unsignalized

intersections, particularly within Alabama's unique traffic and road conditions. By using historical crash data, the study seeks to determine if inadequate sight distance correlates with an increased risk of crashes. This analysis aims to establish a clear connection between ISD and intersection safety, leading to the development of region-specific Crash Modification Factors (CMFs) that quantify the safety benefits of improving ISD. These CMFs will provide transportation agencies with a valuable tool to estimate the potential reduction in crash frequency when ISD is enhanced, supporting data-driven decisions for intersection design and safety interventions. Additionally, the study will evaluate how specific intersection design features, such as left-turn and right-turn lanes, impact ISD and crash risk. This analysis will provide insights into how certain design elements may contribute to either improving or obstructing sight distance, guiding future intersection design improvements.

By pursuing these objectives, the study aims to advance both the methodologies for ISD measurement and the understanding of ISD's impact on traffic safety, providing actionable tools and insights for improving intersection safety across large networks.

1.3 Research Tasks

The research tasks for this study are designed to systematically develop an advanced ISD assessment tool and analyze its impact on traffic safety, particularly at TWSC intersections within Alabama. These tasks address both the development of the tool and its application in the field to assess its effect on crash frequency.

The first task is to conduct a comprehensive literature review. This task involves reviewing current ISD assessment methodologies, including traditional manual methods and more recent approaches that use GIS and LiDAR data. Additionally, the review examines studies on the relationship between ISD and crash frequency at unsignalized intersections, identifying research gaps and limitations in existing methods. The insights gathered from the literature guide the development of an automated ISD measurement tool and the subsequent analysis of its impact on traffic safety.

The second task is to collect data. This task focuses on gathering high-resolution LiDAR data for selected intersections across the Alabama State Highway System. The data collection covers intersections of varying configurations, traffic volumes, and environments, ensuring a representative sample. In addition to the LiDAR data, historical crash data from the past five years (2018-2022) has been obtained. This crash data focuses on accidents that may be influenced by inadequate ISD, such as angle collisions and crashes involving vehicles entering from minor roads. This comprehensive dataset serves as the foundation for tool development and subsequent analysis.

The third task is to develop and validate the automated GIS-based ISD measurement tool. In this task, the primary objective is to create a tool that automates the ISD measurement process, using LiDAR data. The tool incorporates customizable parameters for the observer (driver) and target (oncoming vehicles or obstacles), ensuring flexible and accurate assessments across different intersection geometries. It also calculates the occlusion rate to identify intersections where sight distance is compromised by obstructions. The tool is designed to be scalable, allowing

for its use across large road networks. Validation testing is conducted by comparing the tool's automated ISD measurements with traditional manual measurements at selected intersections.

The fourth task is to apply the validated tool and analyze the impact of ISD on traffic safety. This task involves multiple components. First, the validated tool is applied to measure ISD at the selected unsignalized intersections across Alabama. The measurements are used to assess whether these intersections meet recommended ISD criteria and to identify those with sight distance deficiencies. Following this, the relationship between ISD and crash frequency is analyzed by correlating the ISD data with the historical crash data. This analysis focuses on ISD-related crashes, such as angle collisions and crashes involving vehicles entering from minor roads, which are more likely to be influenced by inadequate sight distance. The goal is to establish a clear connection between ISD deficiencies and higher crash risks. Additionally, this task involves developing region-specific CMFs based on ISD and crash data analysis. The CMFs quantify the safety benefits associated with improving ISD at unsignalized intersections and are calibrated to reflect Alabama's traffic conditions. These CMFs provide transportation agencies with a tool to estimate the potential reduction in crash frequency resulting from ISD improvements. Finally, this task evaluates the impact of various intersection design features, such as left-turn lanes, right-turn lanes, and medians, on ISD and crash risk. Understanding how these features affect visibility, and safety provides insights into optimizing intersection design to improve sight distance and reduce crash risks.

1.4 Organization of the Report

This report begins with the introduction, progresses through a detailed literature review, data collection, methodology, tool application, safety analysis, and finally concludes with key findings, implications, and recommendations for future research.

The second section presents a comprehensive literature review, summarizing existing research on ISD assessment methods, the integration of GIS and LiDAR in traffic engineering, and the influence of ISD on road safety. This review identifies gaps in current methods and highlights the need for more accurate, efficient, and scalable tools for ISD measurement, laying the foundation for the tool's development and subsequent analysis.

The third section details the data collection process, covering the acquisition of high-resolution LiDAR data, historical crash data from 2018 to 2022, and intersection-specific information, such as traffic volumes and geometric configurations. This section explains the selection of intersections to ensure a diverse representation of Alabama's road conditions, providing the necessary dataset for ISD measurement and safety analysis.

The fourth section outlines the study's methodology, including the development of the GIS-based automated ISD assessment tool. It explains the technical steps involved in data processing, observer and target point generation, visibility analysis, and the verification process. This part also describes the methods used for validating and calibrating the CMFs developed based on a recent National Cooperative Highway Research Program (NCHRP) project, as well as the Empirical Bayes (EB) Before-and- After Study method employed for developing the CMFs.

The fifth section focuses on applying the validated ISD tool to selected intersections in Alabama. This part discusses the statistical analysis conducted to explore the differences in ISD measurements under various conditions, such as observer location and vehicle type. It also assesses the tool's accuracy and effectiveness through comparisons with traditional ISD measurement methods, establishing its reliability for large-scale network screening.

The sixth section presents the impact of ISD on intersection safety, analyzing the correlation between ISD and crash frequency, particularly for target crashes directly influenced by sight distance deficiencies. The segment details the calibration of region-specific CMFs based on Alabama's traffic conditions and evaluates how intersection design features, such as left-turn and right-turn lanes, affect ISD and crash risk. These findings offer valuable insights into optimizing intersection design to improve safety.

The final section summarizes the key findings and contributions of the study. It discusses the implications of the research, addresses its limitations, and provides recommendations for future research, including the extension of the ISD assessment tool to other types of intersections and the incorporation of dynamic factors, such as real-time traffic data, in future analyses. This part underscores the potential of the developed tool and methodologies to enhance roadway safety through data-driven intersection design and safety interventions.

2 LITERATURE REVIEW

This section reviews key literature on ISD to identify gaps in current assessment methods and explore opportunities for improvement, covering foundational principles, traditional and modern measurement approaches, and the relationship between ISD and traffic safety. It begins by discussing ISD's critical role in intersection safety, particularly at unsignalized intersections, providing a basis for understanding the limitations of traditional field measurement methods outlined in the AASHTO Greenbook. The review then examines modern ISD measurement approaches, focusing on the use of GIS and LiDAR technologies. The segment also explores studies linking ISD with traffic safety and evaluates safety performance metrics like CMFs to quantify ISD improvements in terms of crash reduction.

2.1 Intersection Sight Distance

In the evolution of intersection design and safety analysis, especially concerning unsignalized intersections, the literature review reveals a critical trajectory from traditional methodologies toward more dynamic, evidence-based approaches. This transition is not only a reflection of advancements in vehicle technology, including autonomous vehicles (AVs), but also a growing recognition of the limitations inherent in existing standards and the need for more precise, real-world reflective measurement tools.

Easa (1998) provided a foundational critique of the AASHTO model for calculating ISD, marking the beginning of this shift. By proposing a revised model that incorporates actual speeds and driver behaviors rather than relying on theoretical or static design speeds, Easa challenges the adequacy of long-standing guidelines and underscores the potential underestimation of ISD needs, setting a precedent for future research and development in this field.

Building on this, Harwood et al. (2000) further advocate for models grounded in gap acceptance and observed driver behaviors, emphasizing a more nuanced understanding of driver decision-making processes at stop-controlled intersections. This approach aligns with the proposed GIS tool's objective to utilize LiDAR data for enhanced ISD measurement, offering a pathway to integrate these insights into practical applications for road safety improvements.

Layton (2012) discusses the evolution of AASHTO's "gap acceptance" models, emphasizing the importance of adapting ISD criteria to better reflect real-world driving conditions and the capabilities of modern vehicles. This evolution highlights the necessity of advanced measurement techniques, such as the proposed GIS tool, to ensure that ISD calculations contribute effectively to safer road designs and traffic management practices.

The studies by Stančerić et al. (2012) and Pranjić et al. (2017) expand the discourse to include the geometric aspects of intersection design and the need for updated standards that accommodate the changing landscape of vehicle technology and traffic behavior. These insights underscore the GIS tool's potential to address the complex dynamics of intersection safety and design, offering more adaptable and responsive solutions to the challenges of unsignalized intersections.

Further, Dabbour et al. (2017)and Dabbour et al. (2021) delve into the specifics of ISD calculation methodologies, proposing revised approaches that better account for the acceleration capabilities and perceptual judgments of drivers. These contributions are invaluable in refining the theoretical underpinnings of ISD measurement and enhancing the practical utility of tools like the GIS application being developed.

Abdulhafedh (2020) provides a comprehensive analysis of Stopping Sight Distance (SSD), Decision Sight Distance (DSD), and Passing Sight Distance (PSD) roles within the broader context of highway safety, articulating the critical importance of accurate and comprehensive sight distance calculations. This analysis not only supports the necessity of the proposed GIS tool but also highlights its potential to inform more effective road design and traffic management strategies.

Lastly, Magyari et al. (2021) brings the discussion into the realm of autonomous vehicles, examining how AV technology may alter ISD requirements and offering insights into the potential for more efficient and safer road use as these vehicles become more common. This perspective is crucial for ensuring that the development of measurement tools and design guidelines keeps pace with technological advancements, aiming to enhance road safety for all users.

Incorporating these diverse yet interconnected strands of research, the literature review underscores the proposed GIS tool's role in navigating the transition towards more dynamic, evidence-based approaches to ISD measurement and intersection design. By aligning with the latest advancements in vehicle technology and road safety research, the tool aims to contribute significantly to reducing traffic accidents and improving safety at unsignalized intersections, marking a critical step forward in the ongoing evolution of traffic engineering and road safety analysis.

2.2 Innovative Technology in ISD Measurement

2.2.1 Advanced Computational and Mathematical Models

In early studies, in addition to field measurements, computational and mathematical models for ISD measurement were proposed and validated. These innovative approaches have revolutionized the way ISD is calculated, especially for roads featuring complex geometries such as 3D alignments. Traditional methods, while useful, often fail to capture the intricate realities of modern road designs, making the precision offered by these advanced models indispensable.

In this area, Easa et al. developed mathematical model in 2004 and 2006, which specifically addresses the limitations inherent in the guidelines provided by the AASHTO (Easa et al., 2004, 2006). This model innovatively includes a wide range of variables, such as the presence of horizontal and vertical curves on the major road and a longitudinal grade and skew on the minor road. By also accounting for obstructions both inside and outside the horizontal curve, it offers much-needed refinement in ISD calculation, a critical aspect previously unaddressed in earlier models. The practical application and efficacy of this model were illustrated through a case study involving a hypothetical intersection with both major and minor roads being two-lane highways, showcasing the model's capability to accurately determine necessary sight distances amidst the complexities of road curves, grades, and obstructions. This example underscored the significant

advantages of utilizing such advanced models, particularly their ability to deliver detailed insights into ISD requirements for complex road alignments, a feat unachievable with traditional methods.

However, the sophistication of these models also presents challenges, particularly the need for detailed and accurate input data, and a dependence on computational resources, which could limit accessibility. Despite these challenges, the future of ISD measurement looks promising, with ongoing technological advancements in data collection methods like LiDAR and GIS expected to further refine the accuracy and applicability of these models. There is also potential for future research to explore integrating real-time data, allowing for dynamic adjustments to ISD calculations in response to changing environmental conditions, thereby advancing road safety measures.

2.2.2 GIS and LiDAR Data Integration for Sight Distance Measurement

An increasing number of studies highlight the integration of GIS and LiDAR data to conduct comprehensive ISD analysis, which offer significant advantages over traditional methods of mathematical analysis models and manual field work.

A study by Castro et al. (2011) leveraged GIS alongside LiDAR data to offer a nuanced methodology that accounts for detailed terrain models and obstacles, such as trees and buildings, which traditional methods often overlook. This approach is instrumental for existing highways lacking design data, employing GPS data to estimate highway alignments—a methodology that proves both practical and reliable for sight distance analysis. The 2014 study by Castro et al developed a GIS-based system, utilizing a trajectory defined by points from a global navigation satellite system (GNSS) receiver, thereby bypassing the need for project-specific information. This system, equipped with tools for identifying 3D alignment issues, significantly contributes to the field by offering a streamlined process for sight distance calculations, with its effectiveness validated through application to a case study.

The transformative potential of employing 3D virtual environments and high-resolution LiDAR data for ISD analysis was highlighted by Jung et al. in the 2018 study. This methodology, demonstrated through a case study in Corvallis, Oregon, not only enhances the precision of sight distance assessments but also introduces adaptability to different vehicle types and movements, thereby setting a new standard for ISD measurement accuracy and efficiency. In parallel, the 2021 study by Kilani et al. introduces an automated method for analyzing ISD in urban environments using mobile LiDAR technology. This novel approach excels in detecting and visualizing obstructions from a driver's perspective, offering a significant leap in the efficiency and accuracy of ISD evaluations.

Similarly, S. A. Gargoum et al. (2021) presents an automated method for assessing sight distance limitations on highways using mobile LiDAR scanning. This method exemplifies the integration of advanced technologies in road safety evaluations, showcasing the ability to automatically identify and classify various obstruction types without fieldwork.

While previous studies have demonstrated the transformative potential of integrating GIS and LiDAR for ISD analysis, significant gaps remain. Past methodologies often focus on specific

applications, such as estimating highway alignments (Castro et al., 2011, 2014) or detecting obstructions in controlled environments (Jung et al., 2018; Kilani et al., 2021) without providing a comprehensive framework adaptable to diverse intersection types or region-specific conditions. These studies also lack calibration to local contexts, such as Alabama's unique traffic patterns and geometric characteristics, and often overlook critical safety performance metrics, such as crash frequency.

2.2.3 Technological Innovations in Sight Distance Evaluation

Traditional methods, while effective to an extent, often fall short in capturing the comprehensive dynamics of modern roadways, particularly in three-dimensional environments. The advent of advanced computational models, GIS, and LiDAR technologies has opened new avenues for precise and comprehensive ISD evaluations, addressing both horizontal and vertical road curvatures and incorporating detailed models of road surfaces and obstructions. This review explores several key studies that have contributed innovative methodologies and frameworks to the field, displaying the evolution of ISD measurement techniques and their implications for road safety.

The 2006 study by Nehate et al. introduced a groundbreaking model for determining ISD using GPS data, marking a departure from traditional two-dimensional analyses. By employing cubic B-splines for road surface and obstruction modeling, this methodology enables detailed evaluations of ISD on 3D combined horizontal and vertical alignments. Verified across Kansas highways, including Highway K-177, this approach has been encapsulated in software, providing a practical tool for transportation departments.

Jha et al.'s 2011 paper presented a novel 3D design methodology for accurately calculating sight distances on highways. This methodology, accounting for the interplay of horizontal and vertical road alignments, overcomes the limitations of existing two-dimensional approaches. By allowing early design simulations to identify and rectify inconsistencies, this approach ensures the adequacy of ISD from a comprehensive 3D perspective, aligning with the objective of developing a GIS tool for ISD measurement using LiDAR data.

The 2021 study by Agina et al. introduced an automated method for assessing PSD on rural highways using mobile LiDAR data. This methodology significantly enhances road safety analysis by precisely identifying passing-allowed zones and proposing enhancements to extend safe passing zones. Further validated by a safety analysis correlating PSD limitations with collision data, this approach exemplifies the integration of advanced technologies in comprehensive road safety evaluations. Similarly, the 2018 study by S. A. Gargoum et al. displays an innovative approach to sight distance evaluation on highways, utilizing mobile LiDAR data for a more efficient and accurate assessment. This method automates the process by leveraging 3D point cloud data to calculate SSD and PSD, identifying obstructions without the need for traditional field measurements. Applied to Alberta, Canada's highway segments, the algorithm successfully pinpointed areas failing to meet minimum sight distance requirements, aligning with collision data and demonstrating the tool's potential for enhancing road safety.

The study by Ma et al. (2021) developed a comprehensive framework for detecting obstacles that restrict 3D highway sight distance using Mobile Laser Scanning (MLS) data. This research utilized a MATLAB-based framework employing linear index-based segmentation and similarity-and-connectivity-based methods for efficient and reliable obstacle detection, overcoming challenges like vehicle noise and data gaps. Demonstrated through real-world highway tests, this framework significantly enhances sight distance evaluations' efficiency and accuracy, marking a notable improvement over traditional method.

Kilani et al. (2021) introduced an innovative automated method for assessing sight distances at urban intersections, utilizing mobile LiDAR data to identify visibility obstacles efficiently. This approach correlates limited sight distances with increased collision risks, providing transportation agencies with a framework to address visibility hazards proactively. Highlighting the potential of mobile LiDAR for urban road safety, this study aligns with the present objectives to enhance ISD measurements.

The 2022 study by Quan et al. introduced a novel method using Google Earth for measuring sight distance at unsignalized intersections for median U-turns on multilane divided highways. By employing Google Earth and Kinovea software, this approach offered a safer and more efficient alternative to field measurements. Validated through field comparisons, this innovative method underscores the potential of leveraging accessible technology for enhancing the accuracy and practicality of ISD measurements.

The review of technological innovations in sight distance evaluation highlights advancements in methodologies and frameworks that enhance ISD measurements and road safety evaluations. These advancements, driven by advanced computational models, GIS, and LiDAR technologies, offer precise evaluations in three-dimensional environments. Key methodologies include automated assessments using mobile LiDAR and MLS data, overcoming traditional limitations. Additionally, novel approaches, such as utilizing Google Earth for ISD measurements, provide safer and more efficient alternatives. Overall, these innovations provide a foundation for this project's objective of developing a GIS tool for ISD measurement using LiDAR data, contributing to more accurate and comprehensive road safety evaluations.

2.3 Impact of ISD on Road Safety

The section is critical for understanding the relationship between ISD and traffic safety. As the second objective of the proposed project entails employing a developed GIS tool for ISD measurement at unsignalized intersections and analyzing the correlation between ISD and crash frequency using historical crash data, this literature review section forms the backbone for establishing the empirical and theoretical grounds for the study. The purpose here is two-fold: firstly, to summarize findings from various research studies that link inadequate ISD to increased crash rates and severity at intersections, thereby highlighting the critical role of ISD in ensuring road safety. Secondly, to discuss theoretical frameworks that support the study of ISDs impact on traffic safety, offering a conceptual basis for the research. This introduction aims to set the stage for a detailed exploration of how ISD directly influences driver behavior, decision-making

processes, and the safety of road users at intersections. By examining empirical studies and theoretical frameworks, this section seeks to underscore the importance of accurate ISD measurement and analysis as essential components in the design and implementation of safety improvements at unsignalized intersections.

2.3.1 Empirical Evidence Linking ISD to Road Safety

Glennon (1987) provides a critical review emphasizing the vital relationship between ISD and road safety, focusing on SSD and ISD as defined by AASHTO since 1940. Glennon underscores the significance of adequate sight distance in preventing collisions with unexpected obstacles, advocating for low-cost improvements such as removing roadside obstructions to enhance road safety. Despite a scarcity of direct studies linking SSD and ISD with crash rates, Glennon highlights key research indicating a reduction in crashes with improved SSD, particularly at crest curves.

Yan et al. (2004) study delves into the geometric models for calculating ISD at signalized intersections, revealing insights into the relationship between ISD and road safety. They emphasize how obstructions from opposing left-turn vehicles can impede sight distance, increasing the risk of accidents and intersection delays. Yan et al. offer geometric models for ISD analysis and suggest design improvements to enhance sight distance, aligning closely with the objective of developing a GIS tool for ISD measurement using LiDAR data.

Liu et al. (2010) analyze the impact of ISD on vehicle speed at intersections, demonstrating how larger static sight distances correlate with higher velocities for turning vehicles and lower speeds for vehicles proceeding directly through intersections. Their findings emphasize the importance of adequate ISD in enabling safe maneuvering decisions at intersections, reinforcing the theoretical framework linking ISD with traffic safety outcomes.

Himes et al. (2016) investigate the correlation between ISD and safety at unsignalized intersections, analyzing data from various states to quantify the impact of ISD on crash frequency. They find that improving ISD can lead to safer intersections, introducing a CMF for ISD that provides a quantitative basis for assessing the safety effects of ISD improvements.

These studies collectively provide empirical evidence supporting the critical impact of ISD on road safety, particularly at intersections. The findings underscore the importance of adequate ISD in reducing crash frequencies.

2.3.2 Methodological Approaches to ISD Measurement and Analysis

Kilani et al. (2021) study focuses on evaluating ISD design in urban road contexts, stressing the importance of providing adequate ISD for safe intersection operation. Utilizing mobile LiDAR point cloud data, Kilani develops a fully automated method for assessing visibility at intersections, identifying obstacles and quantifying their impact on drivers' visual fields. His research also explores the relationship between collision occurrences and limited distances through a safety-

based assessment using the LiDAR dataset, employing the Empirical Bayesian technique for analysis.

The study by Himes et al. (2018) provides a detailed examination of the safety impacts associated with ISD at unsignalized intersections. Through data collection across three states, the research quantifies the relationship between ISD and safety, revealing a nonlinear relationship where decreasing ISD correlates with an increase in target crashes. The methodology employed in this study, leveraging regression models to analyze the ISD-crash frequency relationship, informs the development of the GIS tool, ensuring its empirical and theoretical grounding.

Osama et al. (2016) introduce a reliability analysis framework to evaluate the risk associated with limited sight distance for permitted left-turn movements at signalized intersections. Their study focuses on obstructing vehicles' impact on ISD, utilizing geometric and traffic video data to assess the probability distributions of input variables for reliability analysis. The findings highlight the considerable risk of non-compliance with the requirements of sight distance, especially when the vehicle is obstructed by a bus.

These methodological studies collectively provide empirical and theoretical foundations for the project's objectives. Kilani's automated method for ISD assessment, coupled with empirical evidence linking ISD to road safety, strengthens the GIS tool's development and application. Insights from Himes, Porter, and Eccles enrich the understanding of ISD's role in intersection safety, guiding targeted ISD enhancement strategies. Additionally, Osama, Sayed, and Easa's reliability analysis framework offers practical approaches to evaluating and improving ISD, contributing to a comprehensive approach to intersection safety.

2.3.3 Design and Safety Improvement Strategies

The study by Ibrahim et al. (2012) introduces a methodology for optimizing highway cross-sections' safety, particularly focusing on horizontal curves with restricted sight distance. Their research utilizes reliability analysis to address uncertainties in design parameters and measure the risk associated with deviations from standard design practices. By employing an optimization approach, the study allows designers to proactively manage safety implications, offering a significant advancement in developing safer road designs.

Schattler et al. (2016) evaluates the effectiveness of modified right-turn lane designs at intersections in improving sight distance and reducing crash rates. Their research provides empirical evidence on how geometric modifications, particularly the right-turn lane approach angle, directly impact road safety by enhancing ISD. Combining crash data analysis with driver behavior observations, the study offers insights into the correlation between improved sight distance and reduced crash rates, reinforcing theoretical frameworks and emphasizing the significance of incorporating advanced technological tools and design modifications in enhancing traffic safety at intersections.

The study by Zhou et al. (2021) evaluates the impact of DSD and geometric alignment on driver performance at freeway exit diverging areas, emphasizing the role of DSD in traffic safety. The methodological approach of combining simulated driving data with driver surveys provides a

robust framework for assessing ISD's impact on traffic safety, supporting the development of more effective design and safety improvement strategies for unsignalized intersections.

These studies collectively contribute to understanding and improving ISD measurement and analysis for traffic safety. They offer empirical evidence, methodological approaches, and practical insights that can help the research propose a more comprehensive and responsive approach to sight-restricted intersections.

2.3.4 Behavioral and Psychological Aspects of ISD

Achtemeier et al. (2019) investigate the effects of restricted sight distances on drivers at simulated rural intersections, offering insights into how ISD impacts driver behavior and road safety. Using a driving simulator, the study varied sight distances and oncoming vehicle speeds to observe drivers' gap acceptance and stress levels. Their findings reveal that shorter sight distances increased drivers' stress and led to the acceptance of smaller gaps between vehicles, potentially increasing accident risks. The study underscores the need for nuanced approaches to ISD optimization, as simply enlarging sight distances may not always yield safety gains.

Morris et al. (2019) delve into optimal sight distances at rural intersections through a comprehensive analysis intertwining driving simulation with subjective driver assessments. Their research evaluates driver performance and psychological responses across varying sight distances and oncoming traffic speeds at simulated rural intersections. The findings highlight the significant impact of extended sight distances on improving driver performance and comfort, manifesting in enhanced safety outcomes. The study's methodology, combining quantitative performance metrics with qualitative assessments of driver stress and comfort, offers insights into ISD's impact on traffic safety and could inform future road design and safety interventions.

These studies provide valuable insights into the behavioral and psychological aspects of ISD, enriching this study's understanding of how ISD influences driver behavior and road safety. Incorporating insights from these studies enhances the theoretical and empirical foundations of the dissertation, guiding the development of effective road design and safety interventions aimed at unsignalized intersections.

2.3.5 Innovative Analytical and Predictive Models

The 2018 study by Eccles et al.provides a comprehensive examination of the safety impacts of ISD at unsignalized intersections. By analyzing data from numerous intersections across three states, the study establishes a quantitative relationship between available ISD and safety, highlighting a nonlinear correlation where decreasing ISD correlates with an increase in target crashes. The study underscores the nuanced interplay between ISD and other road and traffic characteristics, emphasizing the importance of precise ISD measurement and analysis in traffic safety improvement efforts.

Sushmitha et al. (2023) emphasize the influence of ISD characteristics on the safety of uncontrolled intersections, leveraging surrogate safety measures. Their research analyzes ISD

variations' impact on critical conflict rates at six uncontrolled three-legged intersections. Findings indicate that improved ISD correlates with enhanced safety, suggesting a significant reduction in the critical conflict rate with increased sight distance. The methodology aligns with innovative approaches intended for the dissertation, supporting the hypothesis that adequate ISD is critical for reducing crash rates and severity at intersections.

Godumula et al. (2023) explores the safety evaluation of horizontal curves on rural two-lane highways using machine learning algorithms. They introduce a priority-based approach to sight distance improvements and advocate for incorporating uncertainties using reliability analysis. Their methodology, including classical topography and video graphic surveys, provides insights into the relationship between sight distance, vehicle speed, and road safety. The emphasis on stochastic aspects of road design and the application of machine learning algorithms aligns with the dissertation's conceptual basis, supporting the need for a more nuanced and data-driven approach to improving road safety through adequate ISD.

These studies significantly contribute to enhancing the methodological foundation for ISD analysis in traffic safety research. Incorporating these methodological advancements into the dissertation enhances its theoretical and practical contributions, guiding the development of effective road safety interventions based on precise ISD analysis methods.

3 DATA COLLECTION

This section outlines the data collection process essential for analyzing ISD at unsignalized intersections in Alabama, focusing on the acquisition of LiDAR data, crash data, and intersection-specific details. The LiDAR data, provided by Alabama Department of Transportation (ALDOT) using the Velodyne HDL-32E system, covers 366 intersections across 53 counties and offers high-resolution spatial information to capture road geometry and visibility obstructions. Additionally, historical crash data from 2018-2022 was obtained through the Critical Analysis Reporting Environment (CARE) software, focusing on intersection-related crashes within a 250-foot radius and filtered to include ISD-related target crashes. Detailed intersection information, such as lane configurations, turn treatments, and traffic volumes, was also collected to assess how these features impact ISD and crash risk.

3.1 Intersection Information

To study the impact of ISD on traffic safety at TWSC intersections, with the support of the ALDOT Maintenance Office, location information for all stop-controlled intersections within Alabama's state highway network was obtained and selected as potential study sites. Both the major and minor roads at these intersections belong to the Alabama State Highway system. The distribution of all intersections is shown in **Figure 2**.

Initially, ALDOT provided location data for 366 TWSC intersections within its jurisdiction, which formed the basis for this study. These intersections represent all stop-controlled intersections. A GIS database was created from this data and reviewed using Google Earth and Street View to assess whether they met the study criteria. The review revealed that 94 of these intersections were either all-way stop-controlled (AWSC) or had been updated to signal-controlled intersections; these were excluded from the study.

Next, the completeness of the LiDAR point cloud data for the study locations was analyzed. Since the point cloud data was collected using MLS mounted on survey vehicles, the coverage directly affected the data completeness. The review found that 25 intersections had point cloud data that only covered parts of the major road sections, rendering the data incomplete. As illustrated in **Figure 3**, the light blue shaded area represents the available LiDAR data coverage, while the red stop sign marks the TWSC intersection location. This figure highlights an example of incomplete data coverage, where the LiDAR data does not fully extend to the surrounding major road segments. Consequently, such intersections were excluded from the study.

Additionally, the availability of Average Annual Daily Traffic (AADT) data for the intersections was critically reviewed. Each intersection considered for the analysis required available AADT data for both the major and minor roads. For four-leg intersections, the AADT data for the major road and at least one approach of the minor road needed to be available, otherwise, the intersection did not meet the study requirements. After this screening process, the review indicated that 18 intersections were excluded from the study (**Figure 4**). The remaining 230 intersections were included in the final analysis. **Table 1** summarizes the reasons for excluding

intersections from the study and provides the corresponding proportions relative to the total number of initially selected intersections.

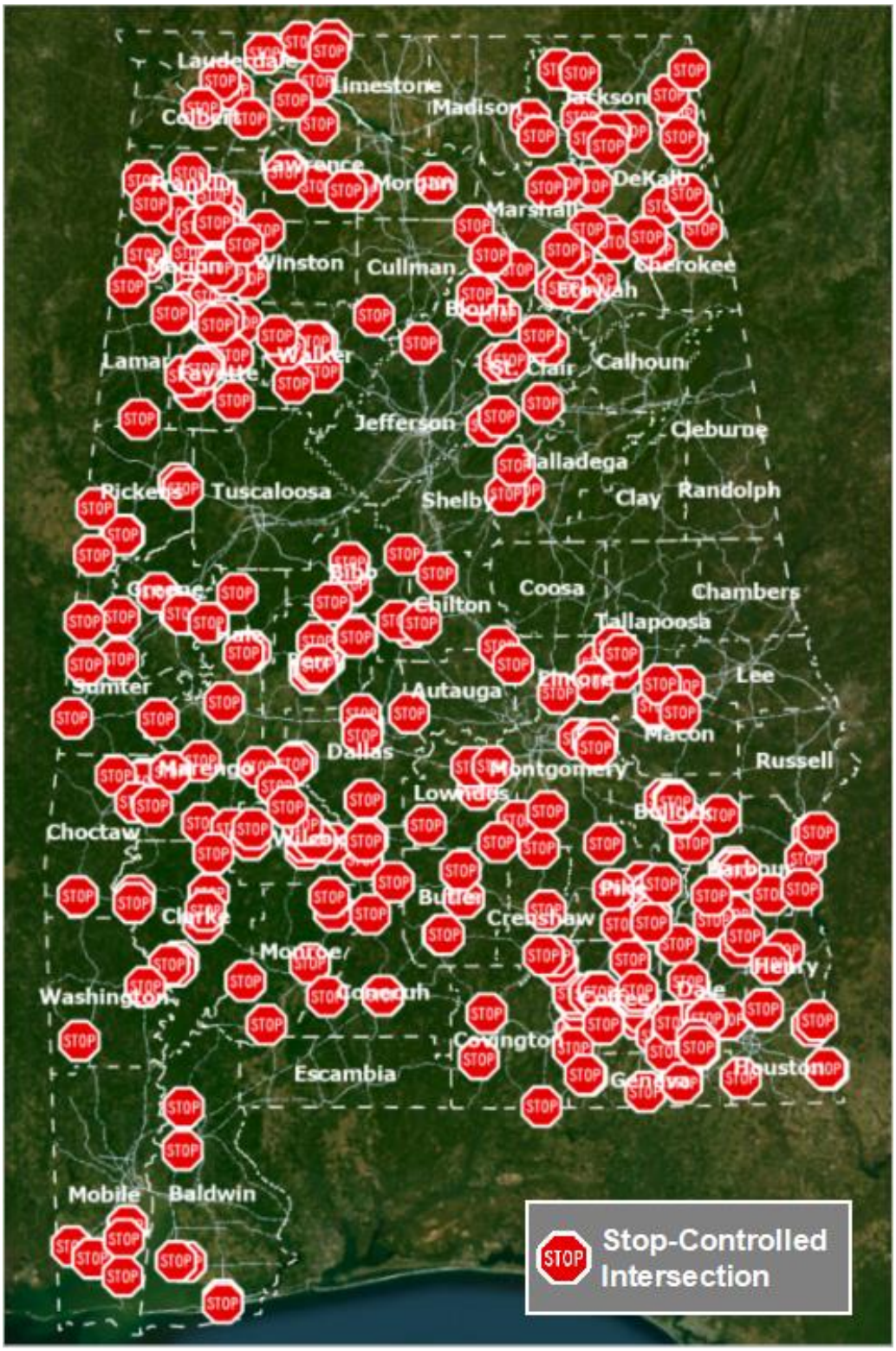

Figure 2 Locations of All the Candidate Intersections

Figure 3 Intersection with Incomplete LiDAR Data

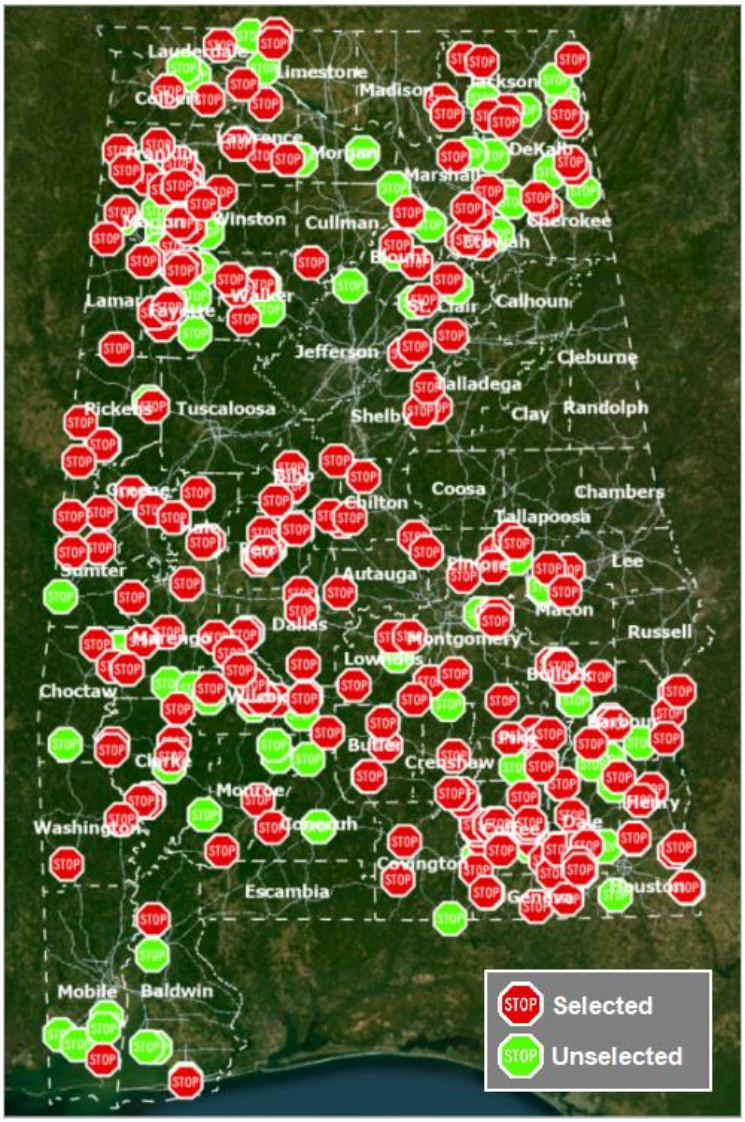

Figure 4 Locations of Selected Intersections and Unselected Intersections

Table 1 Summary of Excluded Intersections and Reasons for Exclusion

Reason for Exclusion	Number of Intersections	Proportion (%)
AWSC or Signalized Update	94	25.68
Incomplete LiDAR Data Coverage	25	6.83
Unavailable AADT Data	18	4.92
Total Excluded Intersections	**137**	**37.43**
Total Retained for Analysis	**230**	**62.57**

The selected study intersections exhibit a diverse range of characteristics, including three-leg (3ST) intersections, four-leg (4ST) intersections, and intersections with skew angles. Although previous studies have indicated that intersections with angles less than 90 degrees can affect safety (Harkey et al., 2021; Kumfer et al., 2019), this study aims to comprehensively analyze the impact of ISD on intersection safety under various conditions. Therefore, intersections with skewed or unusual alignments are included in the study, and these factors will be considered in the safety analysis. Additionally, the lane configurations of the major roads at the study intersections were recorded as potential factors influencing traffic safety. This includes the number of through lanes on the major road, the types of right-turn lanes, the types of left-turn lanes, and the presence of acceleration lanes for vehicles turning left or right from the minor road (Harwood et al., 2003).

The types of left-turn lanes were categorized into three types (**Figure 5**):

- **Left Turn Type 1 :** No left-turn lanes
- **Left Turn Type 2 :** Left-turn channelization defined by raised (curbed) or depressed median
- **Left Turn Type 3 :** Painted left-turn channelization (no median or flush median)

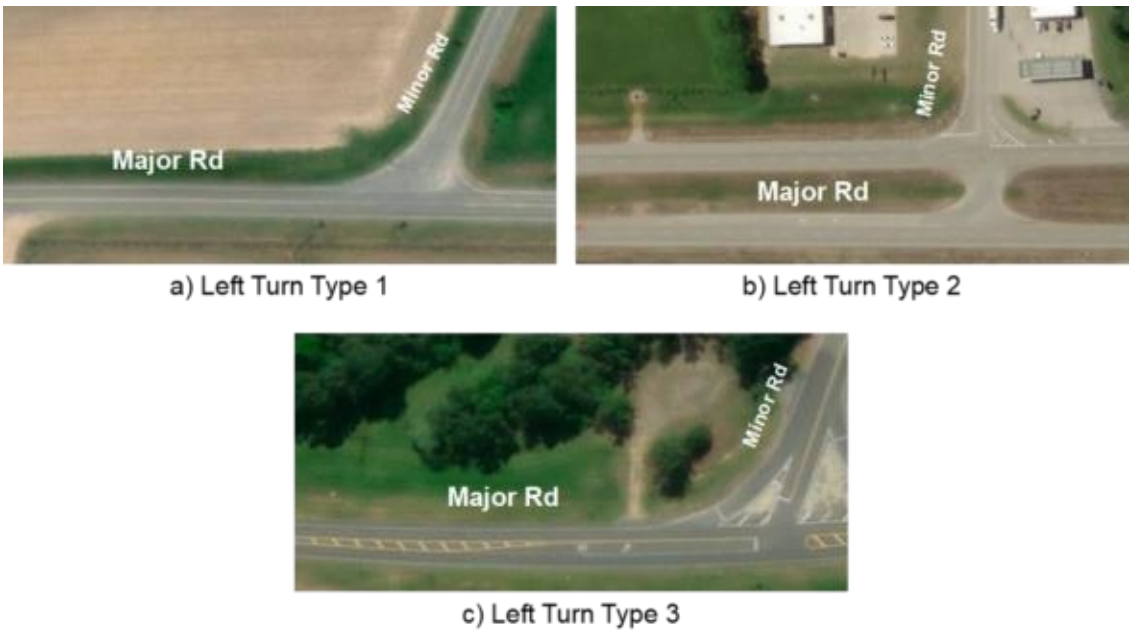

Figure 5 Type of Left-turn Treatment

Similarly, the types of right-turn lanes were classified into four categories (**Figure 6**):

- **Right Turn Type 1:** No right-turn lanes
- **Right Turn Type 2:** Right-turn roadway created by a channelizing island without an exclusive right-turn lane upstream of it (i.e., traffic entered the right-turn roadway from a shared lane used by both through and right-turning traffic)
- **Right Turn Type 3:** Right-turn roadway created by a channelizing island with an exclusive right-turn lane upstream of it (i.e., traffic entered the right-turn roadway from an exclusive right-turn lane)
- **Right Turn Type 4:** Conventional exclusive right-turn lane with no channelizing island.

Figure 6 Type of Right-turn Treatment

These detailed lane configurations were documented to ensure a comprehensive analysis of the various factors that may influence the safety performance of the intersection. These configurations were examined to analyze their impact on ISD-related crash frequency.

Obtaining AADT data is essential for developing a statistical road safety model that accurately reflects the safety conditions of these roads. This data was obtained from the Alabama TDM Public open-source database (Alabama Department of Transportation, 2024) managed by ALDOT, ensuring both credibility and relevance. The dataset is derived from three distinct types of traffic count stations:

- **Permanent:** Permanent counter sites are the Continuous Count Stations located around the state. The sites monitor traffic all year round by utilizing a variety of different sensors (i.e., inductive loops, radar, infrared detection, etc.).
- **Portable:** Portable counter sites collect short duration vehicle classification and/or volume counts. The count duration is typically either 48 continuous hours that will incorporate 2 or 3 days depending on when placed or 168 continuous hours that will incorporate 7-8 days depending on when placed. Every attempt is made to collect traffic data at these locations on a minimum three-year cycle.
- **Virtual:** Virtual counter sites do not actually exist. They represent a section of roadway and contain data collected and transferred from an adjacent site on the route. These counters typically exist at County lines.

For intersections with two Major Road approaches that have different AADTs, the higher AADT of the two is used to represent the AADT for the Major Road (TRB, 2008). Similarly, for intersections with two Minor Road approaches with different AADTs, the higher AADT is used for the Minor Road in intersection-level analyses. In approach-direction level analyses, the specific AADT for the corresponding Minor Road approach is used. If AADT data for a particular approach is unavailable, that approach is excluded from the analysis. This approach helps to avoid interference in the analysis caused by significant differences in AADT between Minor Road approaches within the same intersection.

Table 2 summarizes the data elements of interest used in the study, categorizing them by their description and corresponding data sources. The data elements include key intersection characteristics such as location, traffic control type, intersection legs, speed limits, and turn lane treatments.

Table 2 Data Elements for Intersection Study

Data Element	**Description**	**Data Source**
Location	Geographical coordinates of study the intersection	ALDOT
Traffic control	Type of traffic control (e.g., AWSC, TWSC)	ALDOT; Street View
Num of Legs	Number of intersection legs	Street View
Posted Speed Limit	Speed limit of Major Rd	Street View
Num of through lanes	Number of through lanes on Major Rd	Street View
Median Width	Width of the median at the intersection	Arc GIS Pro
Grade of Approach	The grade of the approaching roads	Proposed Method
Skewed Angle	The angle between the intersecting roads that deviates from 90 degrees	Proposed Method
Left Turn Treatment	Type of left-turn lanes	Street View
Right Turn Treatment	Type of right-turn lanes	Street View

Data Element	Description	Data Source
Major Rd AADT	Average Annual Daily Traffic on the major road	ALDOT
Minor Rd AADT	Average Annual Daily Traffic on the minor road	ALDOT
Left Available ISD	Available ISD to the left	Proposed Method
Right Available ISD	Available ISD to the right	Proposed Method

3.2 Crash Data

For the second phase of this study, which examines the impact of sight distance on road safety, obtaining historical crash data for the selected intersections was essential. To facilitate this, a confidentiality agreement was signed with the ALDOT, granting access to all crash reports within Alabama for the years 2018 through 2022. This period's data encompasses a substantial volume of records: 160,163 for 2018, 159,125 for 2019, 134, 212 for 2020, 151, 954 for 2021, and 144, 256 for 2022. The source of this historical crash data is the CARE, an advanced data analysis software engineered by the Center for Advanced Public Safety (CAPS) at the University of Alabama (Parrish et al., 2003). CARE is specifically tailored for extracting critical insights within the traffic safety domain, facilitating the identification of issues and the formulation of effective countermeasures. Renowned for its speed and analytical prowess, CARE can process and analyze millions of records swiftly, equipped with extensive filtering capabilities to sift through vast datasets.

Each historical crash record in the CARE database contains 235 described variables encapsulating detailed insights into traffic incidents. This dataset is foundational for analyzing traffic crash dynamics, structured across various levels to provide a holistic view of each crash. These variables are categorized into several key areas:

- Administrative Details: Include case numbers and basic administrative data essential for record-keeping and identification purposes.
- Geographical Information: Encompasses precise crash locations (latitude and longitude), dates, times, counties, and cities, providing a spatial and temporal context to each incident.
- Unit Descriptions: Differentiate between involved units (vehicles and non-motorists), detailing vehicle types, commercial vehicle indicators, and specific actions leading up to the crash.
- Driver and Non-Motorist Data: Cover a wide range of information including demographics, licensing details, condition at the time of the crash, and involvement in the incident.
- Vehicle Information: Offers insights into vehicle specifics such as make, model, year, ownership, registration, usage, and the extent of damage resulting from the crash.
- Crash Dynamics and Circumstances: Investigate the environmental conditions, road surface types, and a detailed sequence of events that describe the crash dynamics.

- Environmental and Investigative Factors: Include factors present at the crash site and details from the crash investigation process (witness statements and investigator notes).

The geographical information, driver behaviors, vehicle characteristics, and environmental conditions allowed for an analysis of how ISD influences road safety. By correlating specific variables such as crash location, crash type, and severity with ISD measurements, the study could perform a quantitative analysis of the impact of ISD on crashes.

3.2.1 Intersection Related Crashes

Crashes occurring within a 250-foot radius around the selected intersections are classified as intersection-related, as supported by previous studies (Tegge et al., 2010; Torbic et al., 2021). The choice of a 250-foot cutoff point is consistent with established research and reflects a reasonable balance between including crashes influenced by the intersection and excluding those unrelated to its operation. This distance accounts for typical vehicle interaction zones where conflicts between vehicles from major and minor roads are likely to occur. However, the specific range for defining intersection related crashes can vary based on the unique characteristics of each intersection and the surrounding roadway environment.

To ensure accuracy in identifying relevant crashes, the Conflict Point for each intersection is first determined based on the alignment of the Major Road and Minor Road, serving as a central reference point. Using this Conflict Point, a 250-foot radius impact area is delineated. **Figure 7** visually illustrates this process, highlighting the Conflict Point and the corresponding 250-foot radius impact area.

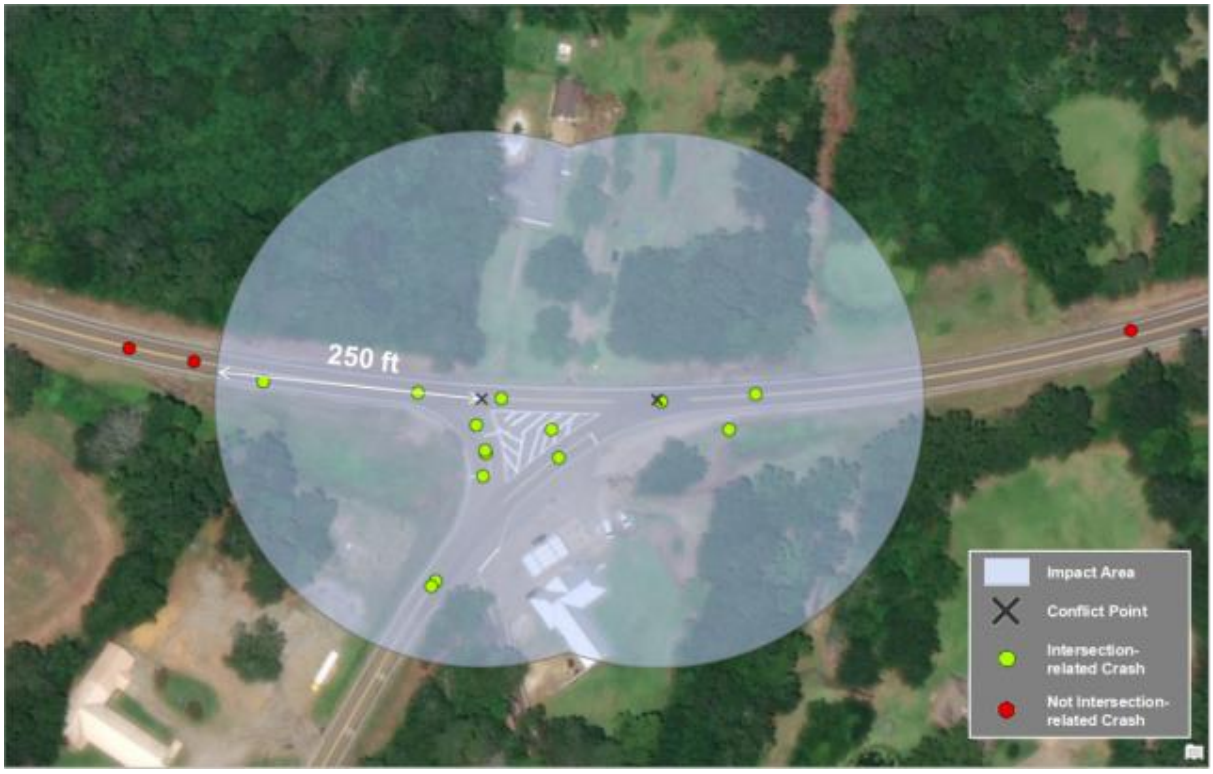

Figure 7 Illustration of Selecting Intersection-related Crash

3.2.2 Target Crashes (ISD-related Crashes)

Previous studies analyzing the impact of ISD on intersection safety have not always used all intersection-related crash data to calculate crash frequency (Eccles et al., 2018). Instead, some studies have filtered a specific type of crashes, termed "Target Crashes," from the broader set of intersection-related crashes to focus on those most relevant to ISD. Target Crashes are defined as those occurring within the intersection's impact area and involving vehicles traveling from both the Major Road and the Minor Road.

To identify Target Crashes, this study first filters out records from the intersection-related crash data that do not meet the criteria for Target Crashes. The filtering rules are as follows:

- Retain only records where the "First Harmful Event" attribute is "Collision with Vehicle in (or from) Other Roadway" or "Collision with Vehicle in Traffic," thereby excluding incidents such as collisions with animals or trees, run-off-road crashes, or overturn/rollover events.
- Exclude records where the "Manner of Crash" attribute is "Rear End (front to rear)," "Head-On (front to front only)," "Unknown," "Causal Veh Backing: Rear to Rear," or "Causal Veh Backing: Rear to Side," to eliminate crashes that do not involve vehicles from both the Major Road and the Minor Road.
- Exclude records where the "Number of Vehicles" attribute is "1 Vehicle," as single-vehicle crashes are not considered Target Crashes.

- Exclude records where the “Vehicle Initial Travel Direction” attribute is “Not on Road,” as these crashes do not occur within the designated roadway.
- Exclude records where the “Vehicle Maneuvers” attribute is “Changing Lanes,” as such crashes typically involve vehicles traveling on the same road (either the Major Road or the Minor Road), rather than between the two.
- Exclude records where the “Trafficway Lanes” attribute is “Not Applicable (Parking Lot),” as these crashes occur in parking lots rather than on the Major Road or Minor Road.

Out of 1,424 intersection-related crashes, a total of 1,034 crashes were removed through the above filtering rules. After completing the initial filtering based on crash attributes, this study also involved a manual review of each crash record. During this manual review process, 42 additional crashes were excluded due to inconsistent or unclear data attributes, leaving 348 crashes identified as ISD-related Target Crashes. This step was necessary because reporting practices may vary between agencies or practitioners, and there could be data entry errors. Researchers carefully examined multiple attributes and the location of each crash to determine whether it truly qualifies as a Target Crash. Additionally, the specific approach on the Minor Road where the vehicle was located, and whether the vehicle on the Major Road was to the left or right of the Minor Road vehicle, were recorded. This information is crucial for distinguishing crashes influenced by left-side ISD from those influenced by right-side ISD.

3.3 Light Detection and Ranging data

Light Detection and Ranging (LiDAR) data is the basis of this research, which is being used to improve ISD measurements and provide accuracy and detail of terrain and obstacles (S. Gargoum et al., 2017). This technology measures distance by illuminating a target with laser light and analyzing the reflected pulses with a sensor. Differences in laser return times and wavelengths are then used to make digital 3D representations of the target. To develop GIS tools for assessing ISD using LiDAR data, understanding key LiDAR parameters is critical for achieving the desired outcomes. Each parameter plays a pivotal role in ensuring the data collected is of high quality and suitable for detailed analysis of road safety at unsignalized intersections (Mehendale et al., 2020).

Point density is one of the most significant parameters, as it refers to the number of data points captured per unit area by the LiDAR system. High point density provides more detailed information about the environment, which is essential for accurately identifying critical features such as road edges, obstacles, and other elements that may obstruct the sight distance at an intersection. In complex intersection environments, a higher point density allows for better detection of subtle obstructions or minor road details that could impact ISD. However, with higher point density comes the challenge of managing larger datasets, which requires more storage and computational resources. Balancing point density to ensure sufficient detail without overwhelming data processing capabilities is key to effective ISD analysis.

The scan angle is another important parameter, as it determines the extent of the environment that can be captured in a single scan. A wide scan angle allows the LiDAR system to cover a broader area, which is particularly beneficial in capturing the full scope of an intersection,

including peripheral objects that might affect the sight distance. For example, a wider scan angle can help identify vehicles, pedestrians, or road signs that are located on the outskirts of the intersection but still influence the driver's line of sight. However, a broader scan angle can also result in reduced accuracy at the edges of the scan, where data points may become less dense and more prone to distortion. Therefore, selecting an appropriate scan angle is essential to ensure that the data collected is both comprehensive and precise.

For this study, the LiDAR data essential for analyzing ISD were supplied by ALDOT, which collected LiDAR data across various regions of Alabama. Given the diversity in acquisition parameters across these datasets, a critical aspect of the project is to account for these differences to ensure that the developed GIS tool remains compatible and adaptable with varied datasets. The data was gathered using the Velodyne HDL-32E sensor, which maintains high-resolution capabilities and reliability in demanding real-world conditions (Mapix Technologies, 2024). The HDL-32E features 32 lasers distributed across a 40° vertical field of view, capturing up to 1.4 million points per second to generate dense point clouds, which are crucial for analyzing road environments, including subtle elevation changes, road edges, and potential sight obstructions.

Its range accuracy of less than 20 mm ensures precise measurements, minimizing errors in ISD calculations, where even minor discrepancies could lead to significant misjudgments. Additionally, the HDL-32E's 360° horizontal field of view enables comprehensive coverage of intersections in a single pass, capturing critical features like signs, barriers, and vegetation that might obstruct a driver's sightline. The sensor's dual return mode further enhances its ability to distinguish between various surfaces, making it particularly effective for identifying objects such as overhanging foliage. With a range of up to 100 meters, the Velodyne HDL-32E is ideally suited for capturing detailed spatial data across large intersection areas, making it an excellent choice for ISD assessments in this research.

A total of 366 study intersections, distributed across 53 counties in Alabama, were included in the LiDAR data request. The requested data covers an area with a 6-mile radius centered around each intersection. The locations of the study intersections and the corresponding LiDAR data coverage areas are illustrated in **Figure 8**.

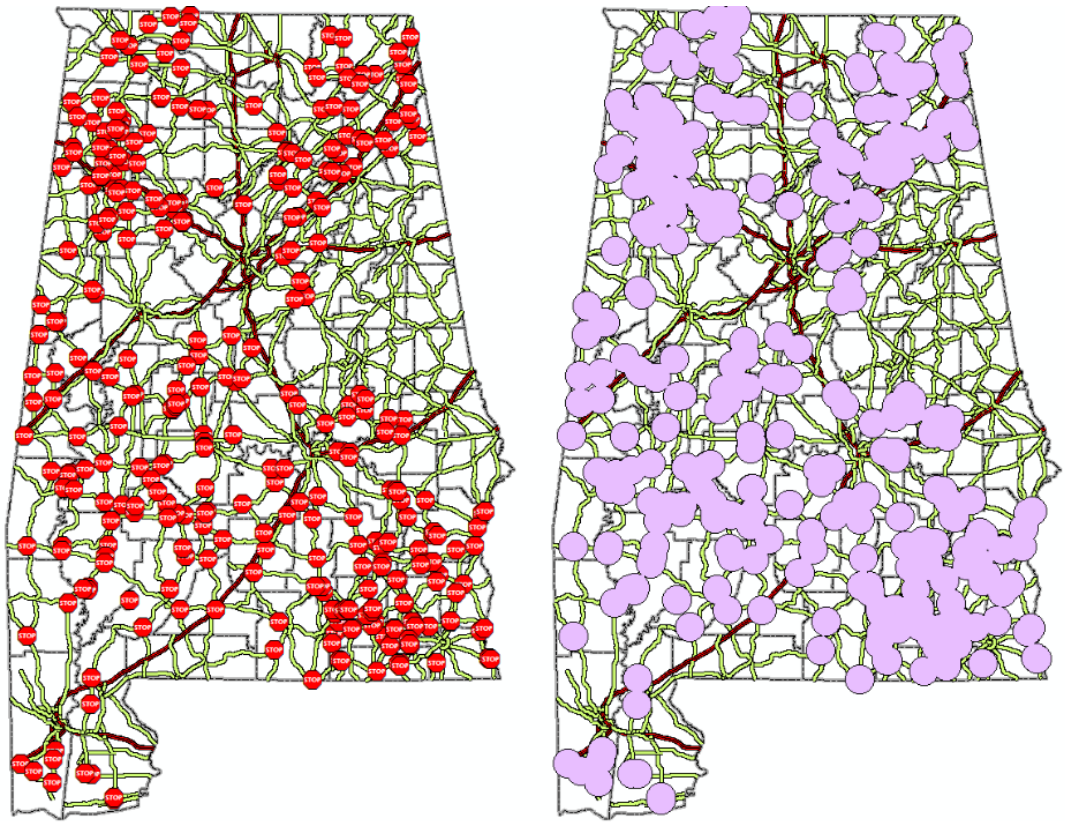

a) Location of study intersections b) Requested LiDAR data area

Figure 8 Study Intersection Locations and Requested LiDAR Data in Alabama

4 ISD ASSESSMENT TOOLS DEVELOPMENT

This section introduces the development of an automated ISD assessment tool using LiDAR data for TWSC intersections. The tool is designed to achieve accurate and efficient ISD evaluations through several key processes, including LiDAR data processing via voxelization to simplify the point cloud, classification of road features, and noise removal. The tool calculates the recommended ISD based on the AASHTO Green Book guidelines (AASHTO, 2018), considering factors such as road speed, lane configuration, and vehicle types. The results are visualized in ArcGIS Pro, offering clear representations of ISD and visibility blockages to help transportation agencies make data-driven decisions for intersection safety improvements.

The section also presents a comprehensive application of the proposed ISD assessment method across diverse intersection scenarios, evaluating its adaptability, robustness, and accuracy when applied to different measurement standards and vehicle types. It emphasizes the tool's ability to compare ISD for passenger cars and trucks, showcasing its capability to handle varying vehicle characteristics. Additionally, the section discusses the limitations of the proposed method, highlighting areas where the tool may require further refinement or where additional factors may need to be considered in future studies.

4.1 Methodology

The methodology for developing the ISD assessment tool involves a comprehensive process that integrates advanced LiDAR data processing with custom-built algorithms. The process begins with the preparation of high-density LiDAR data, followed by a series of steps that include voxelization, classification, and noise reduction to refine the dataset. The workflow further involves generating user-defined observer and target points, constructing lines of sight, and conducting visibility analysis to calculate recommended ISD and blockage rates. The tool is implemented in Python and visualized using ArcGIS Pro, with validation against established transportation standards, including state-specific Department of Transportation guidelines from Alabama and other states.

4.1.1 Data Sources and Preparation

The ISD assessment method begins with the collection and preparation of LiDAR data, which is provided by the ALDOT and collected using the Velodyne HDL-32E laser scanning system. This high-density point cloud data is essential for capturing detailed spatial information of the intersection areas under study. The preparation phase involves the extraction of relevant data points and the reduction of noise to ensure that only stationary objects, which are critical for sight distance analysis, are retained.

4.1.2 Development Environment

The ISD assessment workflow is implemented using Python programming language, with data processing and visualization carried out in ArcGIS Pro 3.3.0. The use of Python allows for the automation of various data processing tasks, enhancing efficiency and accuracy in the analysis. ArcGIS Pro serves as a powerful tool for visualizing the results of the ISD assessment, enabling detailed maps and models to be created that illustrate visibility conditions at intersections.

4.1.3 Workflow

The development of the ISD assessment tool involves a comprehensive multi-step methodology that leverages advanced LiDAR data processing techniques. The workflow used to develop the ISD assessment tool is visualized in **Figure 9** providing a detailed representation of the entire process of developing the tool.

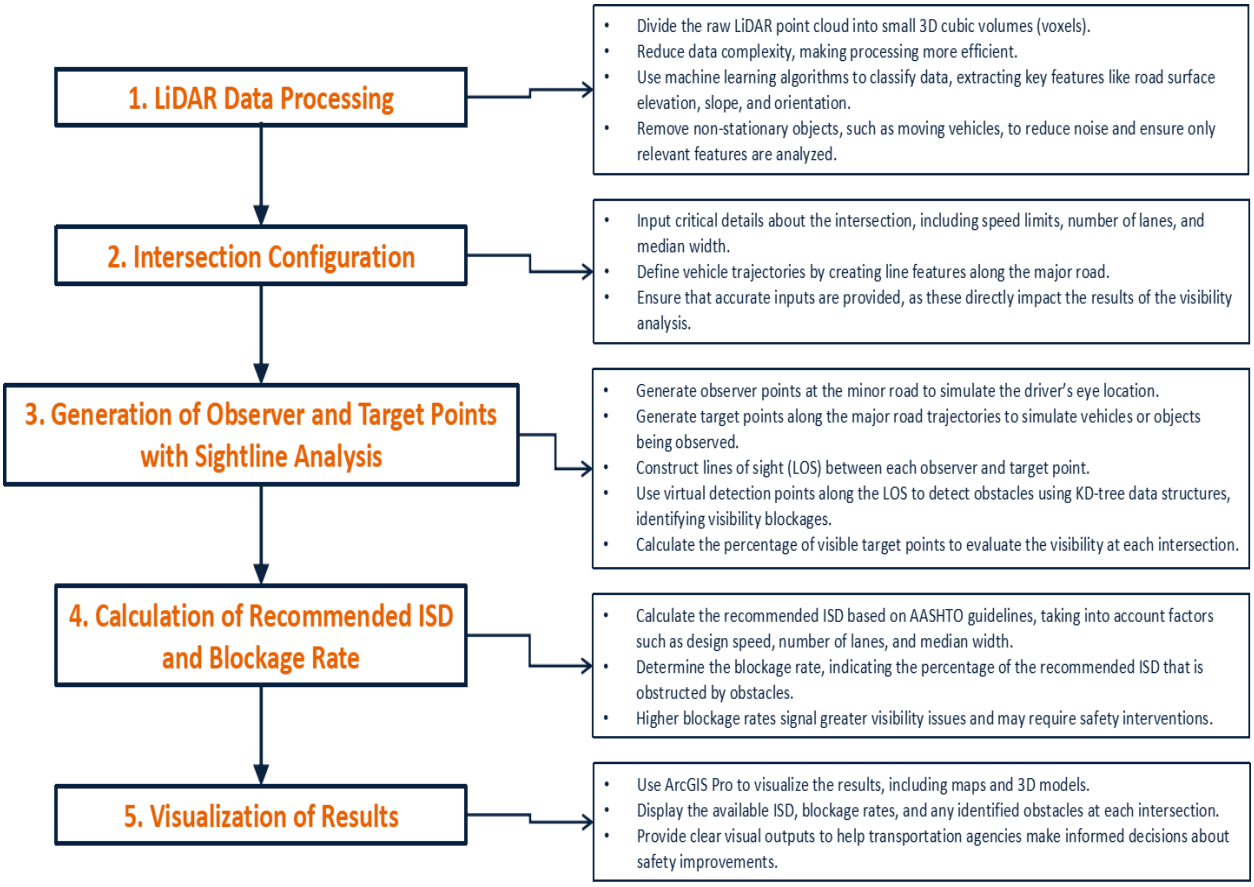

Figure 9 Workflow of ISD Assessment Tool

The workflow begins with voxelization of the raw LiDAR point cloud data. This step breaks the data into a three-dimensional grid of small cubic volumes known as voxels. During this process, the spatial domain is divided into uniform cubic cells, each representing a fixed unit of space within the LiDAR data's coverage area. For this study, the voxel size is set to 0.5 meters,

which provides a balance between computational efficiency and spatial resolution. Points within each voxel are aggregated, with the centroid or representative point retained for further processing. By voxelizing the data, the number of points needing processing is significantly reduced, which enhances computational efficiency while retaining essential spatial information necessary for the ISD analysis. This reduction not only speeds up subsequent steps like classification and visibility analysis but also simplifies handling large-scale datasets without compromising accuracy.

Following voxelization, the classification of the point cloud data is performed to extract meaningful features relevant to the ISD assessment. Machine learning algorithms and heuristic rules are employed to classify the data, isolating key elements such as the road surface, and determining its elevation, slope, and orientation. During this stage, noises, such as moving vehicles or temporary objects captured during scanning, are filtered out, ensuring that only permanent features are considered in the ISD evaluation. This process significantly enhances the accuracy of the subsequent visibility analysis.

Next, intersection configuration is defined by incorporating user inputs. Users are prompted to input critical information about the intersection, including the speed limit of the major road, the number of lanes, and the width of the median if present. Additionally, users define vehicle trajectories by creating line features along the major road approaches to represent the expected vehicle paths. These inputs are vital, as the accuracy of the ISD analysis depends heavily on the precision of the intersection configuration.

Once the intersection is configured, observer and target points are generated. The observer points represent the driver's eye location on the minor road, while the target points simulate the positions of vehicles or obstacles on the major road that the driver observes when looking for gaps to enter the traffic stream. These points are generated by applying specific offsets from the road edge, lateral positions, and heights, ensuring they conform to standard transportation measurement practices.

With the observer and target points established, the tool then constructs a Line of Sight (LOS) between each observer point and its corresponding target points along the vehicle trajectories. Virtual detection points are placed at regular intervals along the LOS, with the interval size matching the voxel size. A KD-tree (K-dimensional tree) data structure, a binary space-partitioning algorithm for organizing points in a k-dimensional space, is utilized to perform efficient nearest neighbor searches within the point cloud data, identifying any obstacles along the LOS path. In this context, the KD-tree allows the tool to quickly locate and analyze points within the LiDAR dataset that are spatially close to each detection point, significantly improving computational efficiency when processing large-scale datasets. If a detection point falls within an occupied voxel, the LOS is marked as obstructed, indicating a visibility blockage.

The tool calculates the percentage of visible target points for each location, which is then used to assess the overall visibility conditions at the intersection. After the visibility analysis is complete, the tool calculates the recommended ISD based on the AASHTO guidelines, incorporating factors such as the design speed of the major road, lane count, and median width. Additionally, the blockage rate, which represents the percentage of the recommended ISD that is

obstructed, is computed. This metric is crucial for identifying intersections with visibility issues, as a higher blockage rate indicates a greater need for safety interventions.

Finally, the processed data and analysis results are compiled and visualized using ArcGIS Pro. The visual outputs include detailed maps and 3D models that display the available ISD, blockage rates, and identified obstacles for each intersection. These visualizations are essential for conveying the assessment results to transportation agencies and other stakeholders, allowing for informed decisions regarding potential safety improvements at problematic intersections.

4.1.4 Tools Application and Validation

Application and validation of the tools used in the ISD assessment method were conducted to ensure accuracy and reliability. The validation process included manual reviews and 3D model comparisons to confirm that the observer positions and visibility assessments accurately reflected real-world conditions. The results demonstrated the robustness and adaptability of the method across different intersection types and measurement standards, confirming its effectiveness in assessing ISD and identifying potential safety issues at intersections.

4.2 LiDAR Data Processing

The processing of LiDAR data in this study includes three primary objectives: voxelizing the LiDAR point cloud data, classifying the voxelized point cloud data, and removing noise from on-road vehicles. Each step is designed to enhance the accuracy and efficiency of ISD evaluations.

Voxelizing the LiDAR point cloud data aims to improve computational efficiency by reducing data complexity. This process involves dividing the point cloud data into a three-dimensional grid of voxels, with each voxel representing a small cubic volume of the data space. Aggregating points within each voxel simplifies the dataset, significantly reducing the number of points that need to be processed (Shalkamy et al., 2020). In addition, voxelized point cloud data will retain the information of the original data and will not negatively affect object recognition and classification (Aijazi et al., 2013; Castro et al., 2014; Nourian et al., 2016). A critical parameter in the voxelization process is voxel size. Previous studies have indicated that the voxel size should be larger than the spacing between the scan lines of the laser scanning system (Jha et al., 2009; Ma et al., 2022). If the voxel size is too small, it may increase the computational burden and overlook potential obstructions. Conversely, if the voxel size is too large, it may result in off-line targets being misidentified as obstructions. Kilani et al.'s 2021 study tested voxel sizes of 0.1m, 0.15m, and 0.2m for line-of-sight analysis, showing similar trends with only slight variations in offset distance. Considering the balance between computational efficiency and data accuracy, as well as the marginal differences observed between 0.15m and 0.2m in Kilani's results, a voxel size of 0.15m was selected for this study.

The second step is the classification of the voxelized point cloud data to extract meaningful features required for ISD analysis. This classification is typically achieved using machine learning algorithms or heuristic rules that consider the spatial and spectral characteristics of the points. By classifying the data, the road surface can be isolated, allowing for the determination of its elevation,

slope, and orientation. Additionally, during the MLS system scanning process, moving vehicles on the road are often recorded. These vehicles temporarily occupy space and should not be considered permanent obstructions in the ISD evaluation. Therefore, identifying and removing these on-road vehicle data is necessary to obtain more accurate ISD assessment results.

Algorithms for object recognition and classification of point cloud data have been a research topic for the past few decades (Che et al., 2019). This study first references several previous studies on ground classification algorithms to classify and filter ground data from the point cloud (Che et al., 2017; Pingel et al., 2013; Zhang et al., 2016). Che et al. (2017) presents a fast ground filtering method based on Scanline Density Analysis (SDA), which efficiently separates ground points from non-ground points by analyzing the density variation in scan lines, thus improving filtering speed and accuracy. Pingel et al. (2013) introduces an improved simple morphological filter for terrain classification of airborne LiDAR data. This method enhances the applicability and accuracy of morphological approaches in complex terrains, making it more effective for processing large-scale airborne LiDAR data. Zhang et al. (2016) proposes an easy-to-use filtering method based on cloth simulation, which distinguishes ground points from non-ground points by simulating the process of a cloth covering the terrain. This method requires minimal parameter tuning and is widely applicable, making it user-friendly for those with little experience.

After filtering out the ground points, this study further utilizes the algorithm proposed by Ma et al. in 2021, which employs an automatic framework to detect obstacles restricting highway sight distance using MLS data. This framework automatically generates boundaries and extracts pavement data from the ground points, as well as identifies and classifies noise data such as moving vehicles on the road.

The third step focuses on removing noise from on-road vehicles to ensure more accurate ISD assessment results by eliminating temporary obstructions. Data classified as noise will be removed to avoid inaccuracies caused by transient objects. After noise removal, linear interpolation will be applied to fill the gaps in the point cloud data, ensuring the continuity and completeness of the road surface information.

After processing the LiDAR point cloud data, the elevation information of any point of interest on the road surface can be accurately obtained. Assuming the 2D coordinates of a point of interest are (X, Y), and the collection of points classified as roadway in the point cloud data is $\{(x_k, y_k, z_k)|k = 0,1,2, \dots, N-1\}$, the elevation of the point of interest can be determined according to the following **Equations 1, 2,** and **3**.

$$d_k = \sqrt{(X - x_k)^2 + (Y - y_k)^2} \qquad \textbf{Equation 1}$$

$$k^* = \arg\min_k d_k \qquad \textbf{Equation 2}$$

$$Z = z_{k^*} \qquad \textbf{Equation 3}$$

Here, d_k represents the Euclidean distance between the point of interest (X, Y) and each point (x_k, y_k, z_k) in the roadway data. The index k^* corresponds to the point with the minimum distance d_k , and z_{k^*} is the elevation of this nearest point, providing the elevation Z for the point of interest.

4.3 Intersection Configuration

In this process, users need to input various information about the study intersection, including the speed limit of the major road, the number of lanes, and the width of the median. This information will be used to calculate the recommended ISD. Additionally, users should create a line feature along the approaches of the major road to represent vehicle trajectories. This trajectory will be used in later steps to generate target points, representing the positions of conflicting vehicles that a driver on the minor road would observe when looking for an acceptable gap to enter the major road. The accuracy of these positions directly impacts the visibility analysis results. In previous studies, vehicle trajectory extraction has primarily been conducted using two methods:

1. Utilizing the scan angle information from LiDAR point cloud data to plot the trajectory of vehicles as they pass through the intersection. (Agina et al., 2021; S. A. Gargoum et al., 2018, 2021; Kilani et al., 2021; Ma et al., 2021)
2. Using road surface data from the point cloud to locate the centerline, representing the vehicle trajectory. (Jha et al., 2011; Tsai et al., 2011)

While these automated methods can enhance analysis efficiency, they come with certain limitations. For instance, when using LiDAR point cloud data to extract vehicle trajectories, the scanning vehicle may only travel through the intersection from one direction on the major road, failing to travel in both directions. Consequently, the vehicle trajectory will be limited to one approach and exit lane of the main road. However, drivers on the minor road are concerned with incoming vehicles on both approaches of the main road (for left turn and through movements), leading to a mismatch between these trajectories. Similarly, using the centerline of the road surface as the vehicle trajectory can also result in a deviation from the actual trajectory. Such inaccuracies are especially significant on multi-lane highways with wide medians or major roads with horizontal curves, where the measurement error due to trajectory deviation is more evident.

This study proposes a method that allows users to customize the vehicle trajectory based on specific research needs. This flexible approach can adapt to various scenarios, yielding more accurate assessment results. Three intersections were selected for this study to compare the impact of vehicle trajectories located at the major road's approaches, centerline, and exits on visibility assessment results. These intersections were chosen due to their unique roadway configurations, geometric features, and varying traffic conditions, providing a diverse basis for analysis. Intersection A is located in Bear Creek, Alabama, at the intersection of US Highway 172 & US Highway 241 (34.282036, −87.72099). Intersection B is located in Brilliant, Alabama, at the intersection of US Highway 278 & US Highway 233 (34.100447, −87.690762). Intersection C is located in Marbury, Alabama, at the intersection of US Highway 31 & US Highway 143 (32.716355, −86.483603). The visualized results of the available ISD for the three types of

trajectories—approach-based, centerline-based, and exit-based—are shown in **Figure 10** highlighting the differences in visibility assessment outcomes for each trajectory type. Bases on the comparison result from **Figure 10** and

Table 3, this study finds that ISD assessment is highly sensitive to the vehicle trajectory on the major road, with significant errors arising when using the centerline or exit instead of the approach for measurement.

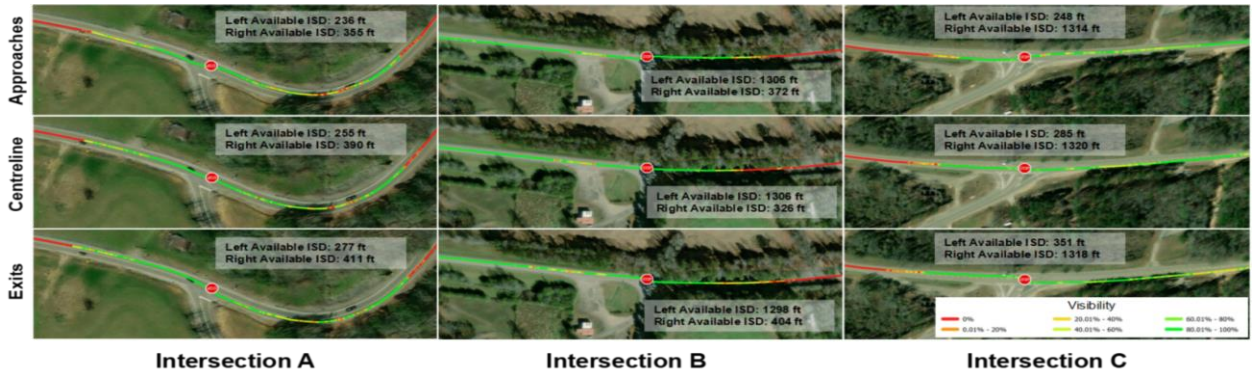

Figure 10 Available ISD for Different Vehicle Trajectories

Table 3 ISD Measurements and Errors for Different Trajectories

Intersection	ISD	Approach (ft)	Centerline (ft)	Error	Exit (ft)	Error
Intersection A	Left ISD	236	255	8.05%	277	17.37%
	Right ISD	355	390	9.86%	411	15.77%
Intersection B	Left ISD	1306	1306	0.00%	1298	0.61%
	Right ISD	372	326	12.37%	404	8.60%
Intersection C	Left ISD	248	285	14.92%	351	41.53%
	Right ISD	1314	1320	0.46%	1318	0.30%

The comparison of ISD values for different trajectories at various intersections demonstrates substantial variations. For instance, at intersection A, the right available ISD increased by 15.77% when measured at the exit compared to the approach, and at intersection C, the left available ISD increased by 41.53%. These findings highlight the critical importance of accurately defining vehicle trajectories for reliable visibility assessments. Therefore, the study recommends that users manually input trajectory features based on satellite imagery or LiDAR point cloud data, as this method provides the most accurate ISD assessment. Using the centerline or exit for such evaluations is not recommended due to the significant measurement inaccuracies they introduce.

4.4 Observer and Target Points Generation

In this process, observer points at the minor road and target points on the major road are generated to construct the line of sight for future visibility analysis. The observer position represents the driver's eye location when the vehicle stops at the minor road, while the targets represent the presumed object height on the road.

4.4.1 Generate Observer Point

To ensure the proposed methodology aligns with transportation agencies' ISD measurements, this study reviewed nearly 200 ISD practice/policy documents from state and local agencies, both in the U.S. and internationally (Eccles et al., 2018). The review revealed significant diversity in measurement methods and parameters. Agencies use a range of equipment, from basic sighting rods and measuring wheels to advanced measuring devices. Parameters for ISD measurement also vary; some agencies adhere to the AASHTO standard (AASHTO, 2018) of 3.5 feet for both driver's eye height and object height, while others use different values. The placement of Decision Points (DP) and Critical Points (CP) also differs, with some agencies basing these points on the roadway centerline, right-of-way lines, or specific offsets from the road edge. Additionally, definitions of what constitutes an obstruction within the sight triangle vary, with agencies setting different maximum heights and widths for objects considered as obstructions.

This diversity highlights the tailored approaches agencies take to address local conditions and specific needs. To address the variability in ISD measurement practices, this study proposes a versatile method for generating observer points. Users create a line feature representing the stop bar or the edge of the major road and input three offset parameters: the horizontal offset from the major road edge, the lateral offset from the minor road, and the vertical offset from the ground to represent the driver's eye height (**Figure 11**). By defining these offsets, the method generates consistent and tailored observer points that accurately reflect the positions from which drivers naturally view potential conflicts at an intersection, accommodating various measurement standards.

Method 1: Offset from Stop Bar

Method 2: Offset from Edge of Major Rd

Figure 11 Observer Positions in Different Practices

To calculate the three-dimensional coordinates of the observer, the user-defined line feature (Stop Bar or Edge of Major Road) is assumed to have a starting point $A = (x_1, y_1)$ and an endpoint $B = (x_2, y_2)$. The midpoint of segment AB is calculated and serves as the observer's approximate position. Two perpendicular segments are considered: the first segment aligns with AB, and the second segment is rotated 90 degrees clockwise from AB, both with a length of d. The expressions for the coordinates are as follows:

For segment L_1 (**Equation 4**)

$$L_1 = \left[\left(\frac{x_1 + x_2}{2}, \frac{y_1 + y_2}{2}\right), \left(\frac{x_1 + x_2}{2}, \frac{y_1 + y_2}{2}\right) + \frac{d}{\sqrt{(y_2 - y_1)^2 + (x_2 - x_1)^2}} . (-(y_2 - y_1), x_2 - x_1)\right]$$

Equation 4

For segment L_2 (**Equation 5)**

$$L_2 = \left[\left(\frac{x_1 + x_2}{2}, \frac{y_1 + y_2}{2}\right), \left(\frac{x_1 + x_2}{2}, \frac{y_1 + y_2}{2}\right) + \frac{d}{\sqrt{(y_2 - y_1)^2 + (x_2 - x_1)^2}} . ((y_2 - y_1), -(x_2 - x_1))\right]$$

Equation 5

As shown in **Figure 12**, if d represents the search radius, and if segment L_1 intersects with the Vehicle Trajectory (**Figure 12a**), the 2D coordinates of the observer are given by **Equation 6**.

a) Segment L_1 intersects the trajectory b) Segment L_2 intersects the trajectory

Figure 12 Different Process of Generating Observer

$$(X_{obs},\ Y_{obs}) = \left(x_1 + \frac{Offset_{Lateral}.(x_2 - x_1)}{\sqrt{(y_2 - y_1)^2 + (x_2 - x_1)^2}} + \frac{Offset_{Horizontal}.(y_2 - y_1)}{\sqrt{(y_2 - y_1)^2 + (x_2 - x_1)^2}},\right.$$
$$\left. y_1 + \frac{Offset_{Lateral}.(y_2 - y_1)}{\sqrt{(y_2 - y_1)^2 + (x_2 - x_1)^2}} - \frac{Offset_{Horizontal}.(x_2 - x_1)}{\sqrt{(y_2 - y_1)^2 + (x_2 - x_1)^2}} \right)$$

Equation 6

The direction of the observer for this configuration is (**Equation 7):**

$$\overrightarrow{Dir} = (y_1 - y_2,\ x_2 - x_1\ )$$ **Equation 7**

If segment L_2 intersects with the Vehicle Trajectory (**Figure 12b**) the 2D coordinates of the observer are (**Equation 8**):

$$(X_{obs},\ Y_{obs}) = \left(x_2 + \frac{Offset_{Lateral}.(x_2 - x_1)}{\sqrt{(y_2 - y_1)^2 + (x_2 - x_1)^2}} - \frac{Offset_{Horizontal}.(y_2 - y_1)}{\sqrt{(y_2 - y_1)^2 + (x_2 - x_1)^2}},\right.$$
$$\left. y_2 - \frac{Offset_{Lateral}.(y_2 - y_1)}{\sqrt{(y_2 - y_1)^2 + (x_2 - x_1)^2}} + \frac{Offset_{Horizontal}.(x_2 - x_1)}{\sqrt{(y_2 - y_1)^2 + (x_2 - x_1)^2}} \right)$$

Equation 8

The direction of the observer for this configuration is **(Equation 9):**

$$\overrightarrow{Dir} = (y_2 - y_1,\ x_1 - x_2)$$ **Equation 9**

Based on the observer's 2D coordinates, the elevation Z of the observer's position on the road surface can be obtained using **Equations 1, 2,** and **3**. Thus, the 3D coordinates of the observer are **(Equation 10):**

$$(X_{obs},\ Y_{obs},\ Z_{obs}) = \left(X_{obs},\ Y_{obs}, Z + Height_{eye}\right) \qquad \textbf{Equation 10}$$

4.4.2 Generate Target Points

Next, target points are automatically generated along the vehicle trajectory, with users able to customize the step length, recommended at 1 ft. The vertical offset from the ground represents the target height on the road, with the AASHTO recommended height being 4.25 ft (AASHTO, 2018). At each position along the trajectory, a set of target points is generated at varying heights up to 4.25 ft, simulating the driver's view of objects at different heights (**Figure 13**). This method ensures a comprehensive visibility assessment by considering multiple heights, representing potential obstacles that a driver might encounter.

The method involves sampling the vehicle trajectory at regular intervals, generating target points at multiple heights for each sampled point, calculating visibility from the observer's position, and applying a user-defined visibility threshold. By creating multiple target points vertically, the method reduces the impact of incidental obstructions on the visibility assessment. For instance, if a location meets or exceeds a visibility threshold of 60%, it is classified as visible; otherwise, it is classified as non-visible. To generate all target points, a set of 2D points $\left\{P_j \middle| P_j = (X_i,\ Y_i),\ j = 0,1,2,\dots,m-1\right\}$ will be created along the user-created vehicle trajectory, where represents the index of the 2D points, and is the total number of 2D points.

Next, for each 2D point P_j , the elevation Z_j will be calculated using **Equations 1, 2** and **3**. Assuming the user-defined target height is $Offset_{Height}$, the number of sub-targets within the target group is n. The 3D coordinates of the i_{th} sub-target at the j_{th} 2D point are given by **Equation 11.**

$$P_{ij} = \left(X_j,\ Y_j,\ Z_j + \frac{Offset_{Height}.i}{n}\right) \qquad \textbf{Equation 11}$$

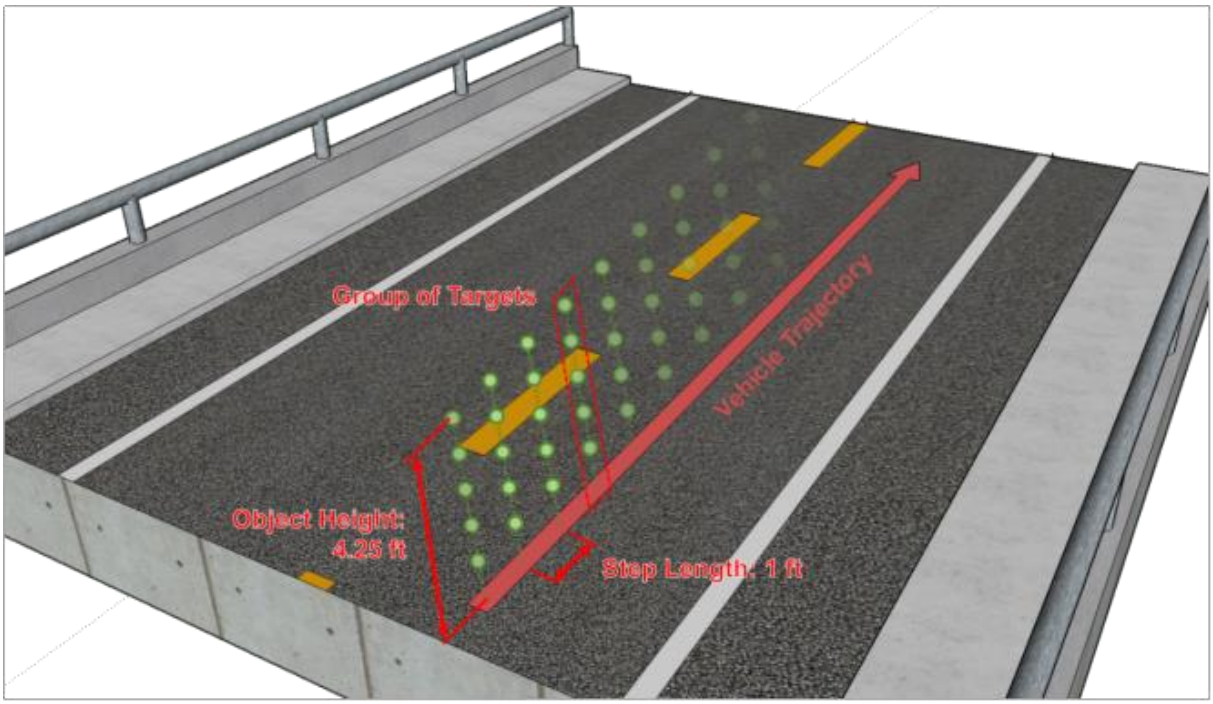

Figure 13 Targets Generation

The more sub-targets within a vertical target group, the more accurate the visibility evaluation at the specified location, although it will increase computational complexity. To balance computational speed and result accuracy, n = 5 is recommended as an optimal configuration.

The proposed method for generating observer and target points offers improvements over previous ISD assessment methods. Unlike traditional approaches that often consider only a single height for targets, this algorithm generates multiple target points at varying heights. This comprehensive approach ensures a more accurate and realistic assessment of visibility, accounting for partial obstructions like hanging traffic signs or roadside vegetation that might block visibility at certain heights but not others.

Furthermore, the method's flexibility allows users to customize parameters, such as the step length and visibility thresholds. This adaptability enables the method to accommodate diverse measurement practices used by different transportation agencies, ensuring that the visibility assessments are relevant and applicable to a variety of scenarios. The ability to generate consistent and tailored observer points based on specific intersection configurations further enhances the precision and reliability of the ISD assessment.

4.5 Visibility Analysis

In the processed point cloud data, all data points except for noise are considered potential obstacles. A set of lines of sight $(LOS_{ij})$is constructed between the observer point and each target point (P_{ij}). For each target group (P_j) containing sub-points, LOS_{ij} is drawn from the observer point to each sub-point in the group. Along each LOS path, virtual detection points are generated

at regular intervals, with the interval (step length) equal to the voxel size of the point cloud data. This ensures optimal spacing for detecting potential obstacles efficiently.

A KD-tree is constructed from the point cloud data to facilitate efficient nearest neighbor searches. The KD-tree is a space-partitioning data structure that organizes points in a k-dimensional space, allowing for fast retrieval of the nearest point to a given query point. For each detection point along the LOS path, the KD-tree is used to find the nearest point in the point cloud data. The distance between the nearest point found by the KD-tree and the detection point is then calculated. If this distance is less than or equal to the voxel size, it indicates that the LOS path intersects an occupied voxel, meaning the line of sight is obstructed. If the distance is greater than the voxel size, the detection point is considered unobstructed. This process is repeated for all detection points along each LOS path. If all the detection points along the path are unobstructed, this target point is visible.

If a certain proportion sub-points of P_j are visible, this proportion is taken as the visibility percentage for P_j . For example, if 60% of the sub-points are visible, the visibility percentage for P_j would be 60% (**Figure 14**). Using a KD-tree significantly reduces the computational complexity of nearest neighbor searches, making the process much faster. KD-trees handle large datasets efficiently, which is essential for LiDAR point cloud data that often contains millions of points. Additionally, the KD-tree provides accurate nearest neighbor results, ensuring reliable visibility assessments.

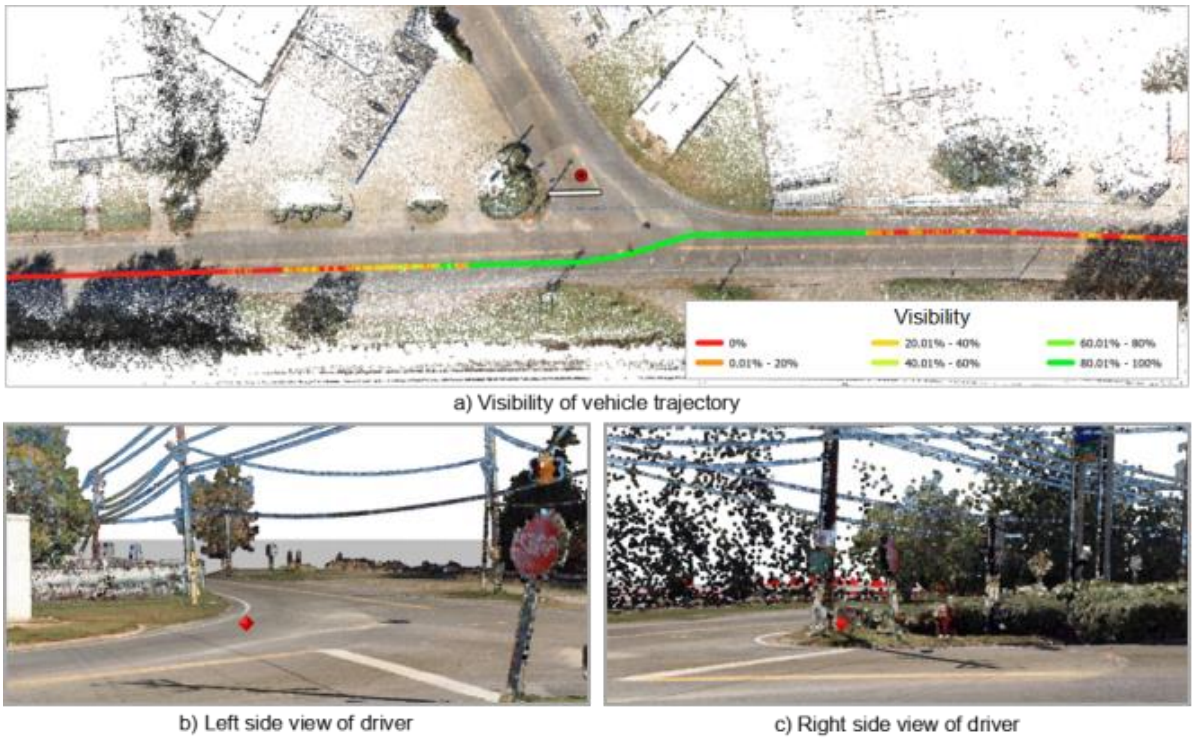

Figure 14 Visualization of ISD Assessment

4.6 Recommended ISD

After determining the visibility for each Minor Road Approach, this study incorporates the AASHTO recommended ISD calculation method. The recommended ISD for each approach and maneuver is calculated, and the blockage rate of the vehicle trajectories within the recommended ISD range is analyzed (**Equation 12).** The equation for calculating the recommended ISD is as follows (**Equation 13):**

$$\text{Blockage Rate} = \frac{\text{Recommended ISD} - \text{Available ISD}}{\text{Recommended ISD}} \qquad \textbf{Equation 12}$$

$$\text{Recommended ISD} = 1.47 \times V_{major} \times t_g \qquad \textbf{Equation 13}$$

Where V_{major} (mph) is the design speed of the Major Road, and t_g (s) is the time gap required for a minor road vehicle to enter the major road. Factors influencing tg include the type of maneuver, vehicle type, major road lanes, median width, and grade of minor road.

For left-turn and crossing maneuver of passenger cars, the base time gaps t_g are 7.5 s and 6.5 s, respectively. Each additional major road lane (including turning lanes) increases the time gap by 0.5 s. The median width should be equivalently treated as the number of lanes. For every 12 ft increase in median width, t_g increases by 0.5 s. For minor road approaches with an upgrade not exceeding three percent, no additional time gap is required. However, for grades exceeding three percent, t_g is increased by 0.2 s for each percent grade.

For right-turn maneuver of passenger cars, the base time gap t_g is 6.5 s. For minor road approaches with an upgrade not exceeding three percent, no additional time gap is required. For grades exceeding three percent, t_g is increased by 0.1 s for each percent grade.

The major road design speed and median width depend on the user's input, while the grade at minor road is computed by the road surface point cloud data within radius 2 ft around the Observer. To fit a plane using the least squares method and subsequently calculate the slope (grade) and aspect, a series of systematic steps are undertaken. Initially, the problem is formulated by representing the plane in the form of the equation z = ax + by + c, where a, b, and c are the coefficients that need to be determined. Given a set of Road Surface 3D points (x_i, y_i, z_i), the objective is to minimize the sum of the squared differences between the observed zi values and the predicted values from the plane equation.

The next step involves setting up the matrix equation AC = Z. Here, A is a matrix constructed from the x and y coordinates of the points, augmented with a column of ones to account for the constant term c. C is a column vector of the coefficients (a, b, c), and Z is a column vector of the coordinates. The least squares solution is obtained by solving the normal equations A^T AC = A^T Z.

Once the plane coefficients a and b are determined, the slope and aspect of the plane can

be calculated. The slope, which represents the grade, is the angle of inclination of the plane and is computed as $\theta = \tan^{-1}\sqrt{a^2 + b^2}$. This angle, expressed in radians, is then converted to a percentage slope by taking the tangent of the angle and multiplying by 100, s = tan θ × 100. The aspect, indicating the compass direction of the slope, is calculated using $\alpha = \tan^{-1}\left(\frac{b}{a}\right)$. To ensure the aspect is within the range of 0 to 360 degrees, any negative values are adjusted by adding 360 degrees. Considering that the road crown slope may have an impact on the grade, this study constructed a slope vector $\vec{v} = \begin{pmatrix} s\cos\alpha \\ s\sin\alpha \end{pmatrix}$, and combine with the direction of the observer $\overrightarrow{Dir}$ calculated above, the final grade can be calculate as Grade $= \vec{v}.\ \widehat{Dir}$.

After calculating the grade, the recommended ISD for different maneuvers can be determined, and the visibility of the vehicle trajectory within the recommended ISD range can be statistic. For example, the intersection presented in **Figure 14** with a major road design speed of 45 mph, a single lane in each direction, a median width of 0 ft, and a grade of 1.41%. The recommended ISD for a left-turn maneuver is 496 ft. Visibility analysis indicates that the driver can see only 163 ft to the left, resulting in a blockage rate of $\frac{496-163}{496} = 67.14\%$, For the right side, the driver can see only 128 ft, the blockage rate is $\frac{496-128}{496} = 74.19\%$. For a right-turn maneuver, the recommended ISD is 430 ft. The driver can see only 163 ft to the left, resulting in a blockage rate of $\frac{430-163}{430} = 62.09\%$..

Calculating the recommended ISD and blockage rate is crucial for transportation agencies to prioritize and address ISD issues. By accurately determining these metrics, agencies can identify intersections with severe sight distance obstructions, allowing them to prioritize these locations for countermeasures. This proactive approach helps in mitigating potential safety hazards before they result in crashes. Transportation agencies can use this information to develop targeted interventions, such as trimming roadside vegetation, regarding slopes, or redesigning intersection layouts to improve sight lines. Furthermore, combining ISD and blockage rate analysis with historical collision data allows agencies to make data-driven decisions for safety investments. By identifying intersections with both high blockage rates and historical crashes, agencies can prioritize these locations for improvements, ensuring that resources are allocated effectively to areas with the greatest need.

4.7 Application

This section presents the comprehensive application of the proposed ISD assessment method using LiDAR data for diverse intersection scenarios. The objective is to evaluate the adaptability, robustness, and accuracy of the method across different measurement standards and vehicle types. The section presents an assessment using distinct transportation agency measurement standards. Additionally, it compares the ISD for passenger cars (PC) and trucks, emphasizing the method's capability to handle different vehicle characteristics.

4.7.1 Different Decision Point

Despite ISD being a critical parameter in traffic safety and capacity analysis, different studies and guidelines have defined varying terms and rules for recommended sight distances and ISD measurement methods(Eccles et al., 2018; Magyari et al., 2021). Notably, significant differences exist in the selection of observer positions, or Decision Points, which can impact ISD measurements. This study includes a thorough review of the criteria used in past research for selecting Decision Points, highlighting the diversity in methodologies and underlying assumptions. Several representative standards are applied to a sample of 230 TWSC intersections to assess whether these differing measurement standards significantly influence ISD evaluations.

Several studies have employed various methodologies for ISD measurement. In a study from Tsai et al. (2011) the DP was determined by offsetting 18 feet from the intersection's Conflict Point towards the Minor Road approach, in addition to the distance from the curb line to the center of the closest travel lane in the direction under consideration. This placed the DP at the center of the Minor Road travel lane.

Jung et al. (2018) proposed an ISD measurement method without specifying a fixed observer position, allowing users to define it flexibly. Similarly, Kilani et al. (2021) allowed users to select any point along the vehicle trajectory as the observation point. Dabbour et al. reviewed multiple methods for calculating Departure Sight Distance, assuming drivers stopped at the stop line or stop sign but did not define specific parameters for generating observer positions (Dabbour et al., 2017, 2021). Harwood et al. (2000) assumed vehicles on the Minor Road would stop 10 feet (approximately 3 meters) from the edge of the Major Road. Morris et al. (2019) made similar assumptions about the stopping distance from the Major Road edge. Himes et al. while analyzing ISD's impact on traffic safety, used observer positions generated based on the Major Road's edge for ISD measurement (Himes et al., 2016, 2018).

Since ISD evaluation results are highly sensitive to the observer's position, it is strongly recommended to generate observer positions based on consistent rules. This approach ensures accuracy and consistency in ISD evaluations, providing reliable data for subsequent analyses of ISD's impact on traffic safety.

Drawing from a review of past studies and ISD practice and policy documents from various transportation agencies, this study selected two representative measurement methods for comparative experiments. **Figure 15** illustrates two methods for determining the DP.

In Method 1: Offset from Stop Bar, the DP is set 10 feet back from the stop bar on the Minor Road and 4 feet from the centerline of the Minor Road travel lane. In Method 2: Offset from Edge of Major Road, the DP is positioned 14.5 feet from the edge of the Major Road and 4 feet from the centerline of the Minor Road travel lane. The Driver's eye height is 3.5 feet. Both methods evaluate the ISD by applying different reference points to determine where the driver typically stops and observes traffic before entering the Major Road. These experiments aim to uncover differences in available ISD under different measurement methods, providing new insights for ISD measurement. This will enable practitioners to conduct more accurate, reliable, and repeatable ISD measurements tailored to actual conditions.

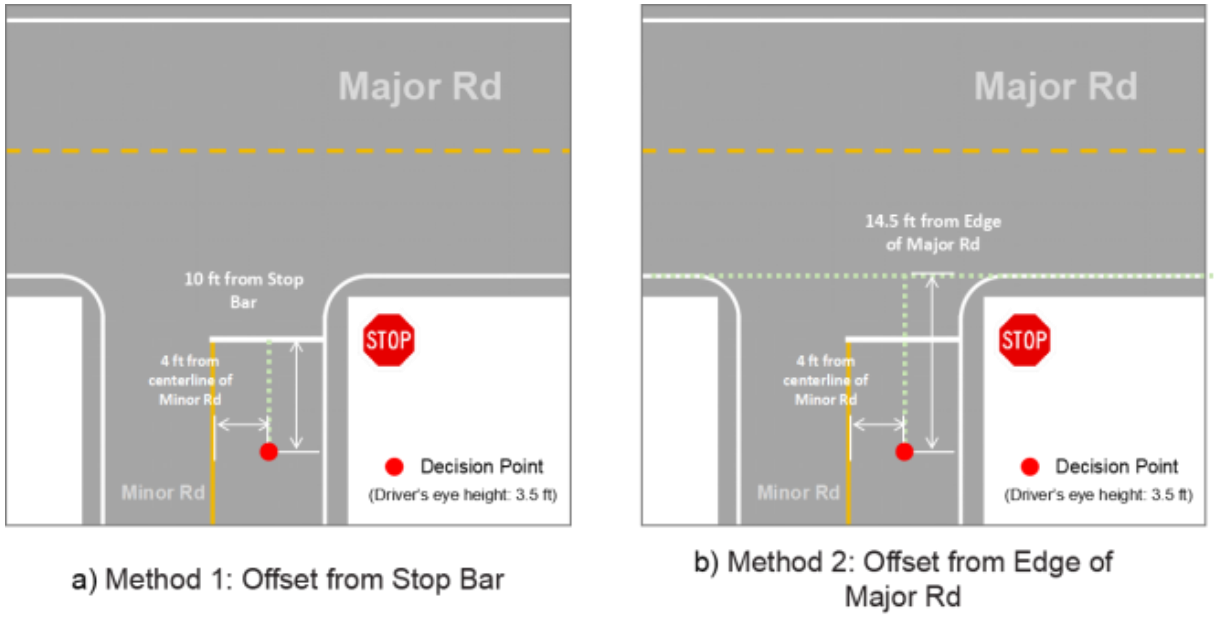

Figure 15 Two Different Methods for Determining DP

In this study, paired t-tests were conducted separately for Left Available ISD and Right Available ISD to compare the assessment results of the two methods (Offset from Stop Bar and Offset from Edge of Major Road) for 342 DP. The results indicate whether there are significant differences between the methods and the variance of the measurement differences. **Figure 16** displays the distribution of differences in ISD assessment between two methods for both Left ISD and Right ISD.

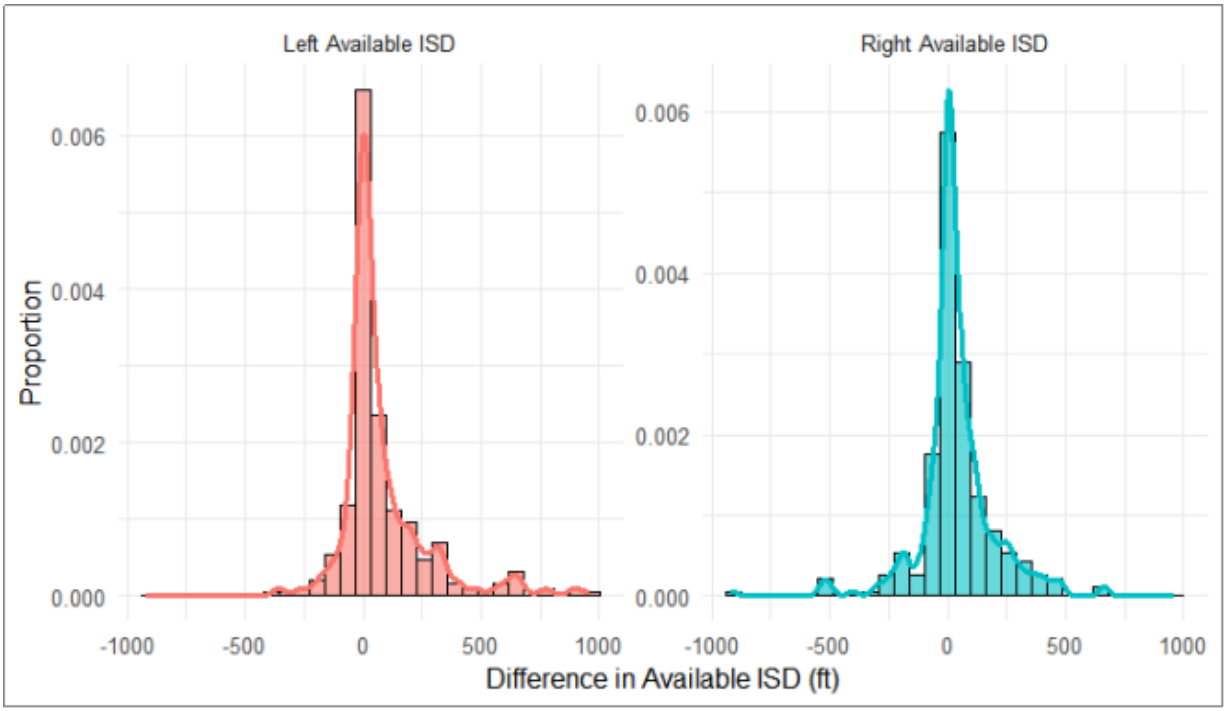

Figure 16 Distribution of Differences in Available ISD (Method 2 vs. Method 1)

The paired t-test (

Table 4) for both Left and Right Available ISD showed significant differences between the two measurement methods.

Table 4 Statistical comparison between M2 and M1 for Left and Right ISD

Metrics	Difference	t-value	Df	p-value	Mean Diff	95% CI Lower	95% CI Upper
Left ISD	M2 vs. M1	7.345	287	2.14×10^{-12}	82.12003	60.11417	104.12589
Right ISD	M2 vs. M1	3.5848	287	0.0003962	34.7743	15.68138	53.86723

For the Left Available ISD, the test yielded a mean difference of 82.12 ft, with a t-value of 7.345 and a p-value of 2.14×10^{-12}. The 95% confidence interval ranged from 60.11 ft to 104.13 ft, indicating a significant difference, with Method 2 producing longer ISD values than Method 1. Similarly, for the Right Available ISD, the mean difference was 34.77 ft, with a t-value of 3.585 and a p-value of 0.0003962. The 95% confidence interval for the mean difference was between 15.68 ft and 53.87 ft, also excluding zero.

The statistically significant p-values for both Left and Right Available ISD suggest that the two methods produce significantly different ISD measurements. The significant differences in ISD assessment between the two methods highlight the importance of selecting a consistent and appropriate observer position. Researchers referencing previous studies on ISD and safety should

ensure that their ISD assessment or measurement methods consist with those used in past studies to avoid deviations. In addition, designing intersections based on measurements from Method 1, which results in lower ISD values, would represent a more conservative design approach. This conservatism may enhance safety by ensuring more restrictive sight distance requirements.

4.7.2 Passenger Car and Truck

This study explores the potential differences in obstruction rates between passenger cars (PC) and trucks at these intersections. By analyzing the impact of these vehicle types on visibility, new insights are provided for improving intersection design. This comprehensive approach clarifies the implications of varying Decision Point criteria and contributes to a better understanding of how vehicle-specific characteristics affect sight distance and safety at TWSC intersections. The analysis is expected to inform future guidelines and practices, enhancing the accuracy and reliability of ISD assessments.

To compare the differences in ISD assessment for different vehicle types, this study examines the available ISD (**Figure 17**) for PC and trucks and analyzes their blockage rates (**Figure 18**) within the recommended ISD.

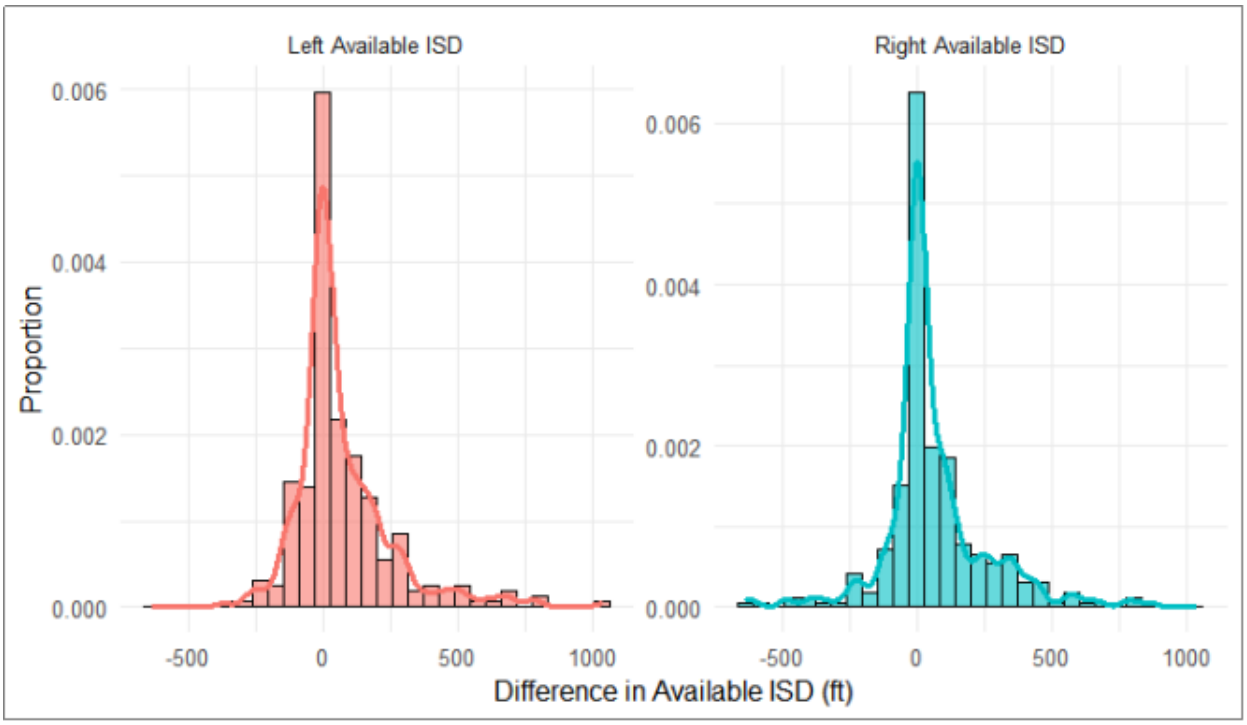

Figure 17 Distribution of Differences in Available ISD (Truck vs. PC)

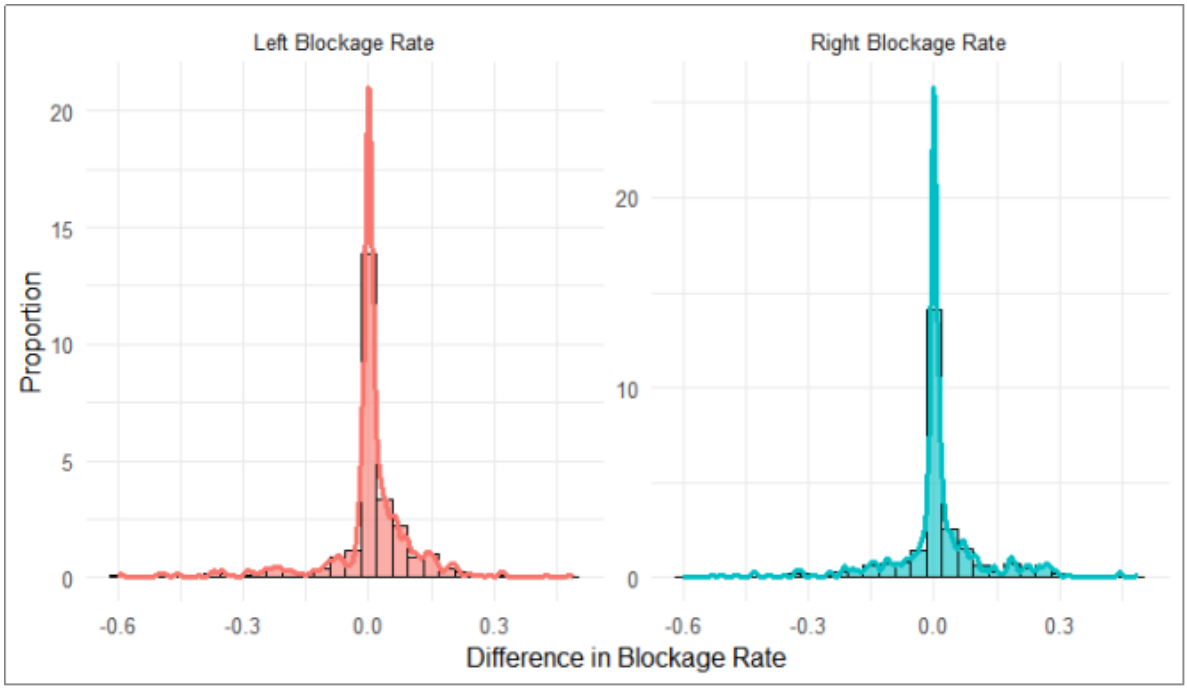

Figure 18 Distribution of Differences in Blockage Rate (Truck vs. PC)

Due to their larger size, longer braking distances, and slower acceleration rates, trucks require longer ISD than PC. These characteristics make it more challenging for truck drivers to safely navigate intersections, particularly when visibility is limited. Traditionally, research on the impact of ISD on safety has predominantly focused on PC, resulting in a lack of comprehensive understanding regarding how trucks are affected by these design parameters.

By addressing these differences, this study underscores the necessity of independently assessing the ISD requirements for trucks to enhance traffic safety. Such focused evaluations can lead to better-informed design decisions, ensuring that intersections are safer and more suitable for all vehicle types, ultimately improving traffic flow and reducing crash frequency.

The statistical results (**Table 5**) indicate that, with a 95% confidence interval, the available ISD for Trucks is significantly longer than that for PC on both the left side [104.13, 60.11] feet and the right side [85.87, 40.60] feet. This difference can be attributed to the higher driver eye height in Trucks, which is approximately 7.6 feet, compared to 3.5 feet in PC, allowing truck drivers to have a better field of view under most conditions. However, given that the recommended ISD for Trucks is longer than that for PC, this study also analyzed the differences in Blockage Rates between the two vehicle types.

Table 5 Comparison of ISD and Blockage Rates between Truck and PC

Metrics	Difference	t-value	Df	p-value	Mean Diff	95% CI Lower	95% CI Upper
Left ISD	Truck vs. PC	6.722	287	9.56×10^{-11}	71.6741	50.68722	92.66093
Right ISD	Truck vs. PC	5.4978	287	8.5×10^{-8}	63.2352	40.59649	85.87388
Left Blockage Rate	Truck vs. PC	0.41669	585	0.6771	0.19%	-0.71%	1.10%
Right Blockage Rate	Truck vs. PC	0.9682	404	0.3335	0.57%	-0.59%	1.73%

The paired t-test results (**Table 5**) for the Blockage Rate show that the 95% confidence interval for the left side sight triangle is [-0.71%, 1.10%], with a t-value of 0.42 and a p-value of 0.6771. For the right-side sight triangle, the 95% confidence interval is [-0.59%, 1.73%], with a t-value of 0.97 and a p-value of 0.3335. These results indicate that there is no statistically significant difference in the Blockage Rates between Trucks and PC.

Therefore, although Trucks have a significantly longer available ISD compared to PC, their Blockage Rates are not significantly higher. This suggests that while trucks benefit from a better field of view due to their higher driver eye height, the actual obstruction rates within the view triangles are comparable for both vehicle types. Consequently, it is necessary to conduct independent analyses of ISD for Trucks during sight distance assessment to gain a more comprehensive understanding of the visibility conditions at study site.

4.8 Limitation of Developed ISD Assessment Method

The application of the proposed ISD assessment method revealed certain limitations. First, in some cases, currently applied classification algorithms are unable to accurately recognize the boundary between the vehicle and the road surface (**Figure 19**). This problem can lead to inaccuracies in recognizing potential obstacles and may affect the overall reliability of the ISD assessment. Secondly, the method struggles with accurately identifying road surfaces on bridges and at interchange facility, often requiring manual calibration to ensure accuracy (**Figure 20**) This need for manual intervention can be time-consuming and may introduce human error into the process.

Additionally, the method relies on manually created vehicle trajectories and stop bar features. While this approach ensures the accuracy of ISD evaluations, it significantly increases the workload and may result in excessive time consumption when scanning large-scale road networks. Future efforts to address these limitations could focus on enhancing the automated classification of vehicles and road surfaces. Developing more advanced algorithms that can better distinguish between vehicles and road surfaces, even in challenging scenarios, would improve the method's reliability and accuracy. Another direction for future work is to streamline the process of creating vehicle trajectories and stop bars. Automating these tasks using advanced mapping technologies and artificial intelligence could significantly reduce the time and labor required for ISD assessments. Implementing these improvements would enhance the method's efficiency and scalability, making it more practical for large-scale road network screening.

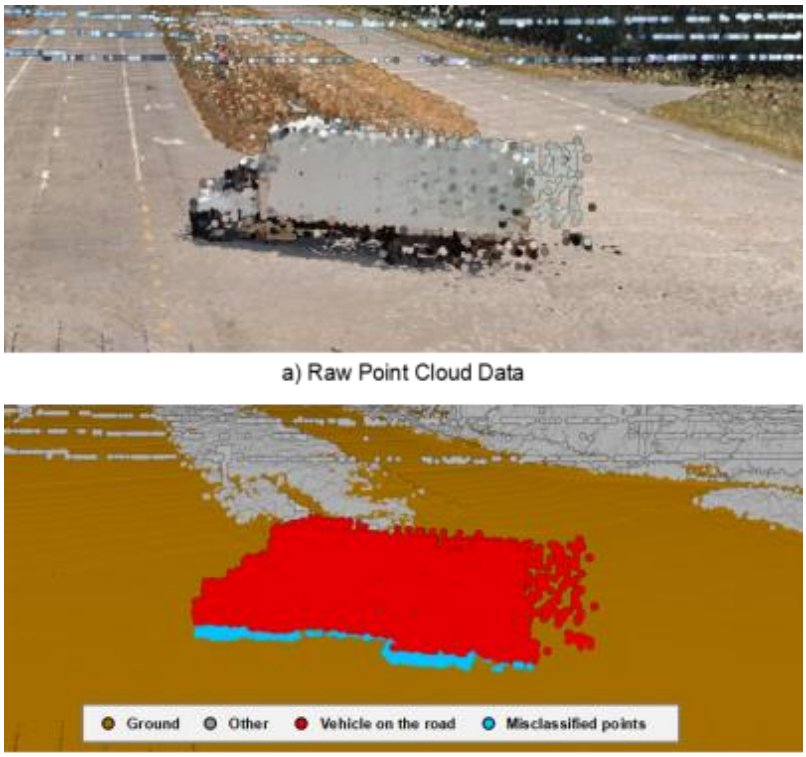

a) Raw Point Cloud Data

b) Classification Results

Figure 19 Vehicle on the Road Classification Error

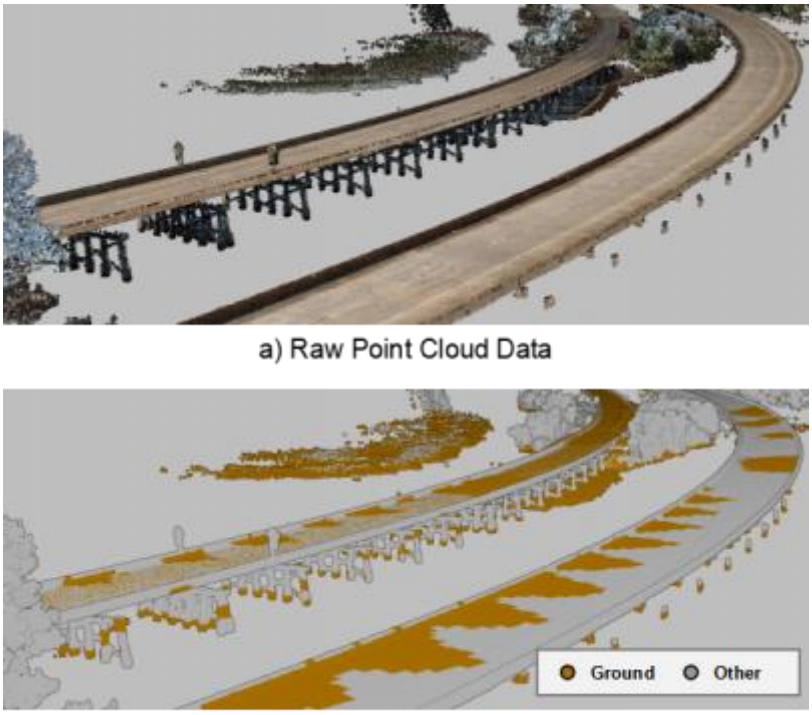

a) Raw Point Cloud Data

b) Ground Classification Results

Figure 20 Ground Classification Error

5 IMPACT OF ISD ON INTERSECTION SAFETY

Many studies have investigated the impact of ISD on intersection safety, with one of the most comprehensive being a study conducted by the National Cooperative Highway Research Program (NCHRP) (Eccles et al., 2018). This study collected extensive data on crashes, traffic volume, and roadway geometry from 832 intersections across North Carolina, Ohio, and Washington. ISD was recorded using standardized field measurement methods. Through a cross-sectional study design and count regression models, the study identified a nonlinear relationship between ISD and crash frequency, particularly highlighting that increasing ISD can significantly reduce crash rates. Additionally, the study found that the traffic volume and speed limits on major roads have a moderating effect on the relationship between ISD and safety outcomes. The research ultimately developed CMFs based on ISD and translated these into practical guidance charts for use by traffic engineers in planning intersection improvement projects.

While the NCHRP's crash prediction models and CMFs, developed using extensive multi-state data, demonstrate effective predictive capability for the relationship between ISD and traffic safety, their applicability may vary significantly across different regions. Alabama's unique roadway geometric features, traffic patterns, climatic conditions, and driving behaviors may differ from those of the states included in the NCHRP's original study. These differences could affect the accuracy of the model's predictions in a local context. Without calibration, the model may fail to fully capture the traffic safety factors specific to Alabama, leading to predictions that do not align with local realities.

In this study, the measurement parameters proposed by NCHRP were first adopted, incorporating a LiDAR-based ISD assessment method to measure the Available ISD at selected intersections in Alabama. This approach ensured consistency in data collection methods with the original NCHRP study. Subsequently, crash data related to ISD, particularly crashes involving minor road vehicles and major road vehicles, were extracted from historical crash records. The NCHRP's target crash prediction model was then applied to predict the crash frequency at these intersections, and the predicted values were compared with the observed crash frequencies to evaluate the model's applicability and accuracy in Alabama.

Based on preliminary comparative analysis, several model optimization strategies were proposed aimed at enhancing the predictive performance of the model. These strategies included adjusting model parameters and developing prediction models tailored to specific scenarios. By comparing the predictive performance of these optimized models, the best-performing model was selected. Using this optimized model, new CMFs were developed to more accurately assess and predict the crash risks at Alabama intersections under varying sight distance conditions. The optimized model better reflects Alabama's specific traffic conditions, providing a more precise tool for crash risk assessment. This improvement not only aids in optimizing intersection design and traffic management but also provides a scientific basis for local traffic authorities to develop more effective safety measures, ultimately contributing to the reduction of crashes and the enhancement of road safety.

5.1 Methodology

5.1.1 Impact of ISD on Intersection Safety

The study begins with the collection of ISD data using the developed framework. Historical crash data related to ISD was also collected to establish a foundation for analyzing the relationship between sight distance and crash frequency. This data collection process is essential for understanding how ISD impacts traffic safety.

The collected ISD and crash data were then applied to the target crash prediction model in the NCHRP report (Eccles et al., 2018). Since Alabama's intersections have unique characteristics, such as rural settings, low traffic volumes, and varying lane configurations, the model required calibration to reflect these local conditions. The calibration process involved modifying key parameters to account for localized factors, including sight distance challenges and specific roadway designs. By aligning the model with Alabama-specific traffic and environmental data, this approach ensures more accurate predictions of crash frequency and better assessments of intersection safety.

Further refinement of the model is achieved through Bidirectional Stepwise Regression, which identifies the most significant variables influencing crash risks while eliminating less impactful factors. Additionally, separate models are developed for different types of facilities, allowing for more tailored predictions based on specific intersection settings.

The performance of the calibrated and optimized models is evaluated using statistical metrics such as McFadden R^2, Mean Squared Error (MSE), Root Mean Squared Error (RMSE) and Mean Absolute Error (MAE). These metrics are used to compare the original NCHRP model with the newly calibrated and optimized versions to identify the most accurate model for predicting crash risks at intersections in Alabama.

Based on the calibrated predictive models, new CMFs are developed. These CMFs offer a more precise tool for assessing and predicting crash risks associated with varying sight distance conditions, providing transportation agencies in Alabama with a valuable resource for improving intersection safety.

5.1.2 Develop CMFs for Countermeasures

This study utilized the Empirical Bayes (EB) Before-and-After study method to analyze the impact of three types of left turn lanes, four types of right turn lanes, and medians on target crashes. Through this analysis, corresponding CMFs were developed. The EB Before-and- After study method is used because it addresses key limitations of simpler before-and-after studies, particularly the issue of regression-to-the-mean (**Figure 21**).

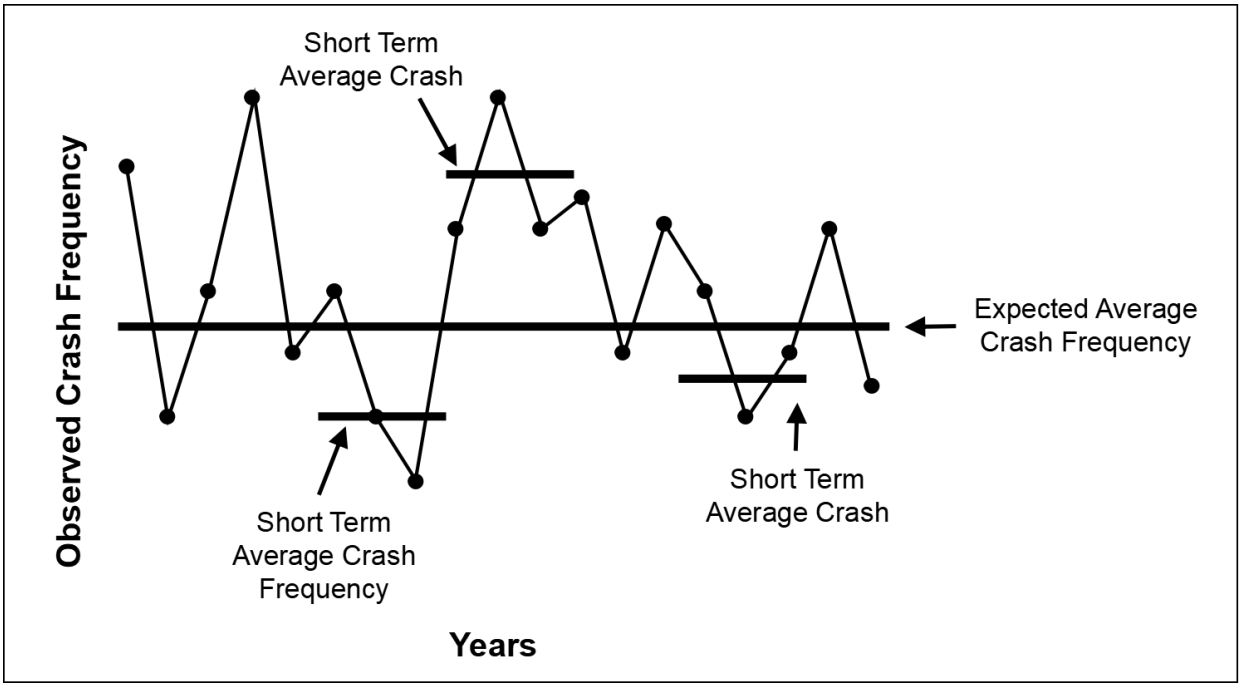

Figure 21 Regression-To-the-Mean in Crash Frequency (AASHTO, 2010)

Regression-to-the-mean occurs when sites with unusually high crash rates are selected for treatment, leading to a natural decrease in crashes over time, regardless of the treatment's effectiveness. This can result in an overestimation of the treatment's impact. The EB method corrects this by incorporating data from similar, untreated reference sites, which helps isolate the effect of the treatment from other factors that could influence crash rates, such as traffic volume changes and time trends. Additionally, the EB method provides more accurate and statistically robust estimates by using a weighted average of observed and predicted crashes, reducing uncertainty and improving the reliability of the CMFs (Gross et al., 2010).

To develop CMFs for countermeasures, the first step involves selecting a reference group of untreated sites that closely match the treated sites in terms of traffic volume and geometric characteristics. The treatments considered in this study include adding different types of left- turn lanes, right-turn lanes, and wide medians at intersections. This reference group serves as a baseline for estimating the number of crashes that would have occurred at the treated sites had the treatments not been implemented. By ensuring the reference group is similar to the treated sites, a more accurate comparison can be made between treated and untreated conditions.

Next, Safety Performance Functions (SPFs) are developed. These SPFs are statistical models used to predict the expected number of crashes based on the characteristics of the sites. The SPFs are created using data from the reference group and are calibrated to accurately reflect the conditions at the study sites. This step ensures that the predicted crashes at the treated sites are consistent with real-world conditions prior to the treatment's implementation.

Once the SPFs are established, the expected number of crashes in the "before" period at the treated sites is calculated. This calculation involves a weighted average of observed and

predicted crashes, providing a reliable estimate of crashes before the treatments were applied. For the "after" period, the estimated number of crashes is adjusted to account for any changes in traffic volumes or conditions, which helps to create an accurate comparison of crash rates before and after the treatment.

Finally, CMFs are calculated by comparing the observed number of crashes in the "after" period with the expected number of crashes had the treatment not been implemented. This comparison allows researchers to determine the effectiveness of the countermeasure. The statistical significance of the CMFs is evaluated by calculating the variance and confidence intervals, ensuring that the findings are robust and reliable. This methodological approach provides a comprehensive way to quantify the safety impact of the treatments and develop CMFs that can guide future safety interventions.

5.2 Applicability of NCHRP Models to Alabama

The NCHRP study (Eccles et al., 2018) developed two prediction models aimed at estimating the frequency of target crashes and target fatal and injury crashes at TWSC intersections, that were designed to quantify the impact of ISD on intersection safety, incorporating various intersection characteristics and traffic conditions as key variables. The prediction models developed in the NCHRP study assume a log-linear relationship between the expected crash frequency and site characteristics. Generalized Linear Modeling (GLM) techniques were employed to construct these models, specifically using a negative binomial error structure to account for over-dispersion in crash data. The prediction model of frequency of total target crashes for the observation is represented as (**Equation 14**):

$$\lambda_i = exp\Big(-8.147 + 0.244 \times \log(MajAADT) + 0.536 \times \log(MinAADT) - 243.0 \times \frac{LmajAADT}{AvailableISD} - 177.8 \times \frac{MmajAADT}{AvailableISD} + 0.334 \times LT + 0.845 \times fourleg - 0.016 \times median - 0.021 \times SpeedLimit + 7.194 \times \frac{SpeedLimit}{AvilableISD} - 0.061 \times grd500\Big)$$

Equation 14

And the second model is designed to predict the frequency of target fatal and injury crashes, which is represented as (**Equation 15**):

$$\lambda_i = exp\Big(-8.234 + 0.115 \times \log(MajAADT) + 0.498 \times \log(MinAADT) - 155.5 \times \frac{LmajAADT}{AvailableISD} + 0.507 \times LT + 0.953 \times fourleg + 0.215 \times median - 0.009 \times SpeedLimit + 6.335 \times \frac{SpeedLimit}{AvilableISD} - 0.054 \times grd500\Big)$$

Equation 15

Where:

λ_i	= expected number of target crashes (or target fatal and injury crashes) for the ith observation, with an observation defined as a minor road and major road approach combination
MajAADT	= major road AADT
MinAADT	= minor road AADT
LmajAADT	= 1 if the major road AADT is less than or equal to 5,000; otherwise, 0
MmajAADT	= 1 if the major road AADT is greater than 5,000 and less than or equal to 15,000; otherwise, 0
LMmajAADT	= 1 if the major road AADT is less than or equal to 15,000; otherwise, 0
AvailableISD	= left or right available ISD at Minor Rd (ft)
LT	= 1 if the Target Crashes involve vehicles from the left side of the major road; otherwise, 0
fourleg	= 1 if study intersection is a four leg intersection; otherwise, 0
median	= 1 if there is a median present on the major road; otherwise, 0
SpeedLimit	= major road post speed limit (mph)
grd500	= measured vertical grade on the major road approach 500 feet prior to the intersection

The approach and direction-level dataset used for validating and optimizing the NCHRP prediction models was derived from a comprehensive collection of intersection data from Alabama. This dataset includes detailed information on critical variables that influence crash frequency, categorized into continuous and categorical variables, as summarized in **Table 6** and **Table 7**.

Table 6 Statistics for Continuous Variables for Study Intersections (Approach and Direction Level)

Variable	Obs.	Min	Max	Mean	St. Dev
Observed Total Target Crashes	510	0	10	0.62	1.31
Observed FI Target Crashes	510	0	8	0.24	0.76
MajAADT	510	420	21320	5326.90	4548.88
MinAADT	510	83	11422	1879.73	1711.20
AvailableISD	510	209	1320	1052.70	297.97
SpeedLimit	510	30	65	52.10	8.62
grd500	510	-6.15	8.20	0.12	2.12

Table 7 Statistics for Categorical Variables for Study Intersections (Approach and Direction Level)

Variable	Category Levels	Frequency	Percentage
LmajAADT	5,000 < AADT (0)	200	39.22%
	0 ≤ AADT ≤ 5,000 (1)	310	60.78%
MmajAADT	AADT ≤ 5,000 or AADT > 15,000 (0)	342	67.06%
	5,000 < AADT ≤ 15,000 (1)	168	32.94%
LMmajAADT	15,000 < AADT (0)	32	6.27%
	AADT ≤ 15,000 (1)	478	93.73%
LT	Right-Directional Analysis Unit (0)	255	50.00%
	Left-Directional Analysis Unit (1)	255	50.00%
fourleg	Three-legged (0)	338	66.27%
	Four-legged (1)	172	33.73%
median	Not Presented (0)	412	80.78%
	Presented (1)	98	19.22%

Continuous Variables (**Table 6**)

- **Observed Total Target Crashes and Observed Fatal and Injury (FI) Target Crashes:** These variables represent the recorded crash counts at the study intersections, with means of 0.62 and 0.24 crashes per intersection, respectively. The wide range in crash counts (0 to 10 for total target crashes and 0 to 8 for FI crashes) highlights variability in intersection safety performance.
- **Major Road and Minor Road AADT (MajAADT and MinAADT):** These variables reflect average annual daily traffic volumes on the major and minor roads. The significant variation (e.g., MajAADT ranging from 420 to 21,320) underscores the diversity in traffic demand at these intersections.
- **Available ISD:** This measures the sight distance available at the intersections, with a mean of 1,052.70 feet and values ranging from 209 to 1,320 feet.
- **Speed Limit:** The posted speed limits at the intersections range from 30 to 65 mph, with a mean of 52.10 mph.
- **Grade (grd500):** This variable captures the grade of the intersection over a 500-foot segment, ranging from -6.15% to 8.20%, with a mean grade close to zero, indicating generally flat or gently sloped intersections.

Categorical Variables (**Table 7**)

- **AADT Categories (LmajAADT, MmajAADT, LMmajAADT):** These variables classify intersections based on major and minor road AADT thresholds (e.g., ≤ 5, 000, 5, 000–15, 000, and > 15, 000 vehicles). Most intersections fall under lower AADT categories, reflecting a predominance of rural or low-traffic locations.
- **Left-Turn Direction (LT):** This variable differentiates intersections based on the directional analysis unit (left or right), with an even distribution across categories.
- **Intersection Type (fourleg):** Approximately 67% of the intersections are three-legged, while 33% are four-legged.
- **Median Presence (median):** This variable indicates whether a median is present at the intersection. Most intersections (80.78%) do not have a median, with only 19.22% featuring a median design.

To evaluate the performance of the prediction models developed by researchers under the NCHRP framework (Eccles et al., 2018) when applied to the Alabama dataset, several statistical metrics were employed: McFadden R2, Mean Squared Error (MSE), Root Mean Squared Error (RMSE), and Mean Absolute Error (MAE). These metrics provide a comprehensive evaluation of the models' accuracy and predictive capability, offering insights into how well the models capture the relationship between intersection characteristics and crash frequency in a different regional context.

- **McFadden** R^2

McFadden R^2 is a pseudo R-squared measure commonly used in models estimated via maximum likelihood, such as logistic regression and count models. It compares the likelihood of the fitted model with the likelihood of a model that only includes an intercept (i.e., a model that does not account for any predictors). McFadden R^2 is calculated as (**Equation 16):**

$$McFadden\ R^2 = 1 - \frac{\ln(L_{full\ model})}{ln(L_{intercept\ model})} \qquad \textbf{Equation 16}$$

Where $\ln(L_{\text{full model}})$ is the log-likelihood of the fitted model, and $\ln(I_{\text{Intercept model}})$ is the log-likelihood of the model with only an intercept. McFadden R^2 values closer to 1 indicate better model fit, with values between 0.2 and 0.4 generally considered indicative of a good fit for prediction models in social sciences. Unlike traditional R-squared, McFadden R^2 is better suited for the logistic regression models employed here and provides a clear, interpretable measure of model performance. Reporting this metric enables a standardized comparison of model fit and helps demonstrate the effectiveness of the calibration and optimization methods applied in this research.

- **Mean Squared Error (MSE)**

MSE measures the average of the squares of the errors, that is, the average squared difference between the observed actual outcomes and the outcomes predicted by the model. MSE is calculated as (**Equation 17):**

$$MSE = \frac{1}{n}\sum_{i=1}^{n}(y_i - \hat{y}_i)^2 \qquad \textbf{Equation 17}$$

Where y_i represents the observed values, $\hat{y}_i$ represents the predicted values, and is the number of observations. MSE is sensitive to large errors due to the squaring of differences, making it useful for identifying models that produce occasional large errors. In this study, MSE is used as one of the primary metrics to evaluate the performance of crash prediction models. By quantifying the average deviation between predicted and observed crash frequencies, MSE provides insight into the overall accuracy of the models. This metric is especially valuable for identifying outlier predictions and assessing the robustness of the model under varying conditions.

- **Root Mean Squared Error (RMSE)**

RMSE is the square root of the MSE and provides a measure of the average magnitude of the prediction errors, expressed in the same units as the observed data. RMSE is calculated as (**Equation 18):**

$$RMSE = \sqrt{\frac{\sum_{i=1}^{n}(y_i - \hat{y}_i)^2}{n}} \qquad \textbf{Equation 18}$$

RMSE provides an interpretable metric to evaluate the average distance between the observed and predicted values, with lower RMSE values indicating better model performance.

- **Mean Absolute Error (MAE)**

MAE measures the average magnitude of the errors in a set of predictions, without considering their direction (positive or negative). It is calculated as (**Equation 19):**

$$MAE = \frac{1}{n}\sum_{i=1}^{n}|y_i - \hat{y}_i| \qquad \textbf{Equation 19}$$

MAE is useful for understanding the average error in absolute terms, providing a straightforward interpretation of model accuracy.

The validation results for the two prediction models, as depicted in the **Figure 22** and quantitative metrics **Table 8** reveal notable differences in their performance. The scatter plots for both the Total Target Crashes and FI Target Crashes models exhibit a clear pattern where most data points fall below the ideal reference line. This trend suggests that both models consistently underestimate the observed crash frequencies. The dispersion of points, particularly within the lower range of crash frequencies, indicates considerable variability in the model predictions, with more pronounced discrepancies at lower observed values.

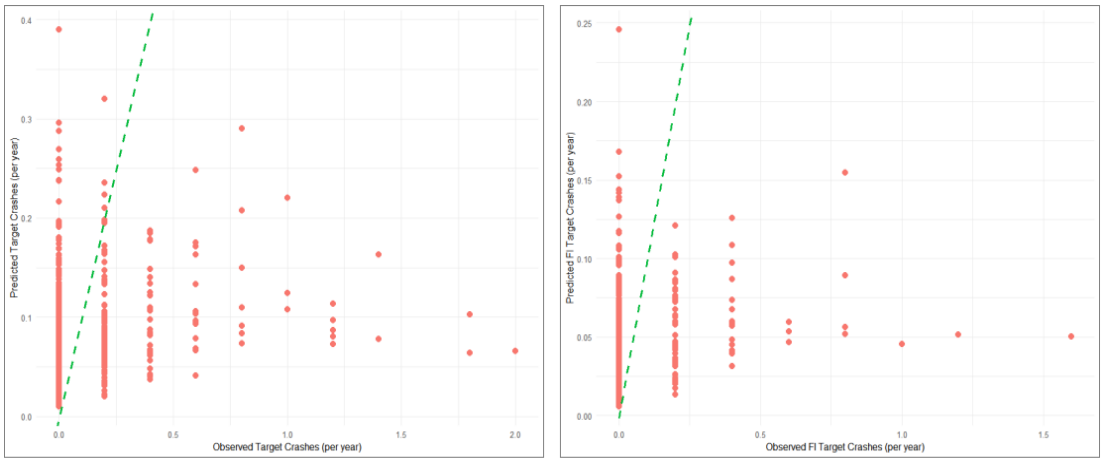

a) Observed vs Predicted Total Target Crashes

b) Observed vs Predicted FI Target Crashes

Figure 22 Comparison of Observed vs Predicted Target Crashes Using NCHRP Models

Table 8 Prediction Performance of NCHRP Models

Model	McFadden R^2	MSE	RMSE	MAE
Total Target Crashes	0.02269676	0.06714414	0.2591219	0.1396654
FI Target Crashes	0.07606794	0.6108492	0.7815684	0.2673819

Quantitative analysis further reinforces these observations. The McFadden R^2 value for the Total Target Crashes model is just 0.0227, indicating that the model explains only 2.27% of the variance in the data. Similarly, the FI Target Crashes model, while having a slightly higher McFadden R^2 of 0.0761, still accounts for less than 8% of the variance, suggesting limited predictive power in both models. In terms of error metrics, the Total Target Crashes model reports an MSE of 0.0671 and an RMSE of 0.2591, which are relatively low. In contrast, the FI Target Crashes model exhibits a much higher MSE of 0.6108 and an RMSE of 0.7816, indicating not only greater overall prediction errors but also increased variability in those errors. Both models face challenges in accurately predicting crash frequencies, especially at the lower end of the observed spectrum. The scatter plots demonstrate a general tendency for the models to underestimate actual crash frequencies, accompanied by noticeable variability and inconsistencies between observed and predicted values. The relatively low McFadden R^2 values indicate that the models have limited explanatory power, and the error metrics underscore significant prediction inaccuracies. These findings highlight the need for further optimization and refinement of the models to enhance their predictive accuracy and reliability.

5.3 Model Calibration and Optimization

The CMFs related to ISD are derived from Crash Frequency prediction models. To improve the accuracy of these models and enhance the reliability of CMFs, this study employed three dis-

tinct methods of calibration and optimization, tailored to reflect Alabama's traffic and roadway conditions.

- **Method 1: Recalibration of NCHRP Model Coefficients**

In the first method, the original set of explanatory variables from the NCHRP model was retained, while the model coefficients were recalibrated using Alabama-specific data. This approach ensured that the model's predictions reflected local traffic conditions, such as rural road characteristics and varying AADT levels, without altering the structure or logic of the original model. By recalibrating the coefficients, the model maintained computational efficiency and interpretability.

A detailed analysis of Alabama's crash data revealed that the variable indicating whether the major road AADT exceeds 15,000 had an insignificant impact on Fatal and Injury (FI) Target Crashes. Therefore, this variable was excluded from the recalibrated FI Target Crashes model to simplify its application. Removing this variable reduced data collection requirements and made the model more practical for use by transportation practitioners. The calibrated Total Target Crashes prediction model and the FI Target Crashes prediction model according to Method 1 are presented in **Table 9** and **Table 10**. respectively.

Table 9 Total Target Crashes Prediction Model (Method 1)

Variable	Coefficient	Std. Error	Z-Score	P-value
Constant	-16.14969	3.46688	-4.658	3.19e-06
$\beta_1(\log(\text{majAADT}))$	0.34841	0.33389	1.044	0.29671
$\beta_2(\log(\text{minAADT}))$	0.84130	0.22621	3.719	0.00020
$\beta_3(\text{LmajAADT/ISD})$	1001.27701	725.06319	1.381	0.16729
$\beta_4(\text{MmajAADT/ISD})$	8890.55610	562.94118	1.582	0.11366
$\beta_5(\text{LT})$	-0.05557	0.25348	-0.219	0.82646
$\beta_6(\text{fourleg})$	0.28467	0.28383	2.683	0.00103
$\beta_7(\text{median})$	-0.02967	0.42458	-0.070	0.94429
$\beta_8(\text{spdlmt})$	0.07892	0.02862	2.787	0.00532
$\beta_9(\text{spdlmt/ISD})$	-13.52462	14.14817	-0.956	0.33911
$\beta_{10}(\text{grd500})$	0.02120	0.06642	0.319	0.74957

Table 10 FI Target Crashes Prediction Model (Method 1)

Variable	Coefficient	Std. Error	Z-Score	P-value
Constant	-15.01772	4.71229	-3.187	0.00144
$\beta_1(\log(\text{majAADT}))$	0.13578	0.44996	0.302	0.76283
$\beta_2(\log(\text{minAADT}))$	0.8434	0.39193	2.152	0.0314
$\beta_3(\text{LT})$	-0.21337	0.42159	-0.506	0.61279
$\beta_4(\text{fourleg})$	1.37017	0.49813	2.751	0.00595
$\beta_5(\text{median})$	0.61126	0.77847	0.785	0.43233
$\beta_6(\text{spdlmt})$	0.06596	0.04607	1.432	0.15219

Variable	Coefficient	Std. Error	Z-Score	P-value
β_7(spdlmt/ISD)	4.96455	9.18132	0.541	0.5887
β_8(grd500)	0.07194	0.12261	0.587	0.55736

- **Method 2: Model Optimization via Adjusted Parameters**

The second method involved optimizing the prediction model by adjusting key parameters to better capture the variability in ISD-related crashes under different scenarios. This approach used Bidirectional Stepwise Regression to refine the model by iteratively adding and removing variables based on their contribution to the Akaike Information Criterion (AIC). This process allowed the model to maintain a balance between complexity and predictive performance.

The optimized model demonstrated improved accuracy in predicting crash frequencies at intersections under varying sight distance conditions. By focusing on significant variables and removing less impactful ones, this method enhanced the model's robustness while simplifying its application. Using this optimized model, new CMFs were developed to provide more reliable assessments of crash risks at Alabama intersections. The calibrated Total Target Crashes prediction model and the FI Target Crashes prediction model according to Method 2 are presented in **Table 11** and **Table 12**, respectively.

Table 11 Total Target Crashes Prediction Model (Method 2)

Variable	Coefficient	Std. Error	Z-Score	P-value
Constant	-17.4865	3.7128	-4.71	2.48E-06
β_1(log(majAADT))	0.5312	0.3847	1.381	0.167279
β_2(log(minAADT))	0.8186	0.2241	3.653	0.000259
β_3(LmajAADT/log(ISD))	8.1874	5.5356	1.479	0.139131
β_4(MmajAADT/log(ISD))	6.0481	3.6906	1.639	0.101252
β_5(fourleg)	0.9816	0.2767	3.548	0.000388
β_6(spdlmt/log(ISD))	0.4394	0.1331	3.302	0.000959

Table 12 FI Target Crashes Prediction Model (Method 2)

Variable	Coefficient	Std. Error	Z-Score	P-value
Constant	-16.966	3.6517	-4.646	3.38E-06
β_1(log(minAADT))	0.9873	0.3378	2.923	0.00347
β_2(fourleg)	1.4413	0.4691	3.072	0.00212
β_3(spdlmt/log(ISD)	0.7539	0.2303	3.273	0.00106

- **Method 3: Facility-Type Specific Models**

In the third method, separate prediction models were developed for four distinct facility types. This approach recognized that different facility types, such as intersections with varying geometric features or traffic volumes, exhibit unique crash patterns. By tailoring the models to

each facility type, the study captured the specific factors influencing crash frequency within each category.

This method provided more accurate and reliable predictions by addressing the unique characteristics of each facility type, such as lane configurations, traffic control devices, and sight distance challenges. The calibrated Total Target Crashes prediction model and the FI Target Crashes prediction model for each facility type are presented in **Table 13** and

Table 14, respectively.

Table 13 Total Target Crashes Prediction Model (Method 3)

Facility Type	Variable	Coefficient	Std. Error	Z-Score	P-value
R23ST	Constant	-19.9783	6.5318	-3.059	0.00222
	$\beta_1(\log(\text{majAADT}))$	0.9809	0.7458	1.315	0.18841
	$\beta_2(\log(\text{minAADT}))$	0.8338	0.3617	2.305	0.02114
	$\beta_3(\text{LmajAADT}/\log(\text{ISD}))$	8.3724	13.3005	0.629	0.52903
	$\beta_4(\text{MmajAADT}/\log(\text{ISD}))$	8.5022	11.0754	0.768	0.44268
	$\beta_6(\text{spdlmt}/\log(\text{ISD}))$	0.2051	0.2169	0.946	0.3442
R24ST	Constant	-15.395	7.6756	-2.006	0.0449
	$\beta_1(\log(\text{majAADT}))$	0.6379	0.6377	1	0.3172
	$\beta_2(\log(\text{minAADT}))$	0.4947	0.4225	1.171	0.2417
	$\beta_3(\text{LmajAADT}/\log(\text{ISD}))$	11.5621	13.7458	0.841	0.4003
	$\beta_4(\text{MmajAADT}/\log(\text{ISD}))$	1.0578	13.6039	0.078	0.938
	$\beta_6(\text{spdlmt}/\log(\text{ISD}))$	0.4309	0.3013	1.43	0.1527
RM3ST	Constant	0.4334	11.9052	0.036	0.971
	$\beta_1(\log(\text{majAADT}))$	-1.0004	1.3156	-0.76	0.447
	$\beta_2(\log(\text{minAADT}))$	0.7428	0.6147	1.208	0.227
	$\beta_3(\text{LmajAADT}/\log(\text{ISD}))$	-129.8055	32894.4	-0.004	0.997
	$\beta_4(\text{MmajAADT}/\log(\text{ISD}))$	-2.157	6.6239	-0.326	0.745
	$\beta_6(\text{spdlmt}/\log(\text{ISD}))$	0.1973	0.3188	0.619	0.536
RM4ST	Constant	-34.9203	13.4336	-2.599	0.00934
	$\beta_1(\log(\text{majAADT}))$	1.1877	1.5306	0.776	0.43775
	$\beta_2(\log(\text{minAADT}))$	0.9135	0.8082	1.13	0.25837
	$\beta_3(\text{LmajAADT}/\log(\text{ISD}))$	52.4078	47.4423	1.105	0.2693
	$\beta_4(\text{MmajAADT}/\log(\text{ISD}))$	39.6741	45.5808	0.87	0.38408
	$\beta_6(\text{spdlmt}/\log(\text{ISD}))$	1.2254	0.7196	1.703	0.08858

Table 14 FI Target Crashes Prediction Model (Method 3)

Facility Type	Variable	Coefficient	Std. Error	Z-Score	P-value
R23ST	Constant	-14.0445	5.8257	-2.411	0.0159
	$\beta_1(\log(\text{minAADT}))$	1.1714	0.5452	2.149	0.0317
	$\beta_2(\text{spdlmt}/\log(\text{ISD}))$	0.1674	0.4126	0.406	0.6849
R24ST	Constant	-12.7405	7.7994	-1.634	0.102
	$\beta_1(\log(\text{minAADT}))$	0.6118	0.7227	0.847	0.397
	$\beta_2(\text{spdlmt}/\log(\text{ISD}))$	0.6969	0.5149	1.353	0.176
RM3ST	Constant	-6.1842	11.3213	-0.546	0.585
	$\beta_1(\log(\text{minAADT}))$	0.6214	1.2126	0.512	0.608
	$\beta_2(\text{spdlmt}/\log(\text{ISD}))$	-0.1686	0.6269	-0.269	0.788
RM4ST	Constant	-25.0776	12.396	-2.023	0.0431
	$\beta_1(\log(\text{minAADT}))$	1.1768	0.7273	1.618	0.1057
	$\beta_2(\text{spdlmt}/\log(\text{ISD}))$	1.6957	1.0074	1.683	0.0923

The three methods represent complementary approaches to improving prediction model performance. Method 1 emphasized maintaining the structure of the original national model while tailoring it to Alabama's conditions. Method 2 refined the model by focusing on significant variables, enhancing both accuracy and usability. Method 3 provided targeted models for specific facility types, offering the highest level of customization.

By comparing the predictive performance of the models derived from these methods, this study identified the most effective approach for developing CMFs tailored to Alabama's unique traffic environment. These advancements not only improve the precision of crash frequency predictions but also provide valuable insights for intersection safety improvements and policy development.

5.4 Validation and Evaluation of Models

The evaluation of different prediction models, as presented in **Table 15** and

Table 16, demonstrates varying levels of performance in predicting total target crashes and FI target crashes.

Table 15 Performance Measures for Different Total Target Crash Prediction Models

Model	Facility Types	Sample Size	McFadden R^2	MSE	RMSE	MAE
NCHRP Model	All	510	0.0227	0.0671	0.2591	0.1397
Method 1	All	510	0.1284	0.0569	0.2385	0.1407
Method 2	All	510	0.1297	0.0564	0.2374	0.1403

Model	Facility Types	Sample Size	McFadden R^2	MSE	RMSE	MAE
Method 3	R23ST	272	0.2032	0.0192	0.1385	0.0826
	R24ST	126	0.0543	0.0544	0.2333	0.1466
	RM3ST	66	0.0526	0.0621	0.2493	0.1741
	RM4ST	46	0.2603	0.1117	0.3342	0.2114

Table 16 Performance Measures for Different FI Target Crash Prediction Models

Model	Facility Types	Sample Size	McFadden R^2	MSE	RMSE	MAE
NCHRP Model	All	510	0.0761	0.6108	0.7816	0.2674
Method 1	All	478	0.1656	0.0189	0.1374	0.0674
Method 2	All	478	0.1523	0.0194	0.1393	0.0688
Method 3	R23ST	268	0.104	0.0047	0.0684	0.0333
	R24ST	122	0.0497	0.0181	0.1345	0.0741
	RM3ST	44	0.0208	0.0189	0.1376	0.0953
	RM4ST	44	0.156	0.0887	0.2978	0.1976

For the Total Target Crash Prediction model, Method 2 emerges as the most effective among the recalibrated models. It consistently outperforms Method 1 across all key performance metrics, including McFadden R^2, MSE, RMSE, and MAE. This indicates that the Bidirectional Stepwise Regression approach used in Method 2 successfully refines the model by selecting the most significant variables and optimizing their coefficients. The primary ad- vantage of Method 2 lies in its ability to strike a balance between model complexity and predictive accuracy. By focusing on the most impactful variables, this model minimizes overfitting and enhances its generalizability, making it particularly well-suited for predicting total target crashes across a wide variety of intersection types in Alabama.

For the FI Target Crash Prediction model, Method 1 proves to be the best prediction performance. This model achieves the highest McFadden R^2 and the lowest MSE, RMSE, and MAE among all models when applied to the entire dataset. These results suggest that the recalibration of coefficients in Method 1 more accurately reflects the local conditions that influence fatal and injury crashes in Alabama. The strength of Method 1 lies in its ability to enhance the predictive power of the original NCHRP model while retaining its foundational structure and logic. This makes Method 1 not only reliable but also interpretable and efficient, providing a robust tool for forecasting FI crashes without the need for significant alterations to the established model framework.

While Method 2 and Method 1 perform well overall, Method 3 shows significant potential, especially in facility-specific contexts, despite not always surpassing the generalized models. By tailoring prediction models to different facility types, Method 3 aims to capture the unique factors that affect crash frequency in specific settings. For example, the R23ST model within Method 3, with its relatively large sample size, exhibits lower error metrics and a higher McFadden R^2 for

total target crashes, making it a reliable choice for that facility type. This suggests that for R23ST facilities, the customized approach of Method 3 is particularly effective. However, other facility-specific models, such as RM3ST and RM4ST, which had smaller sample sizes, did not consistently outperform the generalized models, indicating that their predictive reliability might be limited due to insufficient data. Despite these limitations, the strategy of developing facility-specific models, as demonstrated by Method 3, holds great promise. With more comprehensive datasets, it would be possible to refine these models further, leading to more accurate and reliable predictions across various facility types. This approach could ultimately provide valuable, customized insights that enhance traffic safety management by better reflecting the distinct characteristics of different intersection types.

5.5 Calibrated CMFs and Case Studies

5.5.1 Calibrated CMFs for Total Target Crash

For the Total Target Crash in the approach direction, Method 2 was selected as the calibrated prediction model to create the CMFunction. It can be used to calculate the impact on Total Target Crash after adjusting the ISD in the approach direction. The CMF for Total Target Crash is calculated using the CM function shown in **Equation 20** below:

$$CMF_T = \frac{CMF_{T_1}}{CMF_{T_2}} \qquad \textbf{Equation 20}$$

Where:
CMF_T = CMF for target crashes for left or right approach direction
CMF_{T_1} = Target crash CMF for proposed condition
CMF_{T_2} = Target crash CMF for existing condition

Equation 21 can be used to calculate the Target crash CMF under the proposed condition or existing condition.

$$CMF_{T_i} = \frac{exp\left(8.1874 \times \frac{LmajAADT}{log(ISD_i)} + 6.0481 \times \frac{MmajAADT}{log(ISD_i)} + 0.4394\frac{PSL}{log(ISD_i)}\right)}{exp\left(8.1874 \times \frac{LmajAADT}{log(ISD_{base})} + 6.0481 \times \frac{MmajAADT}{log(ISD_{base})} + 0.4394\frac{PSL}{log(ISD_{base})}\right)}$$

Equation 21

Where:

CMF_{T_i}	= Target crash CMF for proposed condition (i=1) or existing condition (i=2)
LmajAADT	= 1 if the major road AADT is less than or equal to 5,000; otherwise 0
MmajAADT	= 1 if the major road AADT is greater than 5,000 and less than or equal to 15,000; otherwise 0
PSL	= Posted speed limit (mph)

ISD_i = Available ISD for proposed condition (i=1) or existing condition (i=2) (feet)

ISD_{base} = Base ISD for an approach direction (feet). For practical applications, this value is assumed to be 1,320 feet

The CMF charts for ISD under different speed limit conditions were generated using **Equation 21**, as illustrated in Appendix-A for Total Target crashes. For Medium Traffic Volume and Low Traffic Volume scenarios, the calibration process generally results in an increase in CMF, suggesting that the original model may have underestimated the crash risks in these settings, particularly at shorter ISD values. Conversely, in High Traffic Volume conditions, the calibration process significantly reduces the CMF, especially at shorter ISDs, indicating that the original model likely overestimated the crash risks for high traffic volumes. This local calibration provides a more accurate and conservative estimate, tailored specifically to Alabama's unique traffic conditions. Additionally, the sharper increase in CMF with decreasing ISD under low and medium major road traffic volumes, compared to high traffic volumes, can be attributed to two possible factors. First, on roads with lower traffic volumes, drivers might be less vigilant or more prone to risky behaviors, assuming they can safely navigate intersections with limited sight distance due to the infrequent presence of other vehicles. As ISD decreases, this assumption leads to a more dramatic increase in crash risk, which is reflected in the higher CMF post-calibration. Second, intersections on low-volume roads often lack advanced safety features (e.g., Flashing Beacon, warning signs) that are more commonly implemented at high- volume intersections. The absence of these mitigations makes low-volume intersections more sensitive to decreases in ISD, resulting in a steeper rise in CMF. In contrast, high-volume roads benefit from the constant presence of traffic, which encourages more cautious driving and moderates the increase in CMF as ISD decreases.

5.5.2 Calibrated CMFs for FI Target Crash

For the FI Target Crash in the approach direction, Method 1 was selected as the calibrated prediction model to create the CMFunction. It can be used to calculate the impact on FI Target Crash after adjusting the ISD in the approach direction. The CMF for FI Target Crash is calculated using the CM function shown in **Equation 22:**

$$CMF_{TFI} = \frac{CMF_{TFI_1}}{CMF_{TFI_2}} \qquad \textbf{Equation 22}$$

Where:

CMF_{TFI} = CMF for target fatal and injury crashes for left or right approach direction

CMF_{TFI_1} = Target fatal and injury crashes CMF for proposed condition

CMF_{TFI_2} = Target fatal and injury crashes CMF for existing condition

Equation 23 can be used to calculate the Target fatal and injury crashes CMF under the proposed condition or existing condition:

$$CMF_{TFI_i} = \frac{exp\left(4.96455 \times \frac{PSL}{ISD_i}\right)}{exp\left(4.96455 \times \frac{PSL}{ISD_{base}}\right)} \qquad \textbf{Equation 23}$$

Where:

CMF_{TFI_i} = Target fatal and injury crashes CMF for proposed condition (i=1) or existing condition (i=2)
PSL = Posted speed limit (mph)
ISD_i = Available ISD for proposed condition (i=1) or existing condition (i=2) (feet)
ISD_{base} = Base ISD for an approach direction (feet). For practical applications, this value is assumed to be 1,320 feet

In this study, under the traffic conditions in Alabama, the effect of whether the major road AADT is greater than 15,000 on FI Target Crashes is not significant, so to facilitate the practitioner's application, this study develops a generalized CMF for both scenarios where the main roadway AADT is greater than 15,000 or less than or equal to 15,000. The CMF charts for ISD under different speed limit conditions were generated using **Equation 23** and are presented in Appendix-B. The calibrated CMF charts revealed significant differences from the original models across various speed limits. Notably, the calibration process generally resulted in higher CMFs, particularly at shorter ISD values, suggesting that the original models may have underestimated crash risks in these scenarios. However, at higher available ISDs, the calibrated CMFs closely align with the original models, indicating that the original estimates were fairly accurate and required only minor adjustments.

5.5.3 Application Cases

As an example, consider a three-leg intersection with a Major AADT of 4500, a posted speed limit of 55 mph, and a current left-side available ISD of only 400 ft. A practitioner wants to know how the Target Crash Frequency changes when the ISD is upgraded from 400 ft to 600 ft. The Target crash CMF for the existing condition CMF_{T_2} can be calculated using **Equation 21** as,

$$CMF_{T_2} = \frac{exp\left(8.1874 \times \frac{1}{log(400)} + 6.0481 \times \frac{0}{log(400)} + 0.4394\frac{55}{log(400)}\right)}{exp\left(8.1874 \times \frac{1}{log(1320)} + 6.0481 \times \frac{0}{log(1320)} + 0.4394\frac{55}{log(1320)}\right)} = 2.4529$$

The Target crash CMF for the proposed condition CMF_{T_1} can also be calculated using **Equation 21** as:

$$CMF_{T_1} = \frac{exp\left(8.1874 \times \frac{1}{log(600)} + 6.0481 \times \frac{0}{log(600)} + 0.4394\frac{55}{log(600)}\right)}{exp\left(8.1874 \times \frac{1}{log(1320)} + 6.0481 \times \frac{0}{log(1320)} + 0.4394\frac{55}{log(1320)}\right)} = 1.7419$$

The CMF for upgrading the ISD can then be calculated using **Equation 20**:

$$CMF_T = \frac{1.7419}{2.4529} = 0.7101$$

Similarly, based on the calibrated CMF, the CMF of this upgrade for FI Target Crash can be calculated to be 0.7965 using **Equation 22** as below:

$$CMF_{TFI} = \frac{1.2818}{1.6093} = 0.7965$$

Comparing the post-calibration CMF to the pre-calibration CMF reveals significant differences in the estimated safety benefits of improving ISDs in Alabama. When using the post-calibration CMF, the results indicate an expected reduction of 28.99% in Total Target Crashes and 20.35% in FI Target Crashes. On the other hand, the pre-calibration CMF suggests a much lower reduction, with only an 11.95% decrease in Total Target Crashes and a 14.85% decrease in FI Target Crashes. These results suggest that the original model significantly underestimates the safety benefits of upgrading ISDs in Alabama.

5.6 Impact of Intersection Design on ISD-Related Crash

ISD is a critical component of roadway engineering that directly influences traffic safety, particularly at TWSC intersections. These intersections, which lack the traffic signals that guide driver behavior, place a heavy reliance on drivers' ability to make safe decisions based on their visual assessment of oncoming traffic. Properly designed ISD is essential for reducing the likelihood of collisions, especially in scenarios where a minor road intersects a major road without the benefit of traffic signals.

Substantial research has demonstrated the safety impact of specific intersection design features, though findings vary depending on the context and configuration. Left-turn lanes significantly improve traffic safety by reducing crash frequencies at both signalized and unsignalized intersections. For instance, the study by Harwood et al. (2003) showed that these lanes can lead to crash reductions of up to 44% in rural settings and substantial decreases in urban areas (Jonsson et al., 2007). These lanes are particularly effective in mitigating rear-end and angle crashes by separating turning vehicles from through traffic, which is crucial in rural areas where traffic volumes may be lower, but speeds are higher. Additionally, left-turn lanes on rural two-lane highways are considered a cost-effective safety measure, particularly in areas with higher traffic

volumes(Harwood et al., 2000). Beyond their direct impact on crash frequency, left-turn lanes also help reduce uncertainty in crash predictions, further validating their safety benefits at unsignalized intersections (Haleem et al., 2010).

Right-turn lanes also contribute to improved traffic safety by minimizing conflicts between turning and through vehicles, thereby reducing crash rates. Studies have shown that these lanes are effective in both rural and urban settings, contributing to overall crash reduction and offering a high return on investment as part of safety improvement programs (Claros et al., 2022; Harwood et al., 2000). However, some research has observed higher crash frequencies at intersections with right-turn lanes, though it remains uncertain whether this trend is attributable to the presence of the lanes themselves or to sampling bias (Eccles et al., 2018). This suggests that the safety benefits of right-turn lanes might vary depending on the specific intersection context and the surrounding traffic environment.

Medians play a significant role in enhancing traffic safety by providing physical separation between opposing traffic flows and offering refuge for vehicle maneuvers, such as left turns

and U-turns. Studies such as those by Turochy et al. (2022) have emphasized the benefits of wide medians in improving safety by reducing the likelihood of head-on collisions and providing staging areas for crossing vehicles. Implementing low-cost median treatments or wider medians has been associated with significant reductions in crash frequency, particularly for severe crashes (Park et al., 2016; Priyanka, 2022). However, the presence of medians does not always guarantee improved safety. For example, Sushmitha et al. (2023)'sstudy noted that large median openings can increase conflicts by creating more complex interaction zones, and at unsignalized intersections, Himes et al. (2018) found that medians were associated with a slight reduction in overall crash frequency but a significant increase in fatal and injury crashes. This highlights the need for careful median design to ensure that the benefits outweigh the potential risks.

Despite the clear implications for safety, most studies have aggregated target crashes with other types of crashes, potentially masking the unique effects of intersection design on this critical safety measure. By focusing on target crashes, this study aims to provide deeper insights that can inform the design and improvement of intersections specifically to reduce these types of crashes.

This study seeks to address the gap in existing literature by isolating ISD-related crashes and examining how they are influenced by specific intersection design features. The hypothesis driving this research is that the design features that improve overall intersection safety may not have the same impact on target crashes. In fact, certain designs might improve overall safety metrics while having little effect on or even exacerbating the conditions that lead to target crashes.

By conducting a detailed analysis of the effects of different left-turn lane types, right-turn lane types, and median widths on target crash frequency, this study aims to provide actionable insights for transportation agencies. Understanding these relationships is critical for developing targeted interventions that enhance safety at intersections, particularly in contexts where drivers must rely heavily on visual cues to navigate safely.

5.6.1 Empirical Bayes Before-and-After Study

This study employed the Empirical Bayes Before-and-After study method to rigorously evaluate the impact of three types of left-turn lanes, four types of right-turn lanes, and wide medians on the frequency of target crashes. The EB method was chosen due to its ability to address the regression-to-the-mean effect, a common issue in before-and-after studies that can lead to overestimation of treatment effects. By incorporating data from similar, untreated reference sites, the EB method isolates the impact of the treatments and provides more accurate and statistically robust estimates of CMFs.

The study categorized the left-turn lanes, right-turn lanes, and medians into specific types, with a reference group identified for each category. **Table 17** presents the classification of countermeasures and the corresponding sample sizes used in the analysis.

Table 17 Countermeasure Types and Descriptions

Countermeasure	Type	Description	Sample Size	Reference Group
Left-Turn Lanes	Type 1	No left-turn lanes	278	Yes
	Type 2	Channelized left-turn lanes with a raised or depressed median	118	No
	Type 3	Painted left-turn lanes with no physical median	114	No
Right-Turn Lanes	Type 1	No right-turn lanes	210	Yes
	Type 2	Right-turn lanes with a channelizing island but no exclusive lane	138	No
	Type 3	Right-turn lanes with a channelizing island and an exclusive lane	120	No
	Type 4	Conventional exclusive right-turn lanes with no channelizing island	42	No
Medians	No Median	No or narrow medians (less than 30 feet)	412	Yes
	Wide Median	Wide medians (greater than 30 feet)	98	No

- **Crash Prediction Model Development**

In this study, the SPFs were developed using the Target Crashes predictive model from **Table 17**, rather than the HSM-recommended SPFs. Because the HSM-recommended models are designed to predict all intersection-related crashes, whereas the primary objective of this study was to focus solely on target crashes. The Target Crashes model was specifically calibrated to reflect the conditions and characteristics associated with target crashes at the study sites, making it more appropriate for this analysis. By employing a model tailored to the types of crashes under investigation, the study ensured that the predicted crash counts were more relevant and precise, providing a better foundation for the subsequent EB analysis. This targeted approach allowed for a more accurate assessment of the impact of the studied intersection design features on the specific types of crashes that were of primary concern in this research.

- **Calculation of Expected Crashes**

Using the developed target crash prediction models, the expected number of crashes during the "before" period at the treated sites was calculated. This involved combining observed crash data with predictions from the prediction model (**Equation 24**):

$$N_{expected,T,B} = weight \times N_{predicted,T,B} + (1 - weight) \times N_{observed,T,B}$$

Equation 24

Where:

$N_{predicted,T,B}$ = predicted number of target crashes in the "before" period based on the prediction model

$N_{observed,T,B}$ = observed number of target crashes in the "before" period at the treated sites

$weight$ = the degree of variability in crash counts and is derived from the over-dispersion parameter during prediction model calibration

- **Adjustment for the After Period**

To account for changes in traffic volumes or conditions between the "before" and "after" periods, the expected number of crashes in the "after" period without treatment was adjusted as follows **(Equation 25):**

$$N_{expected,T,A} = N_{expected,T,B} \times \frac{N_{predicted,T,A}}{N_{predicted,T,B}}$$

Equation 25

Where:

$N_{predicted,T,A}$ = predicted number of target crashes in the "after" period based on the prediction model

This adjustment ensures that the comparison between the "before" and "after" periods accurately reflects any changes in traffic conditions.

- **Calculation of CMFs, Variance, and Standard Error**

The CMF was calculated to determine the impact of intersection treatments on crash frequency. The CMF is defined as the ratio of the observed number of crashes during the after-treatment period $N_{observed,T,A}$ to the expected number of crashes if the treatment had not been applied $N_{expected,T,A}$. The expected crash count is adjusted to account for any changes in traffic volumes or other conditions between the before and after periods. The formula for CMF is **Equation 26:**

$$\mathrm{CMF} = \frac{\mathrm{N_{observed,T,A}}}{\mathrm{N_{expected,T,A}}} \times \left(1 + \frac{\mathrm{Var(N_{expected,T,A})}}{\mathrm{N_{expected,T,A}}^2}\right)$$

Equation 26

This adjustment factor accounts for the variance in the expected crash number, ensuring that the CMF accurately reflects the treatment's effect while considering uncertainty. The variance of the expected crashes in the after-treatment period $\mathrm{Var}(\mathrm{N}_{\mathrm{expected,T,A}})$ is critical for understanding the reliability of the CMF. It is calculated as follows:

$$\mathrm{Var}(\mathrm{N}_{\mathrm{expected,T,A}}) = \mathrm{N}_{\mathrm{expected,T,A}} \times \frac{\mathrm{N}_{\mathrm{predicted,T,A}}}{\mathrm{N}_{\mathrm{predicted,T,B}}} \times (1 - \mathrm{weight})$$

Equation 27

Here, the "weight" is determined by the over-dispersion parameter from the prediction models, reflecting how much the crash data varies from the predicted values.

To assess the precision of the CMF, the overall variance is computed using (**Equation 28**):

$$\mathrm{Var}(\mathrm{CMF}) = \mathrm{CMF}^2 \times \left(\frac{1}{\mathrm{N}_{\mathrm{observed,T,A}}} + \frac{\mathrm{Var}(\mathrm{N}_{\mathrm{expected,T,A}})}{\mathrm{N}_{\mathrm{expected,T,A}}{}^2}\right) \div \left(1 + \frac{\mathrm{Var}(\mathrm{N}_{\mathrm{expected,T,A}})}{\mathrm{N}_{\mathrm{expected,T,A}}{}^2}\right)^2$$

Equation 28

The Standard Error (SE) of the CMF, which is the square root of the variance, provides a measure of the statistical accuracy of the CMF. This method ensures that the CMF is not only reflective of the true impact of the treatments but also statistically robust, giving confidence in the reliability of the conclusion.

The EB method was applied to calculate the CMFs for Type 2 and Type 3 left-turn lanes, using Type 1 as the reference group. The SEs were computed to provide confidence intervals, ensuring the reliability of the CMFs.

The study calculated CMFs for Types 2, 3, and 4 right-turn lanes, with Type 1 as the reference. Variances and SEs were computed to assess the statistical significance of the findings. The CMF for wide medians (greater than 30 feet) was calculated against the reference group of sites with no or narrow medians. The SE provided a measure of the reliability of this CMF.

This methodology ensures that the effects of regression-to-the-mean are accounted for, and that the CMFs developed are robust, statistically significant, and reflective of the true impact of the intersection design features on crash frequency. The results obtained from this rigorous analysis offer valuable insights for improving intersection safety through targeted design interventions.

5.6.2 Analytical Results and Interpretation

The results of the analysis for different types of left-turn lanes, right-turn lanes, and medians are presented in the following tables. Each table includes the CMF, SE, and Confidence Intervals (CIs) at various levels of confidence. These results provide insights into the effectiveness of each countermeasure in reducing or influencing crash frequency.

- **Left-turn Lanes**

The results of CMF analysis of different types of left-turn lanes on target crashes are shown in

Table 18:

Table 18 Target Crashes CMF for Left-turn Lanes

Countermeasures	Sample Size	CMF	SE	CI (65%-70%)	CI (95%)	CI (99.9%)
Type 1	278	Basic Condition (Reference)				
Type 2	118	0.4672	0.0913	[0.3759, 0.5586]	[0.2846, 0.6498]	[0.1932, 0.7413]
Type 3	114	0.5718	0.1716	[0.4002, 0.7434]	[0.2286, 0.915]	[0.0569, 1.0867]

The CMF of 0.4672 indicates that Type 2 left-turn lanes, which include channelization with raised or depressed medians, are associated with a 53.28% reduction in target crashes. This significant decrease could be attributed to the improved visibility and reduced conflict points provided by the channelization, which helps to separate left-turning vehicles from through traffic, allowing drivers on the minor road to better judge gaps in oncoming traffic. The narrow confidence intervals further support the reliability of this finding.

With a CMF of 0.5718, Type 3 left-turn lanes, which are painted without physical medians, reduce target crashes by 42.82%. However, the wider confidence intervals suggest more variability in effectiveness. This reduction may be due to the delineation provided by the painted lanes, which can help organize traffic flow and reduce confusion at intersections. However, the absence of a physical barrier may still allow some conflicts to occur, explaining the lesser reduction in crashes compared to Type 2.

- **Right-turn Lanes**

The results of CMF analysis of different types of left-turn lanes on target crashes are shown in

Table 19:

Table 19 Target Crashes CMF for Right-turn Lanes

Countermeasures	Sample Size	CMF	SE	CI (65%-70%)	CI (95%)	CI (99.9%)
Type 1	210	Basic Condition (Reference)				
Type 2	138	1.5047	0.3485	[1.1562, 1.8532]	[0.8077, 2.2017]	[0.4591, 2.5503]
Type 3	120	1.2862	0.2749	[1.0113, 1.5611]	[0.7364, 1.836]	[0.4615, 2.1109]
Type 4	42	0.927	0.3249	[0.6021, 1.2519]	[0.2772, 1.5768]	/

The CMF of 1.5047 suggests that Type 2 right-turn lanes, which include a channelizing island but no exclusive lane, are associated with a 50.47% increase in target crashes. This increase might be due to the added complexity introduced by the channelizing island, which could create confusion or reduce visibility for drivers making right turns. The wide confidence intervals

indicate a high level of uncertainty, suggesting that this design may not consistently perform well across different contexts.

With a CMF of 1.2862, Type 3 right-turn lanes, which feature both a channelizing island and an exclusive right-turn lane, show a 28.62% increase in target crashes. Although the addition of an exclusive lane might reduce conflicts with through traffic, the channelizing island

may still introduce visual obstructions or complicate driver decision-making, leading to more frequent crashes.

The CMF of 0.9270 for Type 4 right-turn lanes, which are conventional exclusive lanes without a channelizing island, indicates a slight reduction in crashes but the wide confidence intervals indicate high variability, making the results less conclusive.

- **Wide Median**

The results of CMF analysis of different types of left-turn lanes on target crashes are shown in **Table 20**.

Table 20 Target Crashes CMF for Wide Median

Countermeasures	Sample Size	CMF	SE	CI (65%-70%)	CI (95%)	CI (99.9%)
No Wide Median	210	Basic Condition (Reference)				
Wide Median	138	1.5047	0.3485	[1.1562, 1.8532]	[0.8077, 2.2017]	[0.4591, 2.5503]

The CMF of 0.8792 indicates that wide medians (greater than 30 feet) are associated with a 12.08% reduction in target crashes compared to sites with no or narrow medians. The reduction is likely due to the additional space provided by the median, which can serve as a refuge for vehicles, allowing drivers to stage their crossings in two phases and better judge oncoming traffic. However, the confidence intervals are relatively wide, especially at higher confidence levels, suggesting that the effectiveness of wide medians may vary depending on specific inter- section characteristics and traffic conditions.

6 CONCLUSION AND DISCUSSION

6.1 Key Findings and Contributions of the Study

This study developed an automated GIS-based tool that leverages high-resolution LiDAR data for ISD assessments. The tool addresses the limitations of traditional manual ISD measurement methods, offering a scalable, efficient, and accurate solution applicable across various intersection types. The automated process calculates the recommended ISD, assesses occlusion rates, and provides detailed visual outputs such as maps and 3D models. These capabilities enable transportation agencies to screen large road networks and prioritize high-risk intersections based on visibility issues, ultimately improving resource allocation for safety interventions.

The developed tool overcomes the time-consuming and labor-intensive nature of traditional field measurements and ensures a more standardized evaluation process. In addition, it improves upon previous LiDAR-based ISD assessment tools by enhancing accuracy and efficiency. The study tested several algorithms for generating major road approaches proposed in earlier research, identified their limitations in measurement accuracy, and recommended a more precise method for defining target points. To address the occasional obstructions affecting visibility checks, a more robust evaluation method was introduced, allowing a graded assessment of visibility between observer and target points rather than a simple binary classification of "visible" or "not visible." Furthermore, the method permits the user to generate observer positions based on reference lines, ensuring consistency with the field measurement practices of transportation agencies and maintaining uniform measurement standards across different intersections.

The ISD assessment tool was applied to multiple intersections using various practices and vehicle types, followed by strict manual reviews to validate the tool's accuracy, stability, and scalability. By using different measurement methods, the study found that using the stop bar to define the observer position resulted in significantly shorter available sight distances compared to using the edge of the major road. Specifically, left-side ISD was shorter by approximately 60 to 104 feet, and right-side ISD was shorter by about 15 to 53 feet. This finding indicates that the stop bar-based observer method provides a more conservative sight distance evaluation. When comparing PC and trucks, the study revealed that trucks had a longer available ISD—left-side ISD by 51 to 93 feet and right-side ISD by 41 to 86 feet. Despite these differences in available ISD, there was no statistically significant difference in blockage rates between trucks and PC. The study recommended conducting separate assessments for each vehicle type to ensure a comprehensive evaluation of ISD.

The study also explored the relationship between ISD and crash frequency, focusing on Alabama's unique traffic and road conditions. The analysis specifically targeted crashes directly affected by insufficient sight distance at TWSC intersections. By examining historical crash data from 230 intersections, a strong correlation was established between inadequate ISD and an increased risk of crashes. The study also calibrated the CMFs proposed by the NCHRP study to

better reflect Alabama's traffic characteristics. The calibration results, presented in Appendix A and Appendix B, showed that for medium and low traffic volumes, the calibrated CMFs were higher than the original values, indicating that the original model might have underestimated crash risks in these scenarios. Conversely, for high traffic volumes, the calibrated CMFs were lower, suggesting an overestimation of crash risks by the original model. This calibration process provides a more accurate and reliable estimate of crash risks tailored to Alabama's specific conditions, offering an effective tool for improving intersection safety in the region.

Furthermore, the study assessed the impact of specific intersection design features on target crashes (ISD-related crashes). It found that channelized left-turn lanes with a raised or depressed median and painted left-turn lanes with no physical median on the major road could significantly reduce the frequency of target crashes. The research also indicated that constructing wide medians (greater than 30 feet) might lower target crash frequencies; however, the large error margins suggested that the effectiveness of wide medians may vary depending on specific intersection characteristics and traffic conditions. Statistical analysis also showed that constructing right-turn lanes with a channelizing island, whether with or without an exclusive lane, tended to increase the frequency of target crashes. This could be due to the channelizing island introducing visual obstructions or complicating driver decision-making, resulting in more frequent crashes.

In summary, this study makes several important contributions: the development of an automated, more accurate, and scalable ISD assessment tool using LiDAR data; an analysis of the differences in available ISD for passenger cars and trucks; an investigation into the correlation between ISD and crash risk in Alabama; the calibration of CMFs specific to Alabama's traffic conditions; and an evaluation of the impact of various intersection design features on ISD-related crashes. These contributions provide transportation agencies with a comprehensive framework for enhancing intersection safety through targeted interventions and data-driven decision-making.

6.2 Discussion of Implications

The findings from this research have significant implications for transportation policy and engineering practice, particularly in the areas of intersection safety and roadway design. The GIS-based ISD assessment tool developed in this study marks a major advancement in intersection safety analysis. By automating ISD measurements and integrating LiDAR data, transportation agencies can now evaluate sight distance across a large number of intersections more efficiently and accurately. This allows for more proactive safety measures, such as identifying intersections with inadequate ISD and prioritizing them for design improvements or targeted interventions.

The insights from this study on the relationship between intersection design features, ISD, and crash frequency offer valuable guidance for future intersection improvement project. Ensuring adequate ISD at TWSC intersections, along with other considerations such as turn lanes and medians, can improve intersection safety. This study emphasizes the need for flexible design standards that consider local traffic conditions, intersection geometry, and the specific requirements of road users.

Furthermore, the development of CMFs for ISD-related crashes enhances the ability of transportation agencies to make data-driven decisions regarding intersection safety improvements. The CMFs provide quantitative estimates of the safety benefits associated with increasing ISD, which can be incorporated into broader safety performance models and decision-making frameworks. This approach can lead to more effective resource allocation for intersection improvements and crash reduction strategies.

6.3 Limitations of the Study

While the findings of this study are promising, several limitations must be acknowledged. First, the accuracy of the ISD assessment tool heavily depends on the availability and quality of LiDAR data. In regions where up-to-date LiDAR data is scarce or unavailable, the tool's effectiveness may be significantly reduced. Additionally, inconsistencies in data acquisition parameters across different LiDAR datasets can introduce variations in the analysis, potentially impacting the reliability of the ISD assessment. Addressing these data quality issues is crucial for enhancing the tool's robustness and consistency.

Another challenge lies in the point cloud classification process used in LiDAR data processing. While the current classification algorithm provided sufficient information for ISD assessments, further refinement is necessary. In some instances, the algorithm struggles to accurately recognize the boundaries between vehicles and road surfaces and classify complex intersection environments. This limitation can lead to inaccuracies in identifying potential obstacles, thereby affecting the overall reliability of the ISD assessment. Enhancing the algorithm's ability to distinguish between various objects, particularly when handling large-scale datasets, would significantly improve the tool's accuracy.

The study also relies on user-defined vehicle trajectories and stop bar positions to ensure precise ISD measurements. Although these customizations are critical for maintaining accuracy, they are time-consuming, particularly when applied across large networks of intersections. This poses a considerable challenge for conducting efficient large-scale screenings and assessments. Incorporating more automated processes, such as leveraging advanced mapping technologies and artificial intelligence, could streamline these tasks and improve the tool's scalability for broader applications, making it more practical for use in extensive road network assessments.

Additionally, the relatively small sample size used in this study restricted the development of independent predictive models tailored to different types of traffic facilities. Consequently, the analysis could not produce specific models for various roadway configurations, potentially overlooking the nuances of how ISD impacts crash frequency across different intersection types. Future research involving a larger dataset is necessary to address this limitation and provide more detailed insights into the relationship between ISD and crash frequency for diverse intersection configurations.

Finally, this study exclusively focused on the impact of ISD on Target Crashes, leaving its influence on the crash frequency of all intersection-related incidents unexplored. While the findings offer valuable insights into crashes specifically influenced by sight distance, the broader

effects of ISD on overall intersection safety remain uncertain. Further investigation is needed to assess the comprehensive impact of ISD on various types of intersection crashes, thereby providing a more holistic understanding of its role in intersection safety. Addressing these limitations in future studies will be key to improving the tool's accuracy, scalability, and applicability to diverse intersection safety assessments.

6.4 Recommendations for Future Research

Based on the findings and limitations of this study, several areas for future research are recommended. One promising direction is the expansion of the ISD assessment tool to include a variety of intersection types beyond the current focus on TWSC intersections. Exploring its applicability in signalized intersections, roundabouts, and more complex roadway configurations would not only broaden the scope of the tool but also provide valuable insights into its effectiveness across different traffic environments. Additionally, adapting the tool for use in evaluating sight distance along entire highway corridors or ramp systems could significantly extend its utility, offering a comprehensive approach to assessing roadway safety.

In addition, future research on the ISD assessment tool could incorporate image recognition algorithms to automatically extract road features, such as the approach trajectories of the major road, the stop bar positions of the minor road, and the edges of the major road. Integrating these advanced image processing techniques would significantly enhance the automation of the tool, reducing the need for manual intervention. This improvement would not only increase the accuracy of the ISD assessments but also boost the overall efficiency of large-scale roadway network scanning, making it more practical and time-effective for transportation agencies to implement across diverse traffic environments.

Further research should also delve into the effectiveness of targeted safety interventions aimed at improving ISD at intersections. By evaluating the impact of measures such as the installation of traffic control devices, geometric design modifications, or visibility enhancements, future studies could generate empirical data on the success of these interventions in mitigating ISD-related crashes. This would provide transportation agencies with evidence-based strategies to enhance intersection safety and prioritize resource allocation for improvements.

Another promising area for future exploration involves the integration of machine learning models and advanced predictive algorithms into the ISD assessment process. Employing these models could substantially enhance the accuracy of ISD evaluations and facilitate the development of more sophisticated crash prediction models. Utilizing larger datasets and incorporating more complex variables would enable these models to refine their predictive capabilities, allowing for a more precise identification of high-risk intersections. This, in turn, could inform proactive safety interventions tailored to specific intersection conditions.

Finally, future studies should broaden the analysis to investigate the effects of ISD on all intersection-related crash frequencies, rather than limiting the focus to Target Crashes. Such a comprehensive approach would provide a deeper understanding of ISD's overall influence on intersection safety, offering valuable insights for transportation agencies seeking to develop more

effective crash mitigation strategies. By expanding the scope of ISD-related research, a more holistic perspective on intersection safety can be achieved, ultimately contributing to more robust and far-reaching safety improvements.

REFERENCES

AASHTO. (2010). *Highway Safety Manual* (1st ed., Vols. 1–3). Washington, D.C.: American Association of State Highway and Transportation Officials.

AASHTO. (2018). A Policy on Geometric Design of Highways and Streets. In American Association of State Highway and Transportation Officials (7th ed.). Washington, D.C.: American Association of State Highway and Transportation Officials.

Abdulhafedh, A. (2020). Highway stopping sight distance, decision sight distance, and passing sight distance based on AASHTO models. *Open Access Library Journal*, *7*(3), 1–24.

Achtemeier, J., Craig, C. M., & Morris, N. L. (2019). The effects of restricted sight distances on drivers at simulated rural intersections. *Proceedings of the Human Factors and Ergonomics Society Annual Meeting*, *63*(1), 2122–2123.

Agina, S., Shalkamy, A., Gouda, M., & El-Basyouny, K. (2021). Automated assessment of passing sight distance on rural highways using mobile LiDAR data. *Transportation Research Record*, *2675*(12), 676–688.

Aijazi, A. K., Checchin, P., & Trassoudaine, L. (2013). Segmentation based classification of 3D urban point clouds: A super-voxel based approach with evaluation. *Remote Sensing*, *5*(4), 1624–1650.

Alabama Department of Transportation. (2024). *ALDOT Traffic Data Management Public Portal*.

Castro, M., Anta, J. A., Iglesias, L., & Sánchez, J. A. (2014). GIS-based system for sight distance analysis of highways. *Journal of Computing in Civil Engineering*, *28*(3), 4014005.

Castro, M., Iglesias, L., Sánchez, J. A., & Ambrosio, L. (2011). Sight distance analysis of highways using GIS tools. *Transportation Research Part C: Emerging Technologies*, *19*(6), 997–1005. doi: 10.1016/j.trc.2011.05.012

Che, E., Jung, J., & Olsen, M. J. (2019). Object recognition, segmentation, and classification of mobile laser scanning point clouds: A state of the art review. *Sensors*, *19*(4), 810.

Che, E., & Olsen, M. J. (2017). Fast ground filtering for TLS data via Scanline Density Analysis. *ISPRS Journal of Photogrammetry and Remote Sensing*, *129*, 226–240.

Claros, B., Schroeder, E., Brummett, K., Chitturi, M., Bill, A., & Noyce, D. A. (2022). Safety and economic evaluation of the highway safety improvement program: is there a return on investment? *Transportation Research Record*, *2676*(5), 732–747.

Dabbour, E., & Easa, S. (2017). Sight-distance requirements for left-turning vehicles at two-way stop-controlled intersections. *Journal of Transportation Engineering, Part A: Systems*, *143*(1), 4016004.

Dabbour, E., & Easa, S. M. (2021). Revised method for calculating departure sight distance at two-way stop-controlled (TWSC) intersections. *Transportation Research Record*, *2675*(12), 904–914.

Easa, S. M. (1998). Model for sight-distance analysis of uncontrolled intersections. *Journal of Transportation Engineering*, *124*(2), 156–162.

Easa, S. M., & Ali, Z. A. (2006). Three-dimensional stop-control intersection sight distance: General model. *Transportation Research Record*, *1961*(1), 94–103.

Easa, S. M., Dabbour, E., & Ali, M. Z. A. (2004). Three-dimensional model for stop-control intersection sight distance. *Journal of Transportation Engineering*, *130*(2), 261–270.

Eccles, K., Himes, S., Peach, K., Gross, F., Porter, R. J., Gates, T. J., & Monsere, C. M. (2018). Safety Impacts of Intersection Sight Distance. In Safety Impacts of Intersection Sight Distance (Issue 228). Washington, DC: The National Academies Press. doi: 10.17226/25082

Gargoum, S. A., El-Basyouny, K., & Sabbagh, J. (2018). Assessing stopping and passing sight distance on highways using mobile LiDAR data. *Journal of Computing in Civil Engineering*, *32*(4), 4018025.

Gargoum, S. A., & Karsten, L. (2021). Virtual assessment of sight distance limitations using LiDAR technology: Automated obstruction detection and classification. *Automation in Construction*, *125*, 103579.

Gargoum, S., & El-Basyouny, K. (2017). Automated extraction of road features using LiDAR data: A review of LiDAR applications in transportation. *2017 4th International Conference on Transportation Information and Safety (ICTIS)*, 563–574.

Glennon, J. C. (1987). Effect of sight distance on highway safety. *Transportation Research Board (TRB) State of the Art Report*, *6*, 64–77.

Godumula, D. T., & Ravi Shankar, K. V. R. (2023). Safety evaluation of horizontal curves on two lane rural highways using machine learning algorithms: a priority-based study for sight distance improvements. *Traffic Injury Prevention*, *24*(4), 331–337.

Gross, F., Persaud, B. N., & Lyon, C. (2010). *A guide to developing quality crash modification factors*.

Haleem, K., Abdel-Aty, M., & Mackie, K. (2010). Using a reliability process to reduce uncertainty in predicting crashes at unsignalized intersections. *Accident Analysis \& Prevention*, *42*(2), 654–666.

Harkey, D., Lan, B., Srinivasan, R., Kumfer, W., Carter, D., & Nujjetty, A. P. (2021). *Impact of Intersection Angle on Highway Safety* (Issue FHWA-HRT-20-067). McLean, VA. Retrieved from https://rosap.ntl.bts.gov/view/dot/54782

Harwood, D. W., Bauer, K. M., Potts, I. B., Torbic, D. J., Richard, K. R., Rabbani, E. R., Hauer, E., Elefteriadou, L., & Griffith, M. S. (2003). Safety effectiveness of intersection left-and right-turn lanes. *Transportation Research Record*, *1840*(1), 131–139.

Harwood, D. W., Mason Jr, J. M., & Brydia, R. E. (2000). Sight distance for stop-controlled intersections based on gap acceptance. *Transportation Research Record*, *1701*(1), 32–41.

Himes, S., Eccles, K., Peach, K., Monsere, C. M., & Gates, T. J. (2016). Estimating the safety effects of intersection sight distance at unsignalized intersections. *Transportation Research Record*, *2588*(1), 71–79.

Himes, S., Porter, R. J., & Eccles, K. (2018). Safety evaluation of geometric design criteria: intersection sight distance at unsignalized intersections. *Transportation Research Record*, *2672*(39), 11–19.

Ibrahim, S. E., Sayed, T., & Ismail, K. (2012). Methodology for safety optimization of highway cross-sections for horizontal curves with restricted sight distance. *Accident Analysis \& Prevention*, *49*, 476–485.

Jha, M. K., & Karri, G. A. (2009). Road surface development and sight distance calculation with new visualization methods. *Proceedings of the 2nd WSEAS International Conference on Sensors and Signals: Sensors, and Signals and Visualization, Imaging and Simulation and Materials Science*, 220–225.

Jha, M. K., Karri, G. A. K., & Kuhn, W. (2011). New three-dimensional highway design methodology for sight distance measurement. *Transportation Research Record*, *2262*(1), 74–82.

Jonsson, T., Ivan, J. N., & Zhang, C. (2007). Crash prediction models for intersections on rural multilane highways: Differences by collision type. *Transportation Research Record*, *2019*(1), 91–98.

Jung, J., Olsen, M. J., Hurwitz, D. S., Kashani, A. G., & Buker, K. (2018). 3D virtual intersection sight distance analysis using lidar data. *Transportation Research Part C: Emerging Technologies*, *86*, 563–579. doi: 10.1016/j.trc.2017.12.004

Kilani, O., Gouda, M., Weiß, J., & El-Basyouny, K. (2021). Safety assessment of urban intersection sight distance using mobile lidar data. *Sustainability*, *13*(16), 9259.

Kumfer, W., Harkey, D., Lan, B., Srinivasan, R., Carter, D., Nujjetty, A. P., Eigen, A. M., & Tan, C. (2019). Identification of Critical Intersection Angle through Crash Modification Functions. *Transportation Research Record*, *2673*(2), 531–543. doi: 10.1177/0361198119828682

Layton, R. (2012). *Intersection Sight Distance: Discussion Paper \#3*. Retrieved from https://d1wqtxts1xzle7.cloudfront.net/64626971/12-4-intersection-sight-distance-libre.pdf?1602157137=&response-content-disposition=inline%3B+filename%3DThe_Kiewit_Center_for_Infrastructure_and.pdf&Expires=1732325996&Signature=bdjNcOpIz8Hn9imf6LlthlT1qXt4T

Liu, M., Lu, G., & Li, Y. (2010). The Impact Analysis of Intersection Sight Distance on Vehicle Speed. In Traffic and Transportation Studies 2010 (pp. 295–304).

Ma, Y., Easa, S., Cheng, J., & Yu, B. (2021). Automatic framework for detecting obstacles restricting 3D highway sight distance using mobile laser scanning data. *Journal of Computing in Civil Engineering*, *35*(4), 4021008.

Ma, Y., Zheng, Y., Easa, S., Wong, Y. D., & El-Basyouny, K. (2022). Virtual analysis of urban road visibility using mobile laser scanning data and deep learning. *Automation in Construction*, *133*, 104014.

Magyari, Z., Koren, C., Kieć, M., & Borsos, A. (2021). Sight distances at unsignalized intersections: A comparison of guidelines and requirements for human drivers and autonomous vehicles. *Archives of Transport*, *59*(3), 7–19.

Mapix Technologies. (2024). *Velodyne HDL-32E LiDAR Sensor*.

Mehendale, N., & Neoge, S. (2020). Review on lidar technology. *Available at SSRN 3604309*.

Morris, N. L., Craig, C. M., & Achtemeier, J. D. (2019). *Examining Optimal Sight Distances at Rural Intersections*.

Nehate, G., & Rys, M. (2006). 3D calculation of stopping-sight distance from GPS data. *Journal of Transportation Engineering*, *132*(9), 691–698. doi: 10.1061/(ASCE)0733-947X(2006)132:9(691)

Nourian, P., Gonçalves, R., Zlatanova, S., Ohori, K. A., & Vu Vo, A. (2016). Voxelization algorithms for geospatial applications: Computational methods for voxelating spatial datasets of 3D city models containing 3D surface, curve and point data models. *MethodsX*, *3*, 69–86. doi: 10.1016/j.mex.2016.01.001

Osama, A., Sayed, T., & Easa, S. (2016). Framework for evaluating risk of limited sight distance for permitted left-turn movements: Case study. *Canadian Journal of Civil Engineering*, *43*(4), 369–377.

Park, J., & Abdel-Aty, M. (2016). Evaluation of safety effectiveness of multiple cross sectional features on urban arterials. *Accident Analysis \& Prevention*, *92*, 245–255.

Parrish, A., Brown, D., Stricklin, R., & Turner, D. (2003). Critical analysis reporting environment (CARE). *WIT Transactions on Information and Communication Technologies*, *29*.

Pingel, T. J., Clarke, K. C., & McBride, W. A. (2013). An improved simple morphological filter for the terrain classification of airborne LIDAR data. *ISPRS Journal of Photogrammetry and Remote Sensing*, *77*, 21–30.

Pranjić, I., Deluka-Tibljaš, A., Cvitanić, D., & Šurdonja, S. (2017). Analysis of sight distance at an at-grade intersection. *Road and Rail Infrastructure IV*.

Priyanka, H. K. (2022). *Development of Crash Modification Factor for Low-cost Median Opening Treatments at Unsignalized Intersections of Rural Divided Highways*. Auburn University.

Quan, L., Zhang, B., Zhou, H., & Liu, P. (2022). Developing a Google Earth-based method to measure sight distance for U-turns at unsignalized intersections on multilane divided highways. *Transportation Research Record*, *2676*(1), 152–161.

Schattler, K. L., Hanson, T., & Maillacheruvu, K. (2016). Effectiveness evaluation of a modified right-turn lane design at intersections. *Illinois Center for Transportation Series No. 16-013*.

Shalkamy, A., El-Basyouny, K., & Xu, H. Y. (2020). Voxel-based methodology for automated 3D sight distance assessment on highways using mobile light detection and ranging data. *Transportation Research Record*, *2674*(5), 587–599.

Stančerić, I., Korlaet, Ž., & Dragčević, V. (2012). Sight distance tests at road intersections with unfavourable angles. *Road and Rail Infrastructure II*, 62.

Sushmitha, R., Reddy, V. B. P., & Ravishankar, K. V. R. (2023). INFLUENCE OF SIGHT DISTANCE CHARACTERISTICS ON SAFETY OF INTERSECTIONS USING SURROGATE SAFETY MEASURES. *Signal*, *9*(2,839), 8–890.

Tegge, R. A., Jo, J.-H., & Ouyang, Y. (2010). Development and application of safety performance functions for Illinois. *ICT-10-066 UILU-ENG-2010-2006*.

Torbic, D. J., Cook, D. J., Bauer, K. M., MRIGlobal, J. R. G., Harwood, D. W., Potts, I. B., Porter, R. J., Gooch, J. P., B, K. K., H, V., Medina, J., Taylor, J., & Utah, U. of. (2021). *Intersection Crash Prediction Methods for the Highway Safety Manual* (T. R. Board, of Sciences Engineering, & Medicine, Eds.; Issue 297). Washington, DC: The National Academies Press. doi: 10.17226/26153

TRB. (2008). *Highway Safety Manual Data Needs Guide* (Issue 329). Washington, DC: The National Academies Press. doi: 10.17226/23089

Tsai, Y., Yang, Q., & Wu, Y. (2011). Use of light detection and ranging data to identify and quantify intersection obstruction and its severity. *Transportation Research Record*, *2241*(1), 99–108.

Turochy, R. E., & Zhou, H. (2022). *Development of Guidance for Unsignalized Intersections on Rural Multilane Divided Highways*. *FHWA-930-964*.

Yan, X., & Radwan, E. (2004). Geometric models to calculate intersection sight distance for unprotected left-turn traffic. *Transportation Research Record*, *1881*(1), 46–53.

Zhang, W., Qi, J., Wan, P., Wang, H., Xie, D., Wang, X., & Yan, G. (2016). An easy-to-use airborne LiDAR data filtering method based on cloth simulation. *Remote Sensing*, *8*(6), 501.

Zhou, X., Pan, B., & Shao, Y. (2021). Evaluating the impact of sight distance and geometric alignment on driver performance in freeway exits diverging area based on simulated driving data. *Sustainability*, *13*(11), 6368.

APPENDIX

Appendix A

Calibrated Total Target Crashes CMF

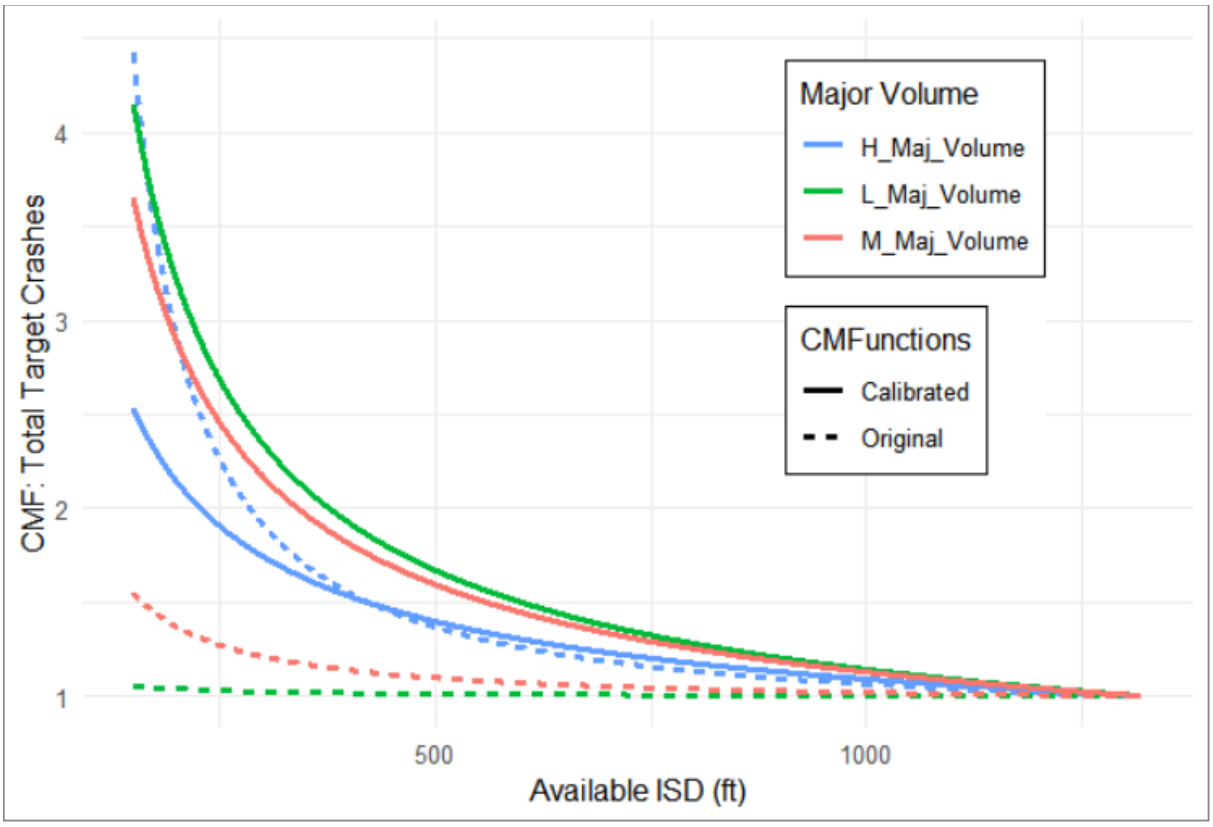

Figure A1 CMF for Target Crashes when Posted Speed Equals 35 mph

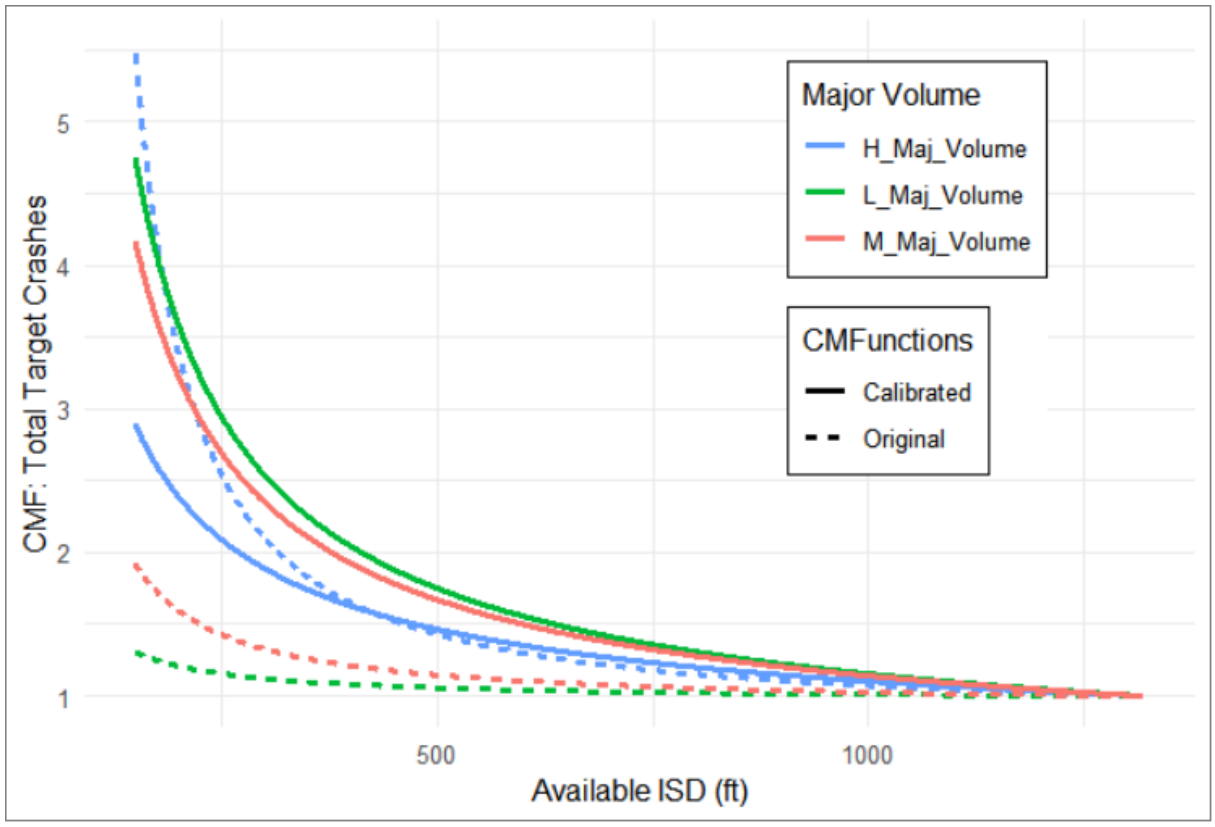

Figure A2 CMF for Target Crashes when Posted Speed Equals 40 mph

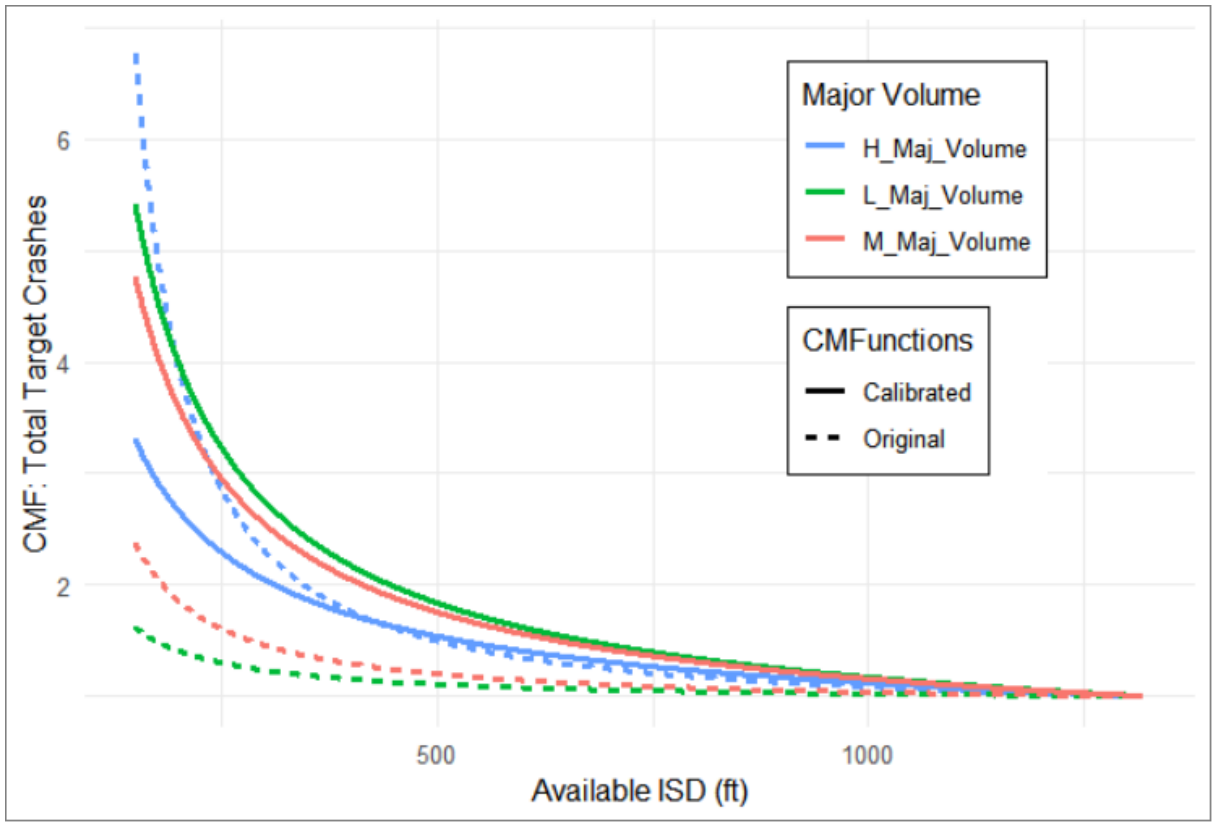

Figure A3 CMF for Target Crashes when Posted Speed Equals 45 mph

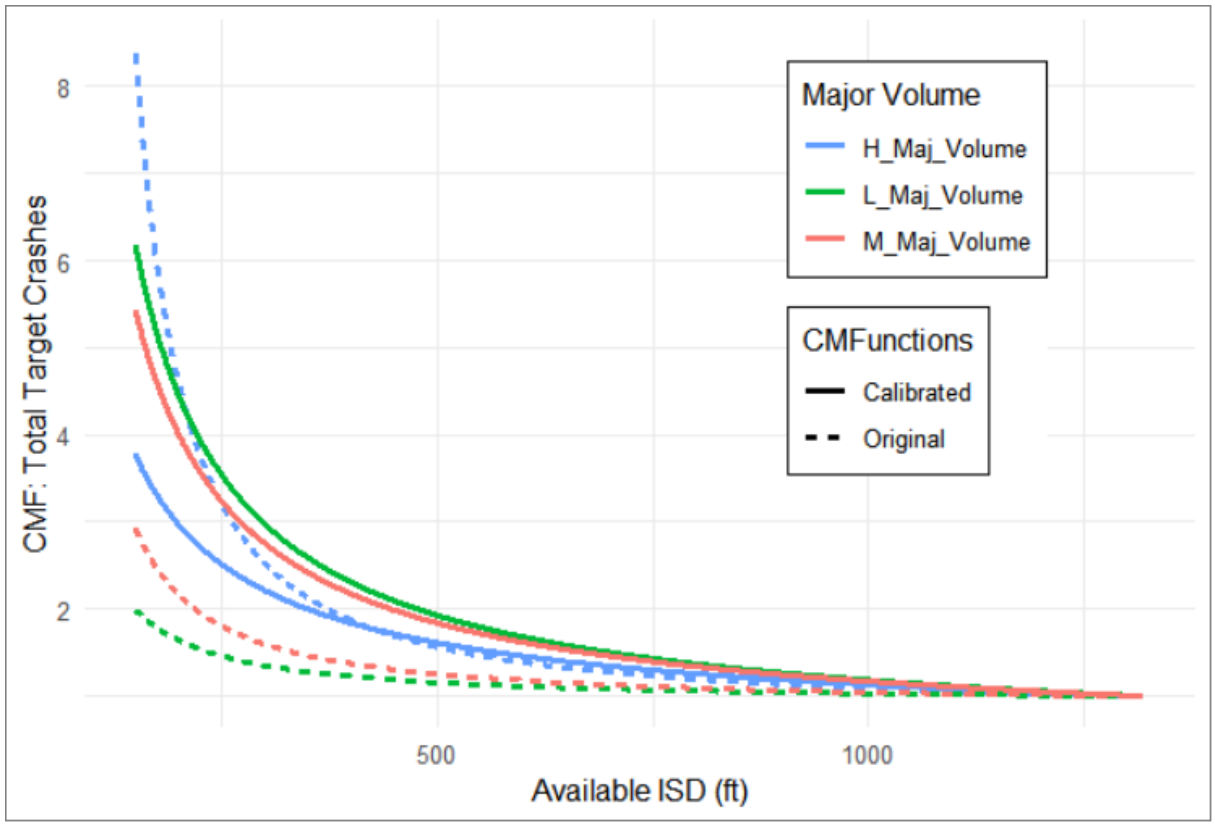

Figure A4 CMF for Target Crashes when Posted Speed Equals 50 mph

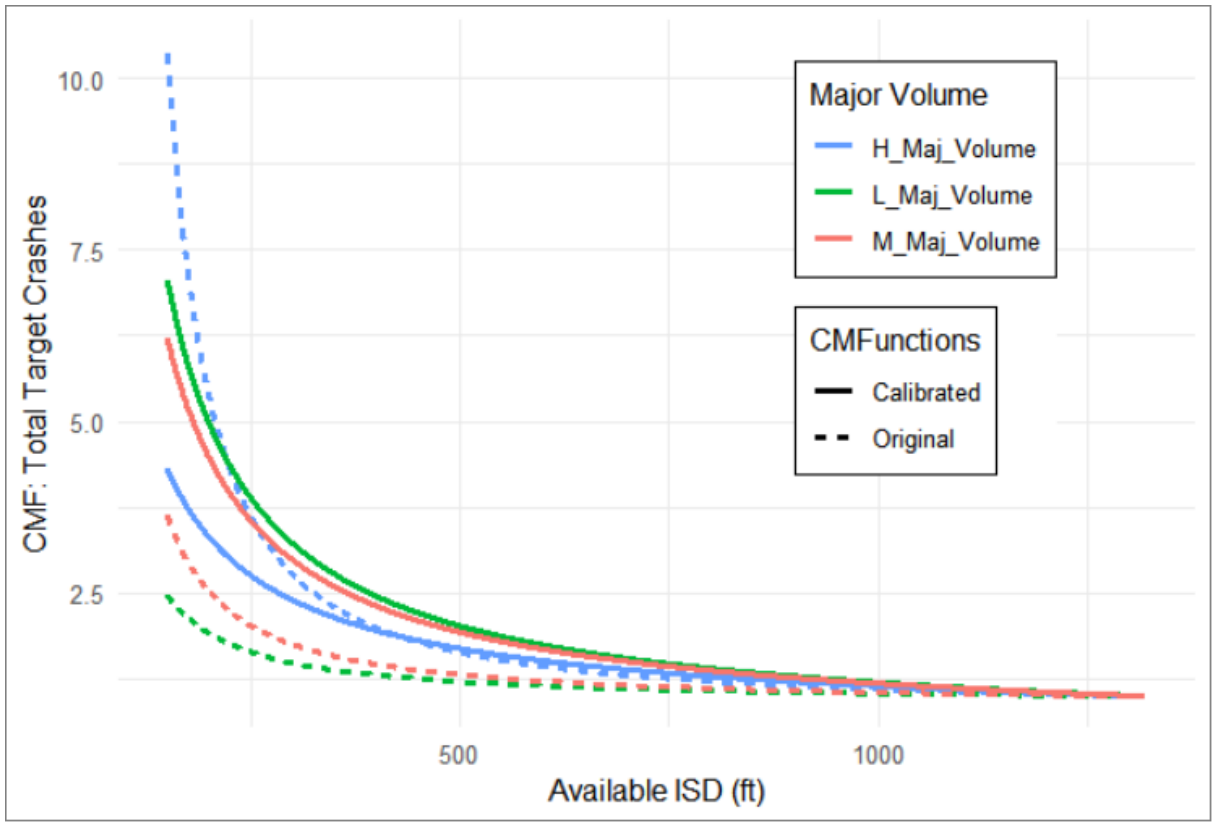

Figure A5 CMF for Target Crashes when Posted Speed Equals 55 mph

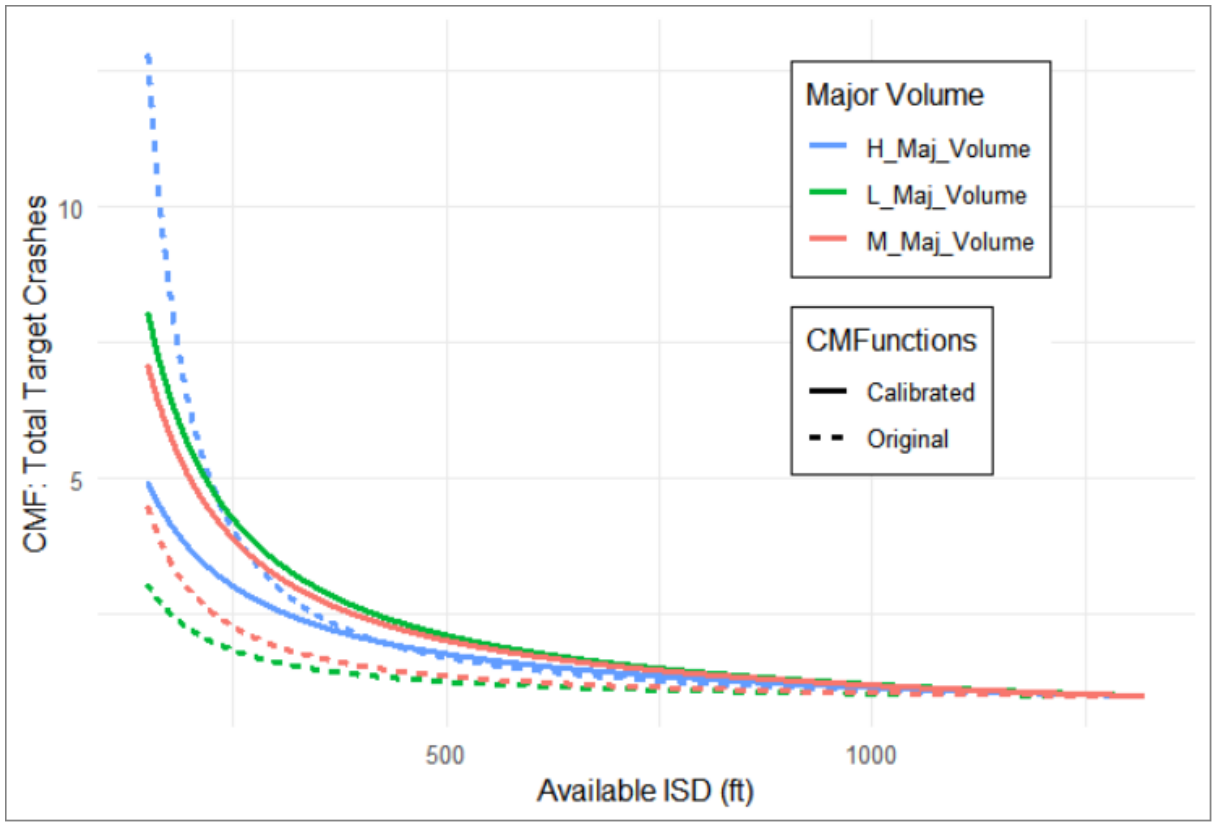

Figure A6 CMF for Target Crashes when Posted Speed Equals 60 mph

Appendix B

Calibrated Fatal and Injury Target Crashes CMF

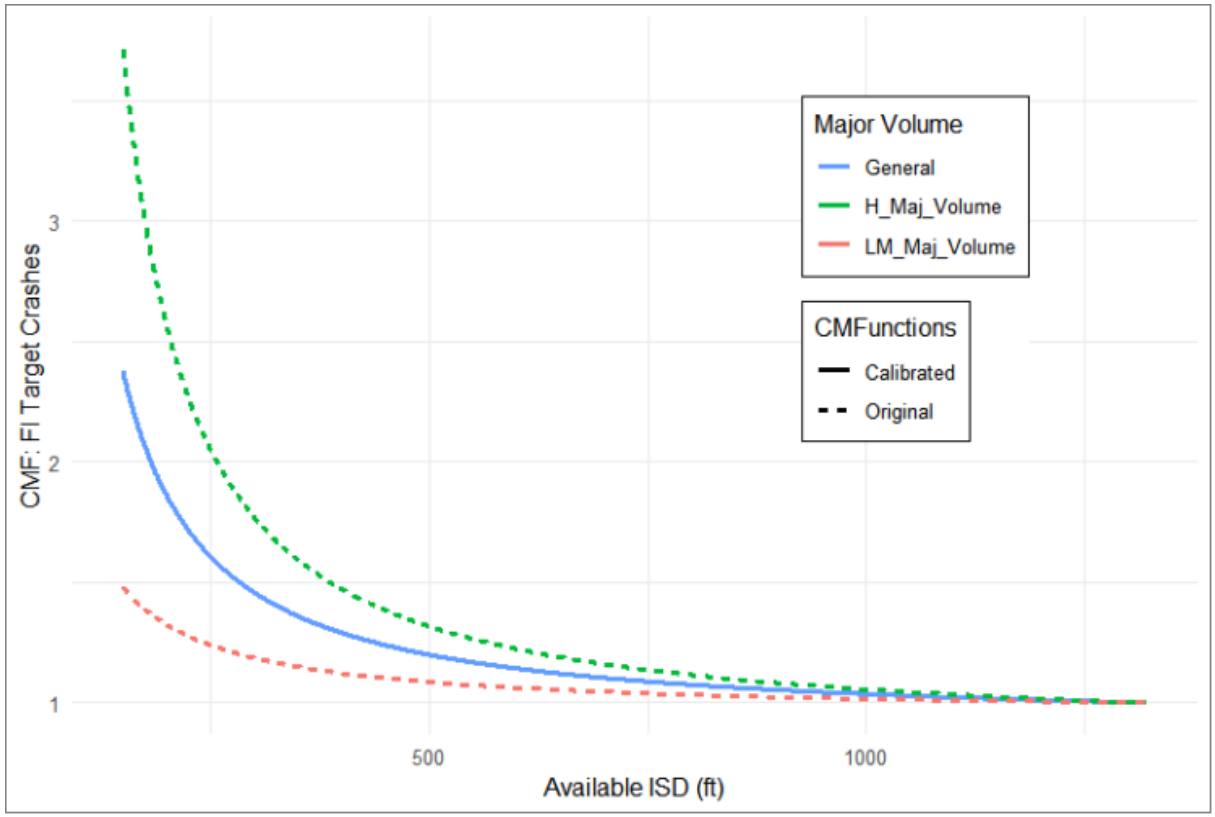

Figure B1 CMF for FI Target Crashes when Posted Speed Equals 35 mph

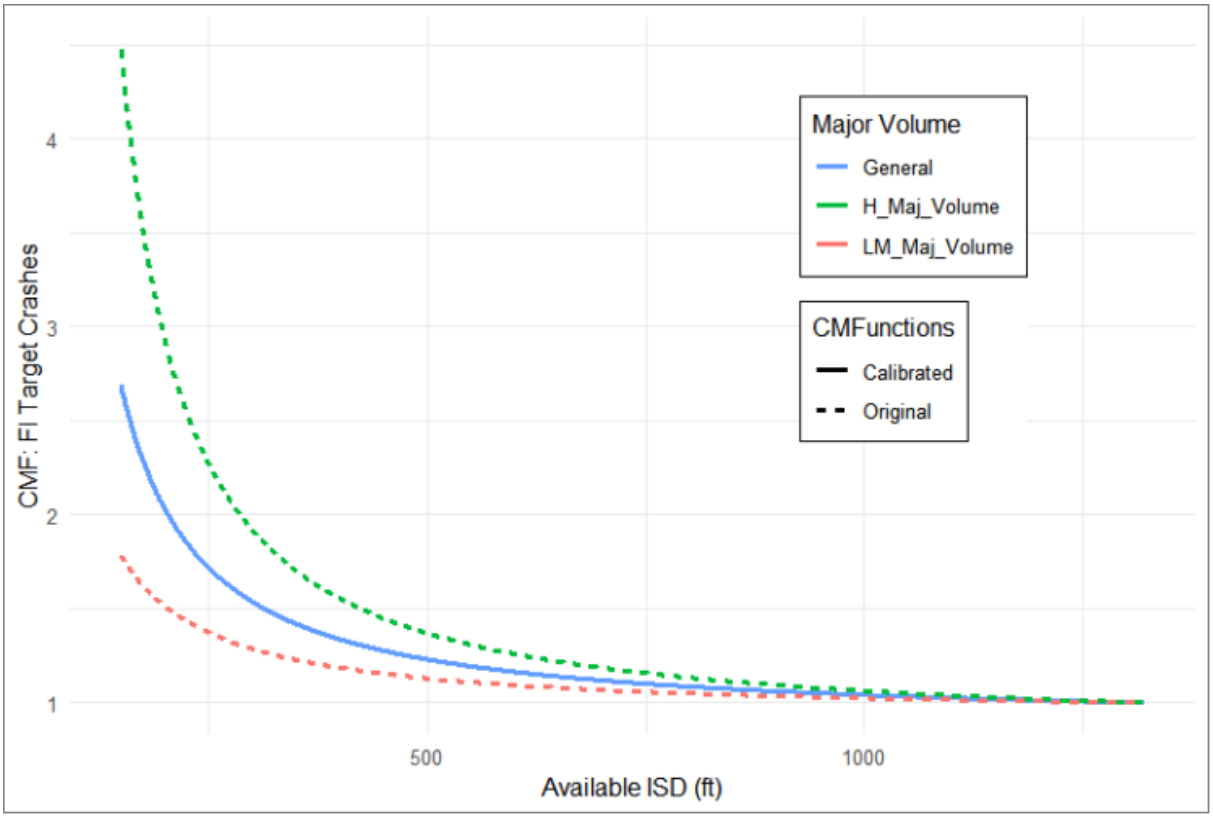

Figure B2 CMF for FI Target Crashes when Posted Speed Equals 40 mph

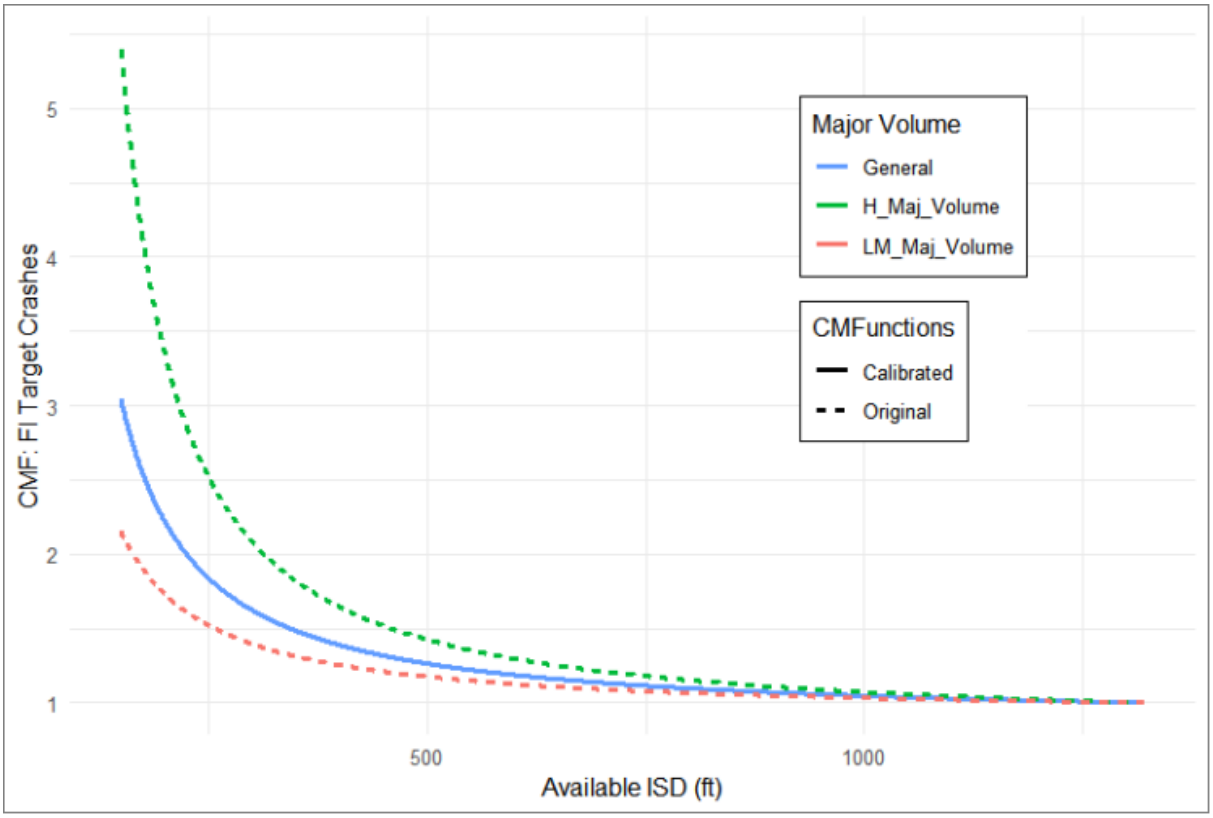

Figure B3 CMF for FI Target Crashes when Posted Speed Equals 45 mph

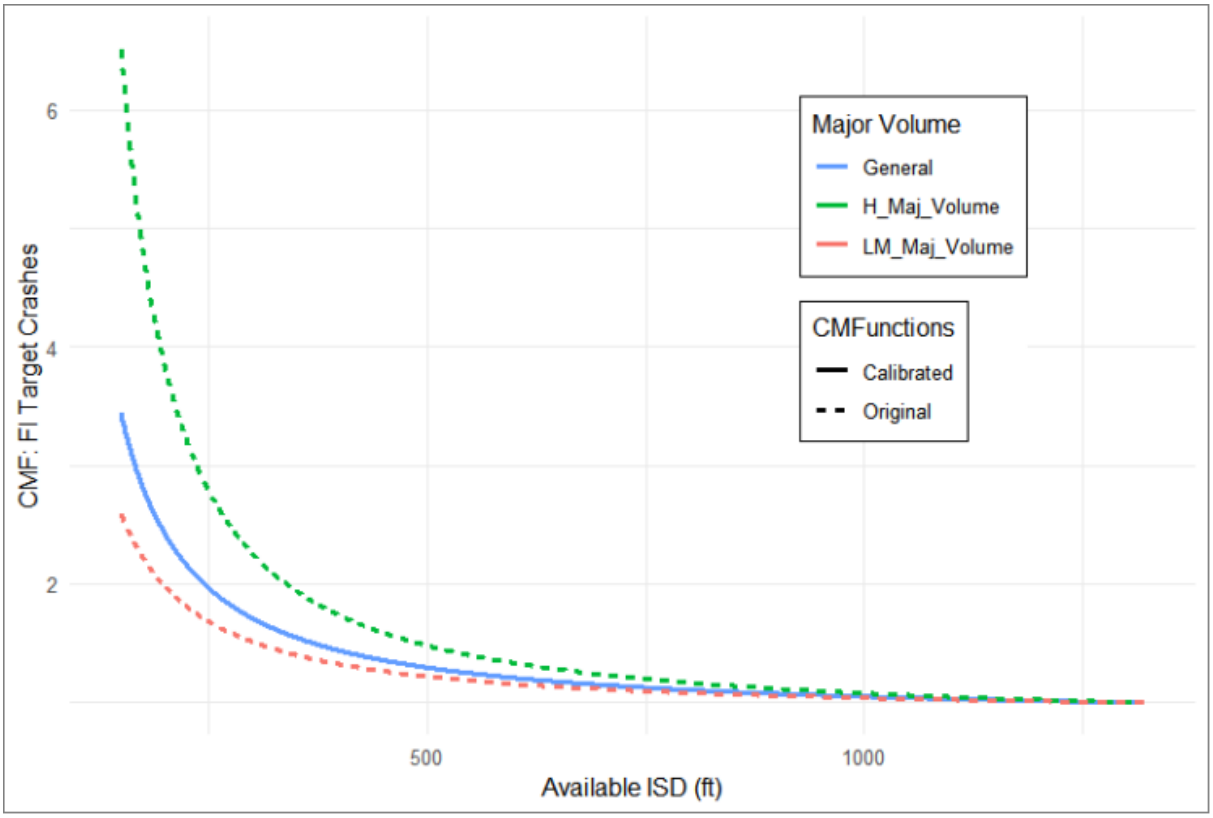

Figure B4 CMF for FI Target Crashes when Posted Speed Equals 50 mph

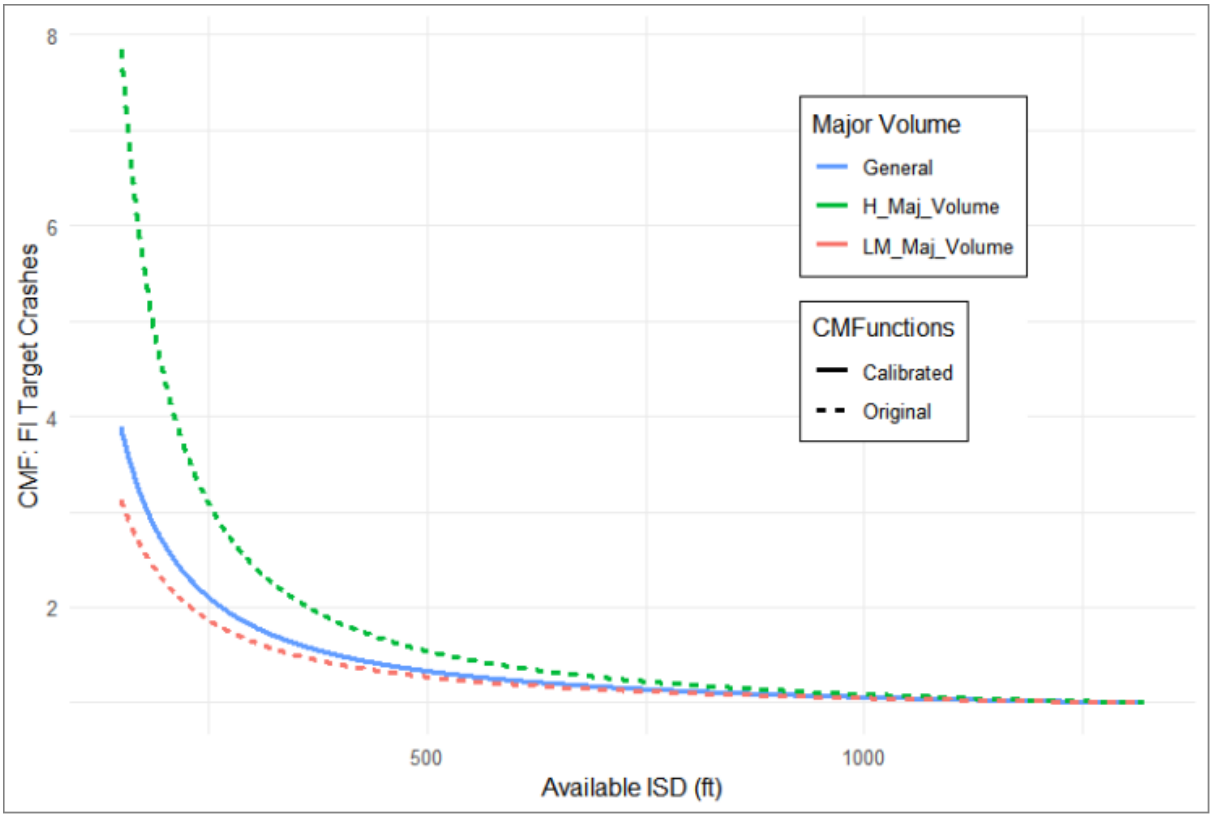

Figure B5 CMF for FI Target Crashes when Posted Speed Equals 55 mph

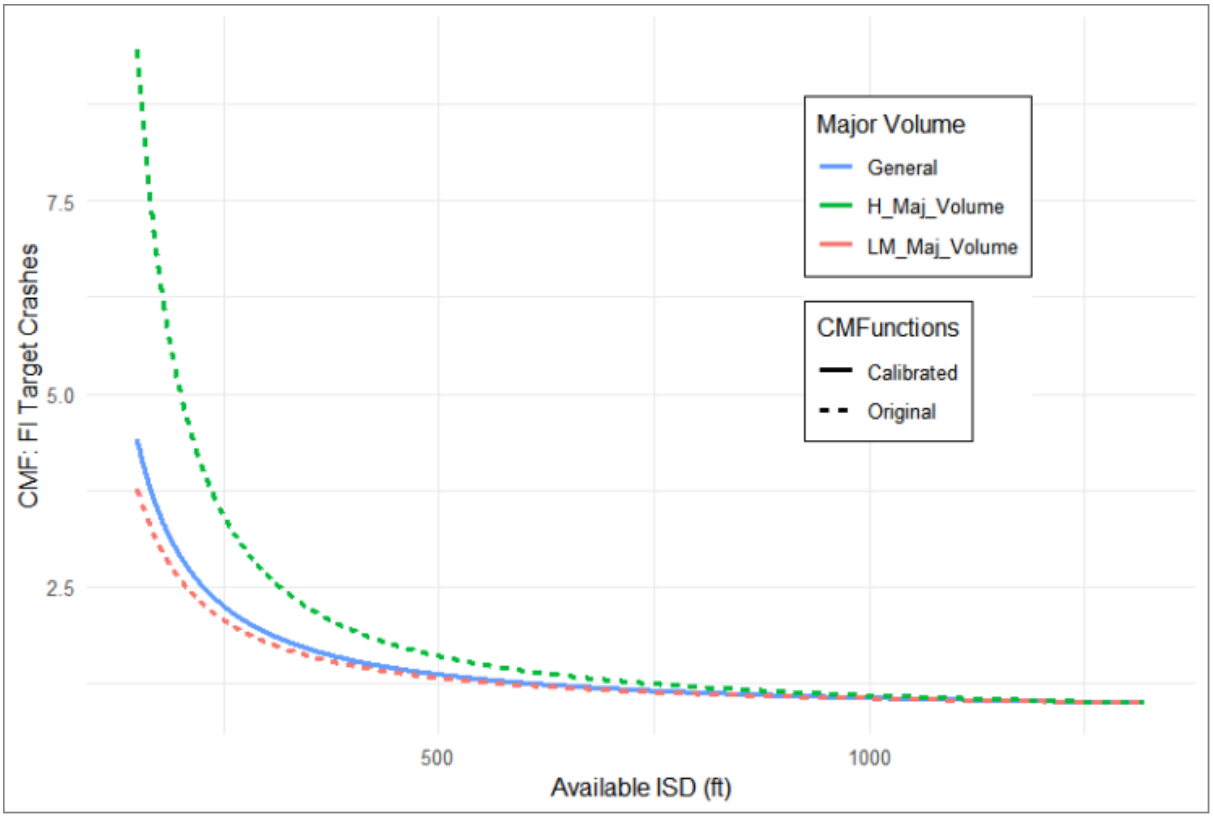

Figure B6 CMF for FI Target Crashes when Posted Speed Equals 60 mph